NASA
Technical
Paper
2683

June 1987

Experimental Cavity Pressure Distributions at Supersonic Speeds

Robert L. Stallings, Jr.,
and Floyd J. Wilcox, Jr.

NASA

NASA
Technical
Paper
2683

1987

Experimental Cavity Pressure Distributions at Supersonic Speeds

Robert L. Stallings, Jr.,
and Floyd J. Wilcox, Jr.

Langley Research Center
Hampton, Virginia

National Aeronautics
and Space Administration

**Scientific and Technical
Information Office**

Summary

An experimental investigation has been conducted to define pressure distributions for rectangular cavities over a range of free-stream Mach numbers and cavity dimensions. These pressure distributions together with schlieren photographs were used to define the critical values of cavity length-to-depth ratio $(l/h)_{cr}$ that separate open type cavity flows from closed type cavity flows. For closed type cavity flow, the shear layer expands over the cavity leading edge and impinges on the cavity floor, whereas for open type cavity flow, the shear layer bridges the cavity. The tests were conducted by using a flat-plate model that permitted the cavity length to be remotely varied from 0.5 to 12 in. Cavity depths and widths were varied from 0.5 to 2.5 in. The flat-plate boundary layer approaching the cavity was turbulent and had a thickness of approximately 0.2 in. at the cavity front face for the test range of Mach number from 1.50 to 2.86. Values of $(l/h)_{cr}$ obtained when decreasing cavity length were generally less than those obtained when increasing cavity length. Values of $(l/h)_{cr}$ ranged from 10 to 13 for the present tests. A large improvement in the correlation of measured cavity centerline pressure distributions for cavities of various depths was obtained when both the cavity width-to-depth ratio (w/h) and length-to-depth ratio (l/h) were held constant rather than l/h alone. The effects of cavity width on the cavity pressure distributions were much greater for cavities having closed or transitional flow fields than cavities having open flow fields. Decreasing cavity width resulted in a reduction in $(l/h)_{cr}$. Three-dimensional effects in the form of large lateral pressure gradients occurred on the rear faces of the cavities that had closed cavity flow fields.

Introduction

Numerous investigations have been conducted over the past several decades to investigate the flow fields over cavities and to define the resulting local pressure distributions and acoustic levels within the cavities (e.g., refs. 1 through 6). These investigations have been conducted over a speed range from subsonic through hypersonic Mach numbers. The results obtained at supersonic speeds are particularly important for application to cavities on contemporary and future aircraft and missile configurations capable of sustained supersonic flight speeds. Some examples of requirements for cavities on these configurations consist of weapon bays for high-speed military aircraft and recessed areas on wrap-around-fin missiles that contain the fins before they are deployed.

Existing data available in the literature show that cavity flow fields can occur that result in large local turning angles of the shear layer over the cavity; this gives rise to large cavity drag levels (e.g., refs. 7 and 8) as well as large impact pressures on components within the cavity. Such cavity flow fields can also result in adverse separation characteristics for a store being launched from the cavity (e.g., refs. 9 and 10). Large fluctuating pressure levels can also occur in cavities, which sometimes are severe enough to cause component failure of hardware within the cavity (ref. 11).

In general, data available in the literature show that at supersonic speeds, there are two fundamentally different types of cavity flow fields which have been classified as open and closed cavity flows. The type of flow field appears to be primarily a function of cavity length-to-depth ratio (l/h). As illustrated in figure 1, for values of $l/h > 13$, the cavity flow field is generally of the closed flow type. For this case, the shear layer expands over the cavity leading edge, impinges on the cavity floor and exits ahead of the rear face. Typical cavity floor pressure distributions for this case consist of low pressures occurring in the expansion region behind the front face followed by an increase in pressure and a pressure plateau occurring in the impingement region. Further downstream, as the shear layer approaches the cavity rear face, the pressure levels again increase and reach a maximum value just ahead of the rear face. The local flows over the cavity front and rear faces for the closed cavity flow field are very similar to the flows over rearward-facing and forward-facing steps, respectively. At $l/h \approx 12$, the cavity flow field is on the verge of changing from closed cavity flow to open cavity flow (decreasing l/h) and is referred to as "transitional cavity flow." For this case, the shear layer turns through an angle to exit from the cavity coincident with impinging on the cavity floor resulting in the impingement shock and the exit shock collapsing into a single wave. The corresponding pressure distribution shows that the extent of the plateau pressures in the impingement region has diminished and the pressure increases uniformly from the low values in the region aft of the front face to the peak values ahead of the rear face. For $l/h < 10$, the high pressures ahead of the rear face venting into the low pressure region downstream of the front face cause the shear layer to flow over or bridge the cavity. This type flow field is generally referred to as "open cavity flow." The pressure coefficients over the cavity floor are slightly positive and relatively uniform with the exception of a small adverse gradient occurring ahead of the rear face that is associated with the shear layer impinging on the outer edge of the rear face.

Because of the large differences in the flow fields for open and closed cavity flows and the resulting varied loadings on the cavities and their contents, it is very important to be able to define the l/h boundary that separates the two types of flow fields, which generally is referred to as the critical value of l/h or $(l/h)_{cr}$. The complexity of the cavity flow field limits the applications of current computational methods for determining local flow conditions in the cavity and therefore experimental techniques are generally relied upon to obtain this information. Unfortunately, the data available in the literature for a particular investigation are generally limited to a single Mach number and a small range of geometric variables. The purpose of the present investigation is to provide critical values of l/h and cavity pressure distributions from a single investigation for a range of supersonic Mach numbers, cavity lengths, cavity depths, and cavity widths. The tests were conducted by using a model that permitted the cavity length to be remotely varied from 0.5 to 12 in. which greatly facilitated determining $(l/h)_{cr}$. Cavity depths and widths were varied from 0.5 to 2.5 in. The boundary layer approaching the cavity was turbulent and had a thickness of approximately 0.2 in. at the cavity front face for the range of test Mach numbers from 1.50 to 2.86.

Symbols

C_p	pressure coefficient, $\frac{p - p_\infty}{q_\infty}$
h	cavity depth, in.
k	height of roughness used for boundary-layer transition, in.
l	cavity length, in.
l_D, l_F	separation distances downstream of a rearward-facing step and upstream of a forward-facing step, respectively, in.
$(l/h)_{cr}$	value of l/h that separates open type cavity flow from closed type cavity flow
M_∞	free-stream Mach number
p	measured surface pressure, lb/ft^2
p_t	free-stream stagnation pressure, lb/ft^2
p_∞	free-stream static pressure, lb/ft^2
q_∞	free-stream dynamic pressure, lb/ft^2
R	free-stream unit Reynolds number per foot
T_t	free-stream stagnation temperature, °R
w	cavity width, in.
x_1, x_2, x_3	axial surface distance on forward plate, cavity floor, and rear plate as defined in figure 3, in.
y_1, y_2	surface distances on cavity front face and cavity rear face as defined in figure 3, in.
z	lateral surface distance on cavity rear face as defined in figure 3, in.
δ	boundary-layer thickness, in.

Abbreviations:

FF	cavity front face
FL	cavity floor
FP	forward plate ahead of cavity
Loc	location
Orif	orifice
RF	cavity rear face
RP	rear plate downstream of cavity

Apparatus and Test Conditions

Wind Tunnel and Test Conditions

The tests were conducted in the low Mach number test section of the Langley Unitary Plan Wind Tunnel (UPWT). This facility is a variable-pressure continuous-flow wind tunnel with two test sections that permit a variation in Mach number from 1.50 to 4.60.

Ahead of each test section is an asymmetric nozzle that permits a continuous variation in Mach number from 1.50 to 2.90 in the low Mach number test section and from 2.30 to 4.60 in the high Mach number test section. The test sections are approximately 7 ft long and have a square cross-sectional area of approximately 16 ft^2. A complete description of the facility is given in reference 12.

The tests were conducted at zero angle of attack for the test conditions shown in the following table:

M_∞	p_t	T_t	R	k
1.50	1051	585	2×10^6	0.0128
2.16	1349	585	2×10^6	.0128
2.86	1934	585	2×10^6	.0215

Models and Instrumentation

Shown in figure 2 are drawings and photographs of the cavity model assembly. The model consisted of a sting-mounted flat plate 41.9 in. long and 34.0 in.

wide that housed a cavity with the cavity forward face being located 10.4 in. downstream of the flat-plate leading edge. In the region ahead of the cavity, the flat-plate leading edge had a sweep angle of 0° that provided a two-dimensional boundary layer approaching the cavity. The outboard sections of the leading edge were swept 30° to reduce the plate planform area in order to reduce tunnel starting loads. Sweeping the leading edge also positioned the tip vortices downstream to minimize the effect of these vortices on the cavity flow field. Starting loads were further reduced by sweeping the plate trailing edge to reduce planform area. The leading-edge wedge angle (5°) was sufficiently small that supersonic attached flow was maintained at the leading edge throughout the test range of Mach number.

Cavity length was remotely controlled by a sliding-block assembly that formed the rear face of the cavity. (See fig. 2(a).) Cavity depth was varied by positioning the cavity floor at the desired locations relative to the flat-plate surface. Depths of 0.5, 1.0, 2.0, and 2.5 in. were tested. Individual cavity rear-face blocks for each cavity depth were constructed and attached to the sliding-block assembly to maintain the remote positioning feature of this assembly. Figure 2(b) is a photograph of the model installed in the low Mach number test section of the UPWT. Shown in figure 2(c) is a photograph of typical block inserts that were installed in the cavity to vary its width. These inserts were constructed to vary width for several depths and lengths as shown in the following table:

l	h	l/h	w	w/h
12	1.0	12	2.5	2.5
			2.0	2.0
			1.5	1.5
			1.0	1.0
			.5	.5
6	1.0	6	2.5	2.5
			2.0	2.0
			1.5	1.5
			1.0	1.0
			.5	.5
6	0.5	12	2.5	5.0
			2.0	4.0
			1.5	3.0
			1.0	2.0
			.5	1.0
3	0.5	6	2.5	5.0
			2.0	4.0
			1.5	3.0
			1.0	2.0
			.5	1.0

A boundary-layer transition strip was applied to the flat-plate leading edge to ensure fully developed turbulent flow on the plate surface at the cavity front face for all test conditions. Two different roughness sizes were used to cover the test Mach number range. At the lower test Mach numbers of 1.50 and 2.16, the transition strip consisted of randomly distributed No. 50 sand elements (0.0128 in. nominal height) in a 0.06-in. band applied 0.40 in. behind the flat-plate leading edge measured in a streamwise direction. At the maximum test Mach number of 2.86, the transition strip consisted of individually placed No. 35 sand elements (0.0215 in. nominal height) arranged in a line that also was 0.4 in. behind the leading edge measured in a streamwise direction. The elements were spaced approximately 0.09 in. between centers.

The model was instrumented with 84 pressure orifices with locations as defined in figure 3. Most of the orifices (orifices 1–72) were located along the plate longitudinal centerline. The remaining orifices were located in lateral rows on the rear face with the number of rows depending on the cavity depth as shown in figure 3.

The pressures were measured by using electrical transducers connected to a pressure scanning system. A total of four scanners were used with tubing from 21 orifices connected to each transducer. Three reference pressures were also connected to each scanner to provide transducer calibration for each test point. The maximum reference pressure for each scanner was selected to approximately match the maximum anticipated pressure to be measured for the particular group of tubes connected to the scanner. The reference pressures and tunnel free-stream pressures were measured independently by precision mercury manometers. The pressure measurements were reduced to coefficient form and are presented in tables I through V.

Accuracy

Accuracy of the system for measuring the cavity pressures is better than 1 percent of the full-scale range of the electrical transducers; this includes all errors of linearity, hysteresis, and repeatability. Transducers with a maximum range of 5.0 lb/in^2 and 7.5 lb/in^2 were used, and accuracies in C_p resulted as follows:

Orifice	Transducer range, lb/in^2	ΔC_p for M_∞ of —		
		1.50	2.16	2.86
1–30, 58–61, 69–72, 81–84	5.0	±0.016	±0.016	±0.019
31–57, 62–68, 73–80	7.5	±0.024	±0.025	±0.029

The accuracy of the precision mercury manometers with which the reference pressures and the tunnel stagnation pressure were measured was ± 0.0035 lb/in^2.

The results of a test section calibration (ref. 12) indicate that the maximum variation in free-stream Mach number in the vicinity of the model installation was ± 0.02 for the test range of Mach number.

Based on pretest calibrations, the cavity sliding-block assembly could be positioned to a given value of x_2 with an accuracy of ± 0.005 in.

Results and Discussion

Schlierens

Effects of l/h. Typical schlieren photographs from the present tests showing both open and closed cavity flow fields are presented in figures 4 and 5 for cavities with depths of 0.5 and 1.0 in., respectively. For a given cavity depth, the cavity length-to-depth ratio was varied by remotely changing the cavity length. The photographs presented in figures 4(a) and (b) are for values of l/h of 24.0 and 16.0 and illustrate closed cavity flow fields. Coincident impingement and exit shocks occurred at $l/h = 11.6$ (fig. 4(c)), corresponding to a transitional cavity flow field as illustrated in figure 1. At $l/h = 11.2$ (fig. 4(d)), the impingement shock is no longer apparent; this indicates an open type cavity flow with this type of flow field existing for all values of $l/h < 11.2$ (figs. 4(e) and (f)). The photographs presented in figure 5 show that for a cavity depth of 1.0 in., closed cavity flow occurred for $l/h > 10.5$, transitional flow occurred for $l/h \approx 10.5$, and open cavity flow occurred for $l/h < 10.5$.

Critical l/h ***values.*** The remotely controlled sliding-block feature of the present cavity model not only expedited pressure data acquisition for a wide range of cavity lengths but also facilitated determination of the critical values of l/h. The procedure for determining these critical values of l/h was as follows. Initially, with the cavity flow field being of the closed flow type, the cavity length was decreased until the flow field changed to open cavity flow as determined by the abrupt disappearance of the combined impingement-exit shock in the schlieren. This critical value of l/h was recorded and identified as being associated with decreasing l/h. After further decreasing the cavity length to well within the open flow region, the cavity length was then increased until the flow field changed back to closed cavity flow as determined by the sudden reappearance of the combined impingement-exit shock. This critical value of l/h was also recorded and identified as being associated with increasing cavity length. The cavity length was then increased to well within the closed cavity flow region before repeating the above procedure. The procedure was repeated four times, and averages of these four critical l/h values were determined for both increasing and decreasing cavity length. The maximum variation of l/h from this mean value was approximately ± 0.12.

Presented in figure 6 are results that were obtained throughout the range of test Mach number for a cavity depth of 0.5 in. The data show that the critical values of l/h obtained by increasing cavity length were greater than those obtained by decreasing cavity length and that the magnitude of this hysteresis effect increased with increasing Mach number. The crosshatched region between these two curves indicates the uncertainty level for determining if the length-to-depth ratio of a fixed geometry cavity at a constant Mach number is critical. For values of l/h above the crosshatched region, the fixed geometry cavity should have closed cavity flow; for values below the crosshatched region, it should have open cavity flow; and for values that fall within the crosshatched region, the flow could be of either type. Also shown in figure 6 are estimated critical l/h values that are assumed to correspond to cavities having lengths that are equal to the sum of the separation distances downstream of a rearward-facing step and upstream of a forward-facing step with the step heights equal to the cavity depths as shown in the following equation:

$$(l/h)_{cr} = (l_D + l_F)/h \tag{1}$$

where l_D and l_F are the separation distances behind a downstream-facing step and ahead of a forward-facing step, respectively. Values of l_D and l_F were obtained from reference 1. The rationale behind such an estimate is that when the sum of the two separation distances is equal to the cavity length, then the high pressure ahead of the cavity rear face will vent into the low pressure region behind the front face and will cause the flow to be forced out of the cavity. This estimate underpredicted the measured critical values throughout the test Mach number range.

Centerline Pressure Distributions

Effects of l/h. Shown in figure 7 are typical cavity centerline pressure distributions for open, transitional, and closed cavity flows for a range of cavity depths and free-stream Mach numbers. Results are presented for the plate surface ahead of the cavity, the cavity front face, the cavity floor, the cavity rear face, and the plate surface downstream of the cavity. Presented in figure 7(a) are data for $M_\infty = 1.50$ and

$h = 0.5$ in. The pressure distributions for $l/h = 24.0$ are for closed cavity flow, for $l/h = 13.0$ for transitional flow just prior to changing from closed to open flow, for $l/h = 12.6$ for transitional flow just after changing, and for $l/h = 8.0$ and 1.0 for open cavity flow. The pressure distributions on the cavity floor for the different types of cavity flow fields are consistent with the hypothetical distributions shown in figure 1 and discussed in the introduction. On the forward plate ahead of the cavity, the pressure coefficients are essentially constant at a value of zero; this indicates that any disturbances created by the cavities are not propagated upstream. The pressure measurements on the cavity front face for $l/h > 1.0$ are invariant with y_1/h; however, the magnitudes of the pressure measurements are sensitive to the type of cavity flow field and are essentially equal to the pressure level at the most forward instrumented station on the cavity floor. In general, for the range of l/h shown, the pressure coefficients on the front face increase with decreasing l/h with the greatest changes occurring for values of l/h at which the flow switches from open to closed cavity flow. On the cavity rear face, large pressure gradients exist and large variations in pressure levels occur with varying l/h. These large gradients, in contrast to the almost constant pressures on the front face, result from the fact that the rear face is exposed to the approaching high energy flow similar to a forward-facing step, whereas the front face is exposed to an almost quiescent region similar to a rearward-facing step. Peak pressures on the rear face for a given value of l/h occurred at the outer edge of the rear face with the exception of the case of transitional cavity flow ($l/h = 13.0$) where a minimum pressure occurred in this region. This trend is observed through the test range of Mach number (figs. 7(a) through (c)). With increasing y_2/h from the outer edge of the cavities ($l/h \neq 13$), the pressures decrease to a minimum value at approximately mid-depth followed by an increase in pressure with further increases in y_2/h toward the cavity floor. The maximum values near the cavity floor are approximately equal to the peak values on the cavity floor for those cases where a pressure orifice was located at $x_2/l = 1$. On the rear plate downstream of the cavity, large pressure gradients occurred for those cavities having the larger values of l/h. The large gradients are associated with closed cavity flow fields and occur in a region of flow separation downstream of the outer edge of the rear face that is formed as the flow exits from the cavity and fails to expand around the 90° corner. For the cavities with open cavity flow fields, the flow essentially bridges the cavity, resulting in minimal separation at the rear corner and hence only small pressure gradients in this region.

The pressure distributions for the 0.5-in-deep cavities presented in figures 7(b) and (c) for Mach numbers 2.16 and 2.86 are somewhat similar to the results shown for $M = 1.50$. One of the most noticeable effects of increasing Mach number is to reduce the magnitude of the peak pressures. Also at $M = 2.86$, transition from closed to open cavity flow occurred when decreasing l/h from 11.6 to 11.2 as compared with 13 to 12.6 for the two lower Mach numbers. This trend is consistent with data obtained from the schlieren tests presented in figure 6. The data obtained on the rear plate shown in figure 7 indicate that increasing Mach number results in an increase in the extent of the separation region downstream of the rear face. This trend was also observed in the schlieren system as evidenced by a downstream movement of the reattachment shock with increasing Mach number.

Shown in figures 7(d), (e), and (f) are cavity pressure distributions for the 1-in-deep cavity at Mach numbers 1.50, 2.16, and 2.86, respectively. For this cavity depth, the maximum cavity length of 12 in. limits the maximum value of l/h to 12 and therefore only transitional and open cavity flow fields would be expected. As discussed previously in the introduction and as shown by the data from the 0.5-in-deep cavity in figures 7(a), (b), and (c), the extent of the flow impingement plateau pressures for the transitional flow field diminished; this resulted in monotonically increasing pressures in this region. The pressure distributions presented in figures 7(d) and (e) show that this is also true for the 1-in-deep cavity at $M_\infty = 1.50$ and 2.16. At $M_\infty = 2.86$, however, the floor pressure distributions for $l/h = 10.5$ (fig. 7(f)) are very similar to pressure distributions shown previously for closed cavity flow in that the plateau pressures occur over a significant range of x_2/l in the flow impingement region. Since the flow has changed to open cavity flow at $l/h = 10.0$, it is not clear why the distributions at $l/h = 10.5$ are not more representative of transitional cavity flow. Another unanticipated variation in the pressure distributions for the 1-in. cavities with $l/h = 12.0$ and 10.5 occurred on the rear face when increasing Mach numbers from 1.50 to 2.16 as may be seen by comparing figures 7(d) and (e). With increasing Mach number, a large increase in pressure level and pressure gradient occurred as compared with a decrease in pressure level shown for the 0.5-in. cavity (figs. 7(a) and (b)). These large pressures also occur on the rear face at $M_\infty = 2.86$ (fig. 7(f)). The flow field associated with these large pressures also results in a bow shock at the outer edge of the rear face as can be seen in figures 5(a) and (b). This bow shock was not apparent for the 0.5-in. cavity flow field (fig. 4(c)). The pressure distributions on the forward plate, front face, and rear plate of the 1-in. cavity through the test range of Mach number and l/h are similar to the results shown for the 0.5-in. cavity. Also, the pressure distributions on the cavity floor and rear face of the 1-in. cavity with open cavity flow ($y_2/h \leq 11.2$) are similar to the results obtained for the 0.5-in. cavity.

Pressure distributions for the 2.0-in-deep cavity were only obtained at Mach numbers 1.50 and 2.16, and these results are shown in figures 7(g) and (h). The maximum value of l/h that could be obtained at this depth was 6 and therefore all the pressure distributions shown are for open cavity flow. Generally, the trends of the variation of C_p with l/h and Mach number that are shown are similar to the open cavity flow results shown previously for the 0.5- and 1.0-in-deep cavities; however, the peak pressure magnitudes on the cavity floors and rear faces are greater than obtained for the more shallow cavities. This trend is consistent with an observation from reference 1 where it was found that as the ratio δ/h increases ($\delta \approx$ Constant with Mach number for present tests), pressure gradients are smoothed out presumably because of the decreased momentum transfer to the cavity.

For the deeper cavities of the present tests ($h = 2.0$ and 2.5 in.) more pressure instrumentation is available on the cavity floor for a given value of l/h simply because l is greater and therefore more pressure orifices are exposed. This more detailed instrumentation on the cavity floor indicates that a different type of flow field occurs for the smallest value of l/h ($l/h = 1$, figs. 7(g) through (j)), as compared with $l/h = 3.0$ and 6.0. This effect of l/h was not apparent for the more shallow cavities ($h = 0.5$ and 1.0) because of the reduced number of orifices on the cavity floor. For the deeper cavities with $l/h = 1$, the data in figures 7(g) through (j) show that a much smaller peak pressure occurs on the cavity floor ahead of the rear face as compared with $l/h = 3.0$ and 6.0. Additionally for $l/h = 1$, lower pressures occurred on the cavity rear face. This change in the pressure distributions may be associated with the flow restructuring from a two-vortex scheme to a single-vortex scheme as observed in reference 13 by flow visualization techniques. For values of l/h ranging from 5.0 to 2.5, Shchukin observed two vortices, as shown in the top of sketch A, of approximately the same size. The rear vortex had considerably greater circulation intensity and its center was located somewhat above the midsection of the cavity. For $l/h \approx 2.0$, the flow pattern restructured to form one vortex as shown in the bottom of sketch A. The one-vortex pattern was retained with increasing cavity depth to $l/h = 1$. Although pressure distributions are not presented in reference 13, the authors state that for the single-vortex case, the pressure

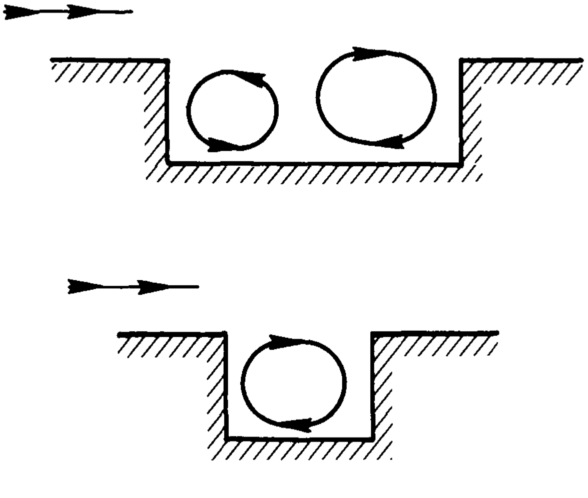

Sketch A

patterns become more symmetrical about the cavity midlength; this trend is consistent with the present data. Also, heat-transfer distributions presented in reference 13 show a large reduction in heat transfer ahead of the rear face for the single-vortex case which could in part be caused by a pressure reduction in this region as measured in the present tests.

Shown in figure 8 are the variations with l/h of the pressure coefficients in the outer-edge regions of the front and rear cavity faces to further illustrate the effect of the cavity flow field on the cavity pressure distributions. The data for the 0.5- and the 1.0-in. cavities (figs. 8(a) and (b)) clearly illustrate the increase in pressure on the front face and the decrease in pressure on the rear face that occurs as the flow changes from closed to open cavity flow ($l/h \approx 10$ to 13). The data also show that for all cavity depths, a decrease in pressure occurs on both the front and rear faces at the very low values of l/h, which is much more pronounced at the larger cavity depths. This decrease in pressure could be associated with the cavity flow restructuring from a two-vortex scheme to a one-vortex scheme discussed previously.

Effects of w/h. Presented in figure 9 are summary plots showing cavity centerline pressure distributions for cavities of different depths at constant or approximately constant values of l/h. The data are presented for the test range of Mach number for values of l/h representative of transitional and open cavity flow. These data indicate that for the transitional cavity flow field, l/h in itself is not a satisfactory correlation parameter. The lack of correlation of data is particularly obvious on the cavity rear face at the higher Mach numbers. This trend may be partially due to a three-dimensional effect created as a result of the cavity width not being scaled properly as depth was varied. The cavity width for the data presented in figure 9 was held constant as depth varied; therefore, the scaling parameter w/h varied as h varied as shown in the figure. Data were obtained, however, for different cavity widths at selected cavity lengths and these data provide an opportunity to examine the effect of w/h. Presented in figures 10 and 11 are data obtained at different depths but constant values of l/h and w/h. The data are again presented for both transitional and open cavity flow and show that much better correlation of the results is obtained when holding both l/h and w/h constant for the different cavity depths than was obtained by holding only l/h constant. There is, however, some lack of agreement of the data along the rear portion of the cavity floor, the rear face, and the rear plate. The disagreement on the floor and rear face generally consists of an increase in pressure level with an increase in cavity depth. This disagreement could result from the variation of the parameter δ/h that occurs with varying h, since for the present test, δ remained approximately constant as discussed previously. The trend of the variation of C_p with δ/h on the floor and rear face consisting of a decrease in pressure with increasing δ/h is consistent with previously published data (ref. 1) and is attributed to the decreased momentum transferred to the cavity with increasing δ/h.

A complete set of data obtained at the various cavity widths is presented in figures 12 and 13 for cavity depths of 0.5 and 1.0 in., respectively. The data are presented with w/h as a parameter at constant values of l and h. The data generally show that the greatest effect of cavity width occurs for the cavities having closed cavity flow fields or for the few cases of open cavity flow where decreasing cavity width caused the flow field to change from open to closed cavity flow. The flow field changed from open to closed flow when decreasing cavity width from $w/h = 4$ to 3 for the 0.5-in-deep cavity with $l/h = 12$ at both Mach numbers 1.50 and 2.16 (figs. 12(a) and (b)), respectively. Therefore, one effect of decreasing cavity width is to reduce the critical value of l/h, since as shown in figure 6, $(l/h)_{cr} = 13$ for the cavity with $w/h = 5$ as compared with $(l/h)_{cr} = 12$ for the cavities with $3 \leq w/h \leq 4$. For the 1.0-in-deep cavity with $l/h = 12$ (figs. 13(a) and (b)), w/h was only varied from 2.5 to 0.5, and for this range of w/h the cavity flow field remained the closed flow type. The data show, however, that increasing w/h resulted in pressure distributions in the flow impingement region changing from distributions typical of closed cavity flow ($w/h = 0.5$) to distributions typical of transitional cavity flow ($w/h = 2.5$). It is quite possible, therefore, that if the range of w/h for the 1.0-in. cavity had been extended from 2.5 to 5, the flow field may have changed from closed flow to open flow and comparable values of $(l/h)_{cr}$ would have been measured for both the 0.5-in. and 1.0-in. cavities.

Results presented in figures 12 and 13 show that the effects of cavity width on the pressure distributions for the cavities having open cavity flow fields were relatively small compared with those for the cavities with closed cavity flows. For open cavity flow, increasing cavity width generally resulted in an increase in pressures on the cavity rear face and on the rear portion of the cavity floor.

Lateral Pressure Distributions

All the pressure distributions presented to this point have been along the cavity centerline and therefore do not give any indication of the lateral variations that may occur as a result of three-dimensional effects created because the cavity had finite width. An example of the complexity of such a flow field is shown in figure 14, reproduced from reference 8. For the closed cavity flow field, a pair of vortices are formed at the outer edges of the cavity side walls as the flow expands into the cavity. At the cavity rear face, the vortices are well developed and are observed to continue downstream of the cavity. The impingement of these vortices on the cavity rear face would be expected to create lateral pressure gradients in this region and in particular toward the outer edge of the rear facc. Also, as the cavity width decreases, there may be an interaction between the vortices which would further complicate the lateral pressure gradients. The vapor screen photographs shown in figure 14 for the case of open cavity flow show a less complicated flow field as there are no apparent vortices or shock waves.

As mentioned in the section "Models and Instrumentation," a lateral array of pressure orifices were installed on the cavity rear face of the present model, the rear face being selected since this was the region believed to have the maximum pressures as well as maximum pressure gradients. Measured pressures from the lateral row of orifices closest to the outer edge of the cavity rear face ($y_2 = 0.25$ in.) are presented in figure 15 for cavity depths ranging from 0.5 in. to 2.5 in. Data are presented through the test range of Mach number for both open and closed cavity flow fields. The data presented in figures 15(a) and (b) for $l/h \geq 12$ are for closed cavity flow and show large lateral pressure gradients with the locations of the peak pressure ranging from the longitudinal centerline to the most outboard instrumentation location. The distributions are relatively symmetrical about the longitudinal centerline. The large pressure gradients and the location of the peak pressures are probably associated with the impingement of the edge vortices on the rear face.

Data presented in figure 15 for $3 \leq l/h \leq 6$ are for open cavity flow, and even for this type flow field, large lateral pressure gradients occur although the magnitudes are considerably less than obtained for closed cavity flow. Also, within this range of l/h for the cavities with depths of 2 and 2.5 in. (figs. 15(c) and (d)), the distributions were in some cases unsymmetrical about the cavity centerline. Results presented in figure 15 for $l/h = 1$ show relatively uniform lateral pressure distributions of small magnitudes which are in all cases symmetrical about the cavity centerline. These differences in the lateral pressure distribution compared with the results shown for $3 \leq l/h \leq 6$ further substantiate the previous discussion concerning changes in the cavity flow field when decreasing l/h to values less than approximately 3.

Shown in figure 16 is the effect of cavity width on the rear face lateral pressure distributions. These results were only obtained for the 0.5- and 1.0-in-deep cavities and for values of l/h of 6 and 12. When the cavity flow field was of the open flow type, the cavity lateral pressure distributions were relatively insensitive to variations in cavity width as shown for $l/h = 6$ in figures 16(a) and (b) and for $l/h = 12$ and $w/h \geq 4$ in figure 16(a). Pressure levels representative of closed type flow fields were measured for the 1-in-deep cavities at $l/h = 12$ for the test range of w/h from 2.5 to 1.0 (fig. 16(b)). These data show that decreasing w/h results in a decrease in the pressure levels and a reduction in the lateral pressure gradient about the centerline. Pressure levels indicative of closed cavity flow were also measured for the 0.5-in-deep cavities at values of $w/h \leq 3$; however, for these reduced width cavities, insufficient instrumentation was available to determine the effect of width on the lateral pressure gradients.

Summary of Results

An experimental investigation has been conducted to define cavity pressure distributions for a range of free-stream Mach numbers and cavity geometries. These pressure distributions together with schlieren photographs were used to define the critical values of cavity length-to-depth ratio $(l/h)_{cr}$ that separate open type cavity flows from closed type cavity flows. For closed type cavity flow, the shear layer expands over the cavity leading edge and impinges on the cavity floor, whereas for open type cavity flow, the shear layer bridges the cavity. The tests were conducted by using a flat-plate model that permitted the cavity length to be remotely varied from 0.5 to 12 in. Cavity widths and depths were varied from 0.5 to 2.5 in. The plate boundary layer approaching the cavity was turbulent and had a thickness of approximately 0.2 in. at the cavity front face for the test range of Mach number from 1.50 to 2.86. The results from these tests are summarized as follows:

(1) Critical cavity length-to-depth ratios obtained when decreasing cavity length were generally less than obtained when increasing cavity length. The magnitude of this hysteresis effect increased with increasing Mach number. Values of $(l/h)_{cr}$ ranged from 10 to 13 for the present tests.

(2) For the transitional cavity flow field, measured pressures in the flow impingement region on the cavity floor downstream of the front face increased monotonically with surface length with no apparent plateau-pressure region through the test range of Mach number for the 0.5-in-deep cavity and at Mach numbers 1.50 and 2.16 for the 1.0-in-deep cavity.

(3) A reduction in pressures occurred on both the front and rear faces of the cavity for values of cavity length-to-depth ratio (l/h) less than approximately 3, which corresponds to the approximate value of l/h where previous investigators have observed a restructuring of the cavity flow from a two-vortex scheme to a one-vortex scheme.

(4) A large improvement was obtained in the correlation of measured cavity centerline pressure distributions for cavities of various depths when both the cavity width-to-depth ratio (w/h) and l/h were held constant rather than l/h alone.

(5) Decreasing cavity width resulted in a reduction of $(l/h)_{cr}$.

(6) The effects of cavity width on the cavity pressure distributions were much greater for cavities having closed or transitional flow fields than cavities having open flow fields.

(7) Three-dimensional effects in the form of large lateral pressure gradients occurred on the rear faces of the cavities that had closed cavity flow fields. These large gradients also occurred for the cavities with open cavity flow fields when $3 \leq l/h \leq 6$. These gradients were generally symmetrical about the cavity longitudinal centerline for the closed cavity flows but in some cases they were asymmetrical for the open cavity flows. Relatively small lateral pressure gradients were measured on the rear faces of the cavities having $l/h = 1$, and these gradients were generally symmetrical about the cavity longitudinal centerline.

References

1. Charwat, A. F.; Roos, J. N.; Dewey, F. C., Jr.; and Hitz, J. A.: An Investigation of Separated Flows. *J. Aeronaut. Sci.*, vol. 28.
   Part I: The Pressure Field., no. 6, June 1961, pp. 457–470.
   Part II: Flow in the Cavity and Heat Transfer., no. 7, July 1961, pp. 513–527.
2. McDearmon, Russell W.: *Investigation of the Flow in a Rectangular Cavity in a Flat Plate at a Mach Number of 3.55.* NASA TN D-523, 1960.
3. Clark, Rodney L.; Kauffman, Louis G., II; and Maciulaitis, Algirdas: Aero-Acoustic Measurements for Mach .6 to 3.0 Flows Past Rectangular Cavities. AIAA-80-0036, Jan. 1980.
4. Nestler, D. E.; Saydah, A. R.; and Auxer, W. L.: Heat Transfer to Steps and Cavities in Hypersonic Turbulent Flow. *AIAA J.*, vol. 7, no. 7, July 1969, pp. 1368–1370.
5. Chang, Paul K.: *Separation of Flow.* Pergamon Press, Inc., c.1970.
6. Emery, A. F.: Heat Transfer and Pressure Distributions in Open Cavity Flow With Varied Recompression Step Profiles. *Proceedings of the Seventh International Symposium on Space Technology and Science, Tokyo, 1967*, AGNE Publ. Inc., c.1968, pp. 345–349.
7. Catani, Umberto; Bertin, John J.; De Amicis, Roberto; Masullo, Sergio; and Bouslog, Stanley A.: Aerodynamic Characteristics for a Slender Missile With Wrap-Around Fins. *J. Spacecr. & Rockets*, vol. 20, no. 2, Mar.–Apr. 1983, pp. 122–128.
8. Blair, A. B., Jr.; and Stallings, Robert L., Jr.: *Supersonic Axial-Force Characteristics of a Rectangular-Box Cavity With Various Length-to-Depth Ratios in a Flat Plate.* NASA TM-87659, 1986.
9. Stallings, Robert L., Jr.: Store Separation From Cavities at Supersonic Flight Speeds. *J. Spacecr. & Rockets*, vol. 20, no. 2, Mar.–Apr. 1983, pp. 129–132.
10. Stallings, Robert L., Jr.; Wilcox, Floyd J., Jr.; Blair, A. B., Jr.; and Monta, William J.: Store Carriage Drag and Separation at Supersonic Speeds. *Langley Symposium on Aerodynamics*, Volume II, Sharon H. Stack, compiler, NASA CP-2398, 1986, pp. 251–268.
11. Clark, Rodney L.: *Evaluation of F-111 Weapon Bay Aero-Acoustic and Weapon Separation Improvement Techniques.* AFFDL-TR-79-3003, U.S. Air Force, Feb. 1979. (Available from DTIC as AD A070 253.)
12. Jackson, Charlie M., Jr.; Corlett, William A.; and Monta, William J.: *Description and Calibration of the Langley Unitary Plan Wind Tunnel.* NASA TP-1905, 1981.
13. Shchukin, V. K.; Gortyshov, Yu. F.; Varfolomeev, I. M.; and Nadyrov, N. A.: Influence of Relative Depth and Reynolds Number on Heat Transfer in Cavities in Compressible Gas Flow. *Soviet Aeronaut.*, vol. 23, no. 3, 1980, pp. 83–86.

Table I. Pressure Coefficients for $h = 0.5$ in. and $w = 2.5$ in.

(a) $M_\infty = 1.50$

Orif	Loc	C_p for l/h of -																				
		24	20	16	14	13	12.532	12	11	10	9	8	7.5	7	6	5	4.8	4	3	2	1.5	1
1	FP	.0016	.0022	.0025	.0016	.0032	.0009	.0015	.0007	.0018	.0011	.0021	.0013	.0017	.0007	.0021	.0022	.0012	-.0002	.0009	.0020	.0010
2		.0048	.0047	.0028	.0050	.0053	.0029	.0039	.0052	.0044	.0047	.0051	.0058	.0047	.0048	.0053	.0051	.0037	.0037	.0046	.0043	.0051
3		.0121	.0103	.0107	.0107	.0115	.0098	.0100	.0112	.0102	.0104	.0106	.0107	.0124	.0101	.0109	.0111	.0100	.0097	.0098	.0101	.0095
4		.0105	.0102	.0111	.0097	.0099	.0100	.0105	.0120	.0120	.0129	.0126	.0118	.0129	.0108	.0107	.0129	.0118	.0110	.0112	.0117	.0111
5	FF	-.1963	-.1968	-.1968	-.1912	-.1504	-.0312	-.0135	.0024	.0119	.0167	.0194	.0228	.0255	.0317	.0397	.0434	.0531	.0705	.0656	.0615	.0540
6	FF	-.1944	-.1938	-.1935	-.1879	-.1478	-.0343	-.0156	.0004	.0092	.0156	.0180	.0218	.0248	.0296	.0368	.0396	.0499	.0733	.0913	.0771	.0760
64	RF	.6270	.6349	.6295	.6079	.5512	.2717	.2349	.2033	.1838	.1747	.1746	.1688	.1665	.1608	.1662	.1686	.1679	.1496	.1091	.0719	.0807
65		.5677	.5866	.5939	.5754	.5136	.2440	.2070	.1729	.1536	.1433	.1418	.1370	.1302	.1243	.1249	.1240	.1253	.1106	.0725	.0637	.0676
66		.5891	.6029	.6000	.5792	.5158	.2432	.2057	.1712	.1489	.1399	.1347	.1289	.1247	.1148	.1165	.1142	.1126	.0942	.0528	.0480	.0485
67		.6752	.6562	.6122	.5781	.5181	.2751	.2327	.1981	.1811	.1798	.1746	.1712	.1670	.1663	.1700	.1683	.1647	.1287	.0690	.0353	.0535
68		.7125	.6566	.5726	.5266	.4794	.3013	.2666	.2484	.2397	.2514	.2524	.2535	.2556	.2635	.2807	.2809	.2796	.2354	.1766	.1059	.1487
69	RP	-.1844	-.1720	-.1430	-.1241	-.1221	-.0732	-.0604	-.0482	-.0366	-.0293	-.0250	-.0224	-.0221	-.0181	-.0166	-.0170	-.0157	-.0138	-.0027	.0011	.0007
70		-.2465	-.2418	-.2255	-.2057	-.1899	-.0812	-.0636	-.0474	-.0343	-.0278	-.0258	-.0247	-.0238	-.0206	-.0193	-.0203	-.0193	-.0178	-.0077	-.0026	-.0005
71		-.2665	-.2713	-.2490	-.2091	-.1629	-.0491	-.0386	-.0292	-.0210	-.0154	-.0131	-.0117	-.0119	-.0097	-.0094	-.0108	-.0083	-.0065	-.0014	.0020	.0035
72		-.0899	-.0997	-.0903	-.0811	-.0695	-.0274	-.0209	-.0170	-.0109	-.0064	-.0049	-.0048	-.0039	-.0033	-.0032	-.0048	-.0029	-.0015	.0030	.0035	.0040
73	RF	.5232	.5843	.6274	.6249	.5921	.2866	.2298	.1806	.1380	.1054	.0926	.0857	.0755	.0613	.0554	.0544	.0527	.0651	.0435	.0411	.0449
74		.7164	.7675	.8005	.7660	.6917	.2779	.2351	.1899	.1671	.1535	.1472	.1414	.1341	.1267	.1288	.1252	.1273	.1233	.0901	.0554	.0504
75		.6681	.7270	.7381	.7140	.6339	.2673	.2250	.1841	.1568	.1412	.1391	.1363	.1286	.1210	.1216	.1197	.1212	.1047	.0488	.0523	.0511
76		.5333	.5930	.6408	.6351	.5958	.2771	.2238	.1756	.1348	.0952	.0759	.0692	.0631	.0514	.0501	.0479	.0462	.0689	.0780	.0414	.0450
11	FL	-.2252	-.2257	-.2254	-.2196	-.1776	-.0376	-.0196	-.0032	.0070	.0133	.0175	.0195	.0220	.0243	.0293	.0293	.0327	.0421	.0418	.0489	.0662
13		-.2437	-.2447	-.2430	-.2381	-.1990	-.0454	-.0270	-.0085	.0031	.0103	.0144	.0165	.0173	.0187	.0221	.0223	.0243	.0197	.0561	.0769	
14		-.2355	-.2370	-.2357	-.2316	-.1958	-.0485	-.0290	-.0111	.0012	.0089	.0135	.0158	.0160	.0172	.0190	.0193	.0170	.0208	.1233		
15		-.2110	-.2116	-.2124	-.2093	-.1817	-.0490	-.0316	-.0133	-.0008	.0064	.0112	.0123	.0136	.0159	.0172	.0159	.0118	.0735			
16		-.1719	-.1720	-.1722	-.1711	-.1545	-.0500	-.0328	-.0157	-.0042	.0045	.0093	.0125	.0135	.0151	.0134	.0123	.0227	.1695			
17		-.1257	-.1245	-.1253	-.1258	-.1187	-.0467	-.0312	-.0153	-.0045	.0037	.0088	.0102	.0134	.0130	.0147	.0154	.0823				
18		-.0773	-.0769	-.0784	-.0776	-.0781	-.0389	-.0259	-.0122	-.0023	.0045	.0089	.0113	.0143	.0128	.0276	.0382	.1917				
20		.0047	.0057	.0043	.0050	.0034	-.0129	-.0059	.0013	.0079	.0123	.0175	.0204	.0184	.0302	.1877						
22		.0646	.0657	.0656	.0714	.0822	.0250	.0256	.0268	.0296	.0312	.0325	.0328	.0428	.1801							
23		.0828	.0832	.0817	.0958	.1164	.0424	.0406	.0397	.0388	.0383	.0379	.0482	.0955								
24		.0963	.0944	.0946	.1183	.1468	.0608	.0555	.0519	.0484	.0431	.0517	.0993	.1850								
25		.1014	.1011	.1019	.1418	.1792	.0783	.0701	.0634	.0585	.0489	.1040	.1896									
26		.1042	.1038	.1036	.1697	.2105	.0990	.0844	.0744	.0646	.0601	.1929										
27		.1019	.1022	.1037	.2062	.2453	.1168	.0992	.0847	.0671	.1073											
28		.0983	.0986	.1031	.2451	.2775	.1306	.1121	.0920	.0771	.1949											
29		.0953	.0958	.1054	.2864	.3138	.1492	.1243	.0964	.1192												
32		.0810	.0811	.2199	.3964	.4130	.1779	.1388	.2223													
33		.0772	.0760	.2876	.4284	.4265	.1793	.1707														
34		.0719	.0711	.3456	.4599	.4435	.1993	.2532														
35		.0676	.0667	.3927	.4763	.4570	.2958															
36		.0632	.0636	.4348	.4961	.5783																
37		.0592	.0601	.4702	.5104																	
38		.0571	.0601	.5013	.6407																	
39		.0550	.0803	.5177																		
40		.0519	.1620	.5260																		
41		.0510	.2647	.5227																		
42		.0496	.3379	.6658																		
43		.0471	.3923																			
44		.0462	.4413																			
45		.0442	.4831																			
46		.0425	.5152																			
47		.0608	.5351																			
48		.1471	.5334																			
49		.2545	.5045																			
50		.3254	.6786																			
51		.3797																				
52		.4246																				
53		.4660																				
54		.4994																				
55		.5112																				
56		.4995																				
57		.4598																				

Table I. Continued

(b) $M_\infty = 2.16$

Orif	Loc	C_p for l/h of -																		
		24	20	16	14	13	12.532	12	11	10	8	7	6	5	4.8	4	3	2	1.5	1
1	FP	.0042	.0033	.0039	.0021	.0038	.0030	.0030	.0035	.0027	.0022	.0018	.0018	.0019	.0018	.0017	.0018	.0017	.0014	.0018
2		.0034	.0026	.0033	.0012	.0028	.0027	.0024	.0024	.0019	.0017	.0017	.0019	.0010	.0008	.0008	.0008	.0009	.0009	.0008
3		.0038	.0032	.0032	.0018	.0033	.0033	.0029	.0028	.0023	.0020	.0020	.0018	.0013	.0015	.0011	.0010	.0010	.0011	.0014
4		.0057	.0057	.0057	.0040	.0057	.0054	.0048	.0047	.0050	.0045	.0042	.0040	.0037	.0038	.0038	.0039	.0038	.0032	.0035
5	FF	-.1748	-.1748	-.1748	-.1745	-.1692	-.0287	-.0129	.0008	.0069	.0134	.0177	.0223	.0262	.0268	.0314	.0327	.0349	.0304	.0274
6	FF	-.1765	-.1766	-.1766	-.1760	-.1713	-.0297	-.0149	-.0010	.0058	.0120	.0167	.0206	.0243	.0246	.0297	.0320	.0388	.0409	.0431
64	RF	.5168	.5197	.4950	.4652	.4421	.1984	.1704	.1458	.1354	.1245	.1146	.1056	.0978	.0960	.0865	.0696	.0529	.0469	.0417
65		.4612	.4803	.4711	.4420	.4151	.1753	.1491	.1261	.1134	.1012	.0900	.0809	.0741	.0725	.0662	.0496	.0390	.0338	.0347
66		.4664	.4753	.4584	.4309	.4077	.1790	.1506	.1251	.1114	.0972	.0847	.0748	.0662	.0639	.0560	.0394	.0250	.0186	.0207
67		.5458	.5127	.4591	.4246	.4116	.2202	.1877	.1598	.1523	.1386	.1287	.1189	.1043	.0997	.0864	.0739	.0447	.0330	.0242
68		.6146	.5468	.4378	.4024	.4097	.2780	.2477	.2265	.2257	.2236	.2200	.2112	.1950	.1899	.1698	.1789	.1500	.1451	.1073
69	RP	.0236	.0352	.0379	.0338	.0344	-.0073	-.0066	-.0054	-.0042	-.0013	-.0005	.0004	.0027	.0026	.0039	.0042	.0062	.0063	.0068
70		-.0416	-.0324	-.0247	-.0241	-.0220	-.0270	-.0244	-.0200	-.0151	-.0103	-.0085	-.0074	-.0056	-.0058	-.0035	-.0006	.0026	.0039	.0039
71		-.0887	-.0778	-.0687	-.0655	-.0630	-.0339	-.0269	-.0194	-.0138	-.0088	-.0071	-.0065	-.0058	-.0061	-.0046	-.0022	.0012	.0025	.0028
72		-.1216	-.1136	-.0986	-.0887	-.0863	-.0290	-.0216	-.0148	-.0109	-.0069	-.0046	-.0041	-.0038	-.0048	-.0039	-.0025	-.0002	.0011	.0012
73	RF	.4328	.5042	.5829	.5573	.5032	.1867	.1409	.1062	.0769	.0480	.0388	.0307	.0230	.0215	.0155	.0133	.0121	.0145	.0178
74		.5882	.6269	.5962	.5445	.5133	.1852	.1605	.1353	.1171	.1040	.0913	.0828	.0746	.0720	.0630	.0519	.0262	.0209	.0207
75		.5561	.5936	.5571	.5092	.4776	.1778	.1516	.1282	.1111	.0970	.0848	.0740	.0646	.0634	.0535	.0319	.0215	.0192	.0208
76		.4247	.4964	.5629	.5283	.4818	.1848	.1342	.1025	.0763	.0426	.0328	.0249	.0172	.0152	.0123	.0270	.0132	.0156	.0182
11	FL	-.1825	-.1828	-.1827	-.1819	-.1780	-.0326	-.0175	-.0038	.0033	.0109	.0133	.0157	.0168	.0170	.0201	.0230	.0222	.0193	.0379
13		-.1869	-.1873	-.1872	-.1865	-.1840	-.0368	-.0220	-.0078	.0017	.0085	.0099	.0116	.0118	.0118	.0115	.0052	.0281	.0542	
14		-.1573	-.1575	-.1577	-.1574	-.1568	-.0395	-.0245	-.0095	-.0002	.0075	.0093	.0107	.0116	.0112	.0062	.0046	.0599		
15		-.1186	-.1189	-.1190	-.1191	-.1202	-.0419	-.0267	-.0117	-.0022	.0060	.0082	.0104	.0081	.0066	.0036	.0353			
16		-.0816	-.0820	-.0824	-.0827	-.0834	-.0413	-.0270	-.0125	-.0037	.0048	.0070	.0084	.0049	.0043	.0101	.0786			
17		-.0498	-.0499	-.0508	-.0509	-.0509	-.0374	-.0245	-.0114	-.0042	.0041	.0065	.0066	.0052	.0063	.0463				
18		-.0233	-.0243	-.0245	-.0246	-.0223	-.0292	-.0188	-.0084	-.0025	.0047	.0078	.0067	.0139	.0222	.0984				
20		.0130	.0118	.0119	.0123	.0242	-.0094	-.0038	.0021	.0052	.0112	.0102	.0170	.1111						
22		.0379	.0398	.0408	.0429	.0756	.0180	.0189	.0205	.0202	.0200	.0255	.1226							
23		.0461	.0478	.0490	.0562	.1016	.0304	.0290	.0278	.0264	.0228	.0655								
24		.0517	.0535	.0540	.0744	.1280	.0431	.0395	.0353	.0324	.0321	.1305								
25		.0547	.0577	.0579	.1009	.1537	.0556	.0492	.0431	.0378	.0712									
26		.0566	.0592	.0593	.1339	.1745	.0678	.0594	.0511	.0416	.1399									
27		.0568	.0590	.0594	.1666	.1943	.0792	.0685	.0576	.0443										
28		.0555	.0583	.0593	.1938	.2122	.0917	.0761	.0609	.0512										
29		.0547	.0573	.0610	.2142	.2309	.1008	.0848	.0637	.0836										
32		.0524	.0522	.1820	.2648	.2990	.1248	.0942	.1634											
33		.0502	.0499	.2276	.2892	.3209	.1260	.1189												
34		.0488	.0495	.2545	.3120	.3357	.1342	.1878												
35		.0489	.0492	.2731	.3344	.3620	.2251													
36		.0486	.0485	.2902	.3562	.4564														
37		.0479	.0482	.3106	.3879															
38		.0467	.0471	.3348	.4806															
39		.0459	.0468	.3575																
40		.0436	.0661	.3792																
41		.0423	.1569	.4040																
42		.0409	.2466	.5131																
43		.0392	.2874																	
44		.0371	.3146																	
45		.0368	.3370																	
46		.0340	.3605																	
47		.0320	.3759																	
48		.0358	.3785																	
49		.0935	.4007																	
50		.2213	.5453																	
51		.2787																		
52		.3101																		
53		.3367																		
54		.3559																		
55		.3570																		
56		.3423																		
57		.3741																		

Table I. Concluded

(c) $M_\infty = 2.86$

Orif	Loc	C_p for l/h of -								
		24	20	16	12	11.6	11.2	8	4	2
1	FP	.0018	.0011	.0001	.0019	.0005	.0018	.0011	.0015	.0016
2		.0027	.0007	.0010	.0007	.0018	.0014	-.0007	.0007	-.0008
3		.0020	.0001	.0003	-.0004	-.0005	.0011	-.0009	.0009	-.0001
4		.0006	.0007	.0014	.0006	.0007	.0008	-.0002	.0007	-.0002
5	FF	-.1263	-.1262	-.1264	-.1262	-.1259	-.0071	.0088	.0209	.0201
6	FF	-.1284	-.1285	-.1284	-.1284	-.1281	-.0080	.0069	.0198	.0195
64	RF	.3596	.3786	.3932	.3305	.3222	.1076	.0832	.0533	.0300
65		.3379	.3568	.3684	.3095	.3006	.0950	.0705	.0443	.0219
66		.3289	.3459	.3509	.2971	.2871	.0954	.0691	.0368	.0134
67		.3439	.3447	.3409	.2890	.2811	.1278	.1020	.0596	.0323
68		.3639	.3303	.3047	.2739	.2688	.1881	.1768	.1315	.1217
69	RP	.0522	.0559	.0506	.0431	.0426	.0057	.0050	.0060	.0052
70		.0122	.0143	.0150	.0121	.0140	-.0065	-.0069	-.0004	.0017
71		-.0170	-.0138	-.0116	-.0103	-.0090	-.0125	-.0085	-.0038	.0021
72		-.0381	-.0344	-.0294	-.0281	-.0274	-.0129	-.0085	-.0047	-.0004
73	RF	.5328	.6675	.9431	.6835	.6239	.0801	.0335	.0096	.0074
74		.4422	.4216	.3613	.3220	.3161	.1033	.0692	.0399	.0114
75		.3872	.3796	.3405	.3031	.3061	.0955	.0662	.0336	.0124
76		.5293	.6476	.7903	.5783	.5351	.0787	.0324	.0103	.0082
11	FL	-.1272	-.1276	-.1273	-.1275	-.1272	-.0121	.0068	.0125	.0134
13		-.1233	-.1234	-.1232	-.1234	-.1231	-.0140	.0039	.0083	.0178
14		-.0986	-.0978	-.0987	-.0989	-.0990	-.0161	.0024	.0029	.0355
15		-.0698	-.0696	-.0685	-.0709	-.0703	-.0174	.0013	.0000	
16		-.0468	-.0470	-.0471	-.0489	-.0478	-.0173	-.0000	.0034	
17		-.0306	-.0310	-.0311	-.0318	-.0306	-.0145	-.0008	.0314	
18		-.0160	-.0156	-.0159	-.0167	-.0141	-.0096	.0004	.0608	
20		.0021	.0023	.0014	.0098	.0337	.0014	.0061		
22		.0148	.0138	.0128	.0929	.1212	.0173	.0130		
23		.0195	.0171	.0175	.1324	.1483	.0236	.0138		
24		.0229	.0202	.0206	.1574	.1612	.0301	.0209		
25		.0233	.0236	.0241	.1736	.1739	.0357	.0523		
26		.0267	.0252	.0258	.1835	.1783	.0415	.0962		
27		.0284	.0271	.0275	.1874	.1893	.0465			
28		.0299	.0281	.0289	.1961	.2001	.0490			
29		.0304	.0279	.0325	.2067	.2180	.0508			
32		.0314	.0295	.1730	.2563	.2778	.1265			
33		.0305	.0279	.1961	.2984	.3248				
34		.0277	.0283	.2106	.3375					
35		.0281	.0271	.2190						
36		.0274	.0267	.2220						
37		.0272	.0258	.2320						
38		.0268	.0276	.2474						
39		.0268	.0492	.2719						
40		.0267	.1134	.2973						
41		.0242	.1727	.3508						
42		.0244	.2032	.3998						
43		.0232	.2171							
44		.0237	.2315							
45		.0246	.2411							
46		.0243	.2622							
47		.0279	.2791							
48		.0657	.2993							
49		.1496	.3355							
50		.1919	.3871							
51		.2129								
52		.2278								
53		.2430								
54		.2605								
55		.2646								
56		.2760								
57		.3069								

Table II. Pressure Coefficients for $h = 1.0$ in. and $w = 2.5$ in.

(a) $M_\infty = 1.50$

Orif	Loc	C_p for l/h of -															
		12	11.5	11	10	9	8	7.5	7	6	5	4.8	4	3	2	1.5	1
1	FP	.0017	.0042	.0064	.0061	.0043	.0041	.0065	.0042	.0028	.0041	.0045	.0051	.0046	.0039	.0027	.0041
2	↓	.0036	.0068	.0082	.0078	.0069	.0053	.0093	.0061	.0071	.0056	.0071	.0077	.0056	.0072	.0056	.0070
3	↓	.0076	.0118	.0115	.0121	.0115	.0095	.0107	.0095	.0117	.0097	.0105	.0111	.0104	.0111	.0099	.0112
4	↓	.0095	.0117	.0127	.0113	.0126	.0105	.0125	.0101	.0111	.0112	.0112	.0121	.0109	.0116	.0108	.0115
5	FF	-.1869	-.1779	-.0045	.0087	.0127	.0146	.0179	.0208	.0272	.0342	.0386	.0514	.0708	.0587	.0346	.0320
6	↓	-.1858	-.1772	-.0055	.0074	.0120	.0146	.0173	.0190	.0253	.0340	.0365	.0493	.0674	.0457	.0286	.0228
7	↓	-.1848	-.1759	-.0094	.0054	.0124	.0146	.0185	.0196	.0263	.0341	.0366	.0474	.0590	.0415	.0277	.0324
62	RF	.6862	.6589	.2527	.2336	.2412	.2735	.3018	.3027	.2933	.2481	.2451	.2515	.2106	.1520	.0709	.0428
63	↓	.6620	.6368	.2017	.1746	.1759	.1959	.2093	.2192	.2020	.1641	.1624	.1598	.1240	.0835	.0415	.0187
64	↓	.7594	.7228	.2256	.2028	.2109	.2497	.2651	.2867	.2629	.2191	.2133	.2138	.1565	.0875	.0415	.0145
65	↓	.8162	.7586	.2491	.2411	.2486	.2955	.3149	.3342	.3269	.2774	.2689	.2707	.1996	.1064	.0487	.0223
66	↓	.8555	.7974	.2870	.2872	.3157	.3597	.3903	.4097	.4145	.3543	.3523	.3566	.2664	.1528	.0760	.0392
67	↓	.8666	.7998	.3164	.3412	.3696	.4317	.4631	.4916	.4888	.4337	.4316	.4456	.3391	.2253	.1354	.0740
69	RP	-.3399	-.3292	-.1026	-.0695	-.0623	-.0654	-.0686	-.0682	-.0678	-.0620	-.0598	-.0557	-.0403	-.0209	-.0081	.0026
70	↓	-.3357	-.3228	-.0792	-.0516	-.0465	-.0567	-.0647	-.0708	-.0681	-.0536	-.0484	-.0489	-.0362	-.0177	-.0038	.0027
71	↓	-.2946	-.2739	-.0462	-.0249	-.0187	-.0199	-.0275	-.0298	-.0289	-.0213	-.0192	-.0194	-.0143	-.0082	.0005	.0038
72	↓	-.1510	-.1414	-.0269	-.0126	-.0058	-.0016	-.0076	-.0064	-.0089	-.0080	-.0066	-.0059	-.0043	-.0007	.0039	.0062
73	RF	.7180	.7002	.2904	.1880	.1547	.1449	.1400	.1364	.1183	.1102	.1019	.0988	.0898	.0487	.0263	.0268
74	↓	.8993	.8534	.3076	.3066	.3180	.3564	.3742	.3961	.3726	.3061	.2990	.3088	.2717	.1569	.0608	.0302
75	↓	.8484	.7958	.3147	.2935	.3098	.3538	.3692	.3913	.3732	.3063	.2954	.3173	.2743	.1565	.0607	.0307
76	↓	.6920	.6728	.2763	.1820	.1461	.1398	.1351	.1341	.1149	.1072	.1062	.1000	.0964	.0504	.0275	.0271
77	↓	.7082	.6843	.2650	.2320	.2367	.2661	.2744	.2841	.2677	.2247	.2171	.2211	.1848	.1148	.0749	.0452
78	↓	.6736	.6530	.2417	.2156	.2188	.2462	.2584	.2685	.2514	.2140	.2100	.2129	.1803	.1292	.0779	.0451
79	↓	.6610	.6413	.2406	.2169	.2163	.2485	.2560	.2680	.2516	.2095	.2107	.2136	.1811	.1288	.0771	.0443
80	↓	.6704	.6520	.2570	.2302	.2256	.2544	.2606	.2703	.2568	.2168	.2121	.2206	.1868	.1105	.0718	.0459
11	FL	-.1925	-.1856	-.0136	.0034	.0105	.0146	.0147	.0175	.0233	.0281	.0305	.0411	.0492	.0313	.0240	.0302
13	↓	-.2000	-.1924	-.0183	.0014	.0072	.0132	.0110	.0146	.0187	.0163	.0166	.0218	.0298	-.0083	.0158	.0356
14	↓	-.1988	-.1932	-.0194	-.0003	.0078	.0125	.0106	.0141	.0157	.0164	.0168	.0243	.0370	.0137	.0241	.0449
15	↓	-.1991	-.1928	-.0196	-.0005	.0074	.0127	.0102	.0135	.0161	.0195	.0205	.0272	.0419	.0338	.0552	
16	↓	-.1991	-.1926	-.0193	-.0002	.0066	.0106	.0080	.0109	.0165	.0214	.0227	.0299	.0287	.0562	.0802	
17	↓	-.2011	-.1929	-.0189	-.0010	.0067	.0113	.0082	.0110	.0150	.0209	.0226	.0311	-.0012	.1438		
18	↓	-.2025	-.1948	-.0187	-.0011	.0062	.0095	.0077	.0103	.0155	.0218	.0233	.0310	-.0077	.1804		
19	↓	-.1995	-.1929	-.0196	-.0017	.0058	.0077	.0067	.0089	.0156	.0225	.0253	.0284	.0146			
20	↓	-.1965	-.1896	-.0193	-.0027	.0043	.0072	.0051	.0088	.0158	.0225	.0235	.0163	.0591			
22	↓	-.1677	-.1633	-.0144	.0032	.0068	.0077	.0122	.0124	.0183	.0227	.0227	.0124	.2655			
23	↓	-.1475	-.1438	-.0156	.0015	.0055	.0054	.0109	.0121	.0207	.0204	.0180	.0366				
24	↓	-.1213	-.1186	-.0166	.0005	.0045	.0044	.0105	.0139	.0222	.0168	.0158	.0831				
25	↓	-.0912	-.0922	-.0153	-.0018	.0037	.0062	.0127	.0147	.0226	.0168	.0196	.2032				
26	↓	-.0609	-.0620	-.0150	-.0011	.0036	.0074	.0139	.0182	.0250	.0240	.0412	.3195				
27	↓	-.0279	-.0317	-.0133	-.0008	.0038	.0099	.0166	.0204	.0271	.0489	.0756					
28	↓	.0028	-.0022	-.0111	-.0001	.0058	.0122	.0197	.0238	.0323	.0891	.1661					
29	↓	.0336	.0274	-.0076	.0029	.0078	.0167	.0235	.0292	.0376	.1999	.3264					
30	↓	.0625	.0561	-.0037	.0042	.0102	.0212	.0278	.0351	.0471	.3150						
31	↓	.0858	.0856	.0044	.0101	.0142	.0255	.0359	.0414	.0685							
32	↓	.1061	.1109	.0101	.0133	.0199	.0302	.0411	.0465	.1129							
33	↓	.1255	.1336	.0167	.0184	.0230	.0353	.0465	.0521	.2491							
34	↓	.1411	.1531	.0233	.0218	.0294	.0400	.0521	.0576	.3618							
35	↓	.1540	.1732	.0312	.0281	.0347	.0455	.0534	.0783								
36	↓	.1649	.1918	.0391	.0342	.0383	.0473	.0583	.1219								
37	↓	.1739	.2127	.0483	.0390	.0430	.0478	.0750	.2431								
38	↓	.1849	.2330	.0565	.0471	.0479	.0533	.1158	.3700								
39	↓	.2002	.2595	.0652	.0503	.0481	.0688	.2264									
40	↓	.2246	.2876	.0714	.0569	.0502	.1113	.3561									
41	↓	.2525	.3198	.0801	.0604	.0509	.2135										
42	↓	.2862	.3503	.0897	.0645	.0519	.3342										
43	↓	.3258	.3781	.0985	.0674	.0683											
44	↓	.3608	.4119	.1039	.0673	.1010											
45	↓	.3971	.4403	.1094	.0658	.1937											
46	↓	.4270	.4609	.1110	.0693	.2956											
47	↓	.4531	.4820	.1185	.0778												
48	↓	.4799	.5059	.1222	.1116												
49	↓	.4977	.5241	.1206	.1927												
50	↓	.5115	.5391	.1227	.2773												
51	↓	.5322	.5538	.1233													
52	↓	.5474	.5719	.1451													
53	↓	.5631	.5754	.2170													
54	↓	.5837	.5391	.2871													
55	↓	.5784	.5996														
56	↓	.5329	.7299														
57	↓	.6102															

Table II. Continued

(b) $M_\infty = 2.16$

Orif	Loc	C_p for l/h of -																
		12	11.5	11	10.5	10	9	8	7.5	7	6	5	4.8	4	3	2	1.5	1
1	FP	.0016	.0019	.0023	.0022	.0019	.0014	.0019	.0019	.0016	.0014	.0016	.0020	.0019	.0018	.0021	.0020	.0017
2		.0017	.0025	.0031	.0026	.0024	.0021	.0025	.0024	.0019	.0016	.0022	.0021	.0027	.0022	.0022	.0018	.0021
3		.0012	.0015	.0020	.0018	.0018	.0011	.0013	.0012	.0009	.0008	.0013	.0014	.0015	.0015	.0010	.0008	.0011
4		.0030	.0039	.0041	.0040	.0039	.0037	.0038	.0043	.0037	.0034	.0032	.0038	.0041	.0040	.0031	.0036	.0033
5	FF	-.1711	-.1709	-.1704	-.1708	.0073	.0085	.0104	.0116	.0123	.0142	.0178	.0187	.0230	.0262	.0175	.0132	.0131
6		-.1729	-.1723	-.1719	-.1723	.0069	.0083	.0103	.0114	.0123	.0147	.0171	.0185	.0237	.0249	.0161	.0117	.0087
7		-.1647	-.1640	-.1637	-.1643	.0053	.0082	.0097	.0114	.0124	.0142	.0166	.0179	.0224	.0231	.0158	.0119	.0170
62	RF	.8155	.8135	.7977	.7739	.1448	.1331	.1304	.1278	.1227	.1140	.1082	.1072	.1090	.0846	.0472	.0350	.0242
63		.7188	.7177	.7153	.6935	.1035	.0929	.0898	.0876	.0829	.0746	.0687	.0664	.0657	.0463	.0220	.0190	.0099
64		.9787	.9693	.9269	.8651	.1299	.1199	.1159	.1139	.1079	.0965	.0864	.0834	.0818	.0529	.0216	.0185	.0033
65		1.1413	1.1256	1.0754	1.0064	.1619	.1535	.1493	.1449	.1389	.1250	.1110	.1081	.1065	.0701	.0291	.0209	.0076
66		1.3253	1.2808	1.2268	1.1532	.2101	.2041	.2032	.1976	.1904	.1721	.1537	.1489	.1449	.1020	.0532	.0356	.0200
67		1.4494	1.4052	1.3808	1.2885	.2707	.2700	.2702	.2630	.2524	.2297	.2023	.1960	.1880	.1420	.1059	.0781	.0485
69	RP	-.0797	-.0721	-.0671	-.0563	-.0171	-.0150	-.0143	-.0142	-.0172	-.0181	-.0129	-.0120	-.0063	-.0034	.0023	.0052	.0077
70		-.1168	-.1129	-.1114	-.1014	-.0276	-.0237	-.0222	-.0217	-.0239	-.0234	-.0194	-.0188	-.0156	-.0104	-.0005	.0025	.0061
71		-.1496	-.1495	-.1499	-.1387	-.0238	-.0195	-.0168	-.0157	-.0175	-.0174	-.0138	-.0142	-.0133	-.0085	-.0004	.0011	.0039
72		-.1765	-.1762	-.1759	-.1632	-.0153	-.0125	-.0106	-.0094	-.0115	-.0112	-.0078	-.0081	-.0080	-.0043	.0015	.0023	.0034
73	RF	.7729	.8126	.8355	.8337	.1006	.0716	.0612	.0584	.0550	.0512	.0454	.0426	.0408	.0229	.0146	.0063	.0113
74		1.2261	1.2325	1.1970	1.1318	.1970	.1741	.1628	.1574	.1519	.1401	.1364	.1388	.1594	.1113	.0341	.0188	.0153
75		1.1751	1.1990	1.1357	1.0669	.1843	.1610	.1543	.1473	.1425	.1322	.1294	.1297	.1501	.1045	.0339	.0196	.0157
76		.7515	.7729	.7927	.7869	.0914	.0678	.0582	.0552	.0525	.0476	.0428	.0398	.0410	.0231	.0144	.0064	.0123
77		.7991	.8118	.8036	.7778	.1415	.1246	.1169	.1129	.1080	.0994	.0925	.0923	.0963	.0629	.0337	.0270	.0244
78		.7574	.7541	.7606	.7348	.1342	.1197	.1122	.1088	.1046	.0972	.0911	.0902	.0927	.0677	.0442	.0354	.0242
79		.7431	.7500	.7444	.7216	.1279	.1141	.1083	.1061	.1021	.0946	.0897	.0875	.0908	.0655	.0433	.0353	.0243
80		.7784	.7783	.7845	.7473	.1331	.1160	.1101	.1073	.1027	.0943	.0883	.0863	.0892	.0598	.0324	.0257	.0246
11	FL	-.1749	-.1748	-.1744	-.1747	.0044	.0076	.0091	.0101	.0108	.0133	.0158	.0160	.0203	.0205	.0132	.0097	.0135
13		-.1820	-.1822	-.1812	-.1820	.0032	.0065	.0056	.0047	.0039	.0041	.0058	.0059	.0079	.0085	.0070	.0024	.0228
14		-.1835	-.1835	-.1823	-.1834	.0025	.0060	.0050	.0041	.0030	.0033	.0049	.0053	.0071	.0123	-.0034	.0094	.0246
15		-.1844	-.1848	-.1836	-.1846	.0022	.0061	.0050	.0048	.0042	.0044	.0057	.0066	.0096	.0164	-.0023	.0278	
16		-.1832	-.1837	-.1824	-.1836	.0020	.0053	.0048	.0047	.0049	.0056	.0080	.0078	.0115	.0132	.0077	.0372	
17		-.1780	-.1784	-.1772	-.1785	.0019	.0054	.0048	.0054	.0056	.0069	.0091	.0095	.0140	-.0021	.0403		
18		-.1679	-.1682	-.1670	-.1683	.0016	.0048	.0046	.0054	.0063	.0079	.0098	.0109	.0154	-.0062	.0537		
19		-.1525	-.1532	-.1520	-.1532	.0016	.0039	.0040	.0055	.0063	.0088	.0104	.0113	.0137	.0059			
20		-.1358	-.1362	-.1351	-.1362	.0010	.0036	.0041	.0053	.0061	.0090	.0114	.0119	.0069	.0265			
22		-.0975	-.0962	-.0980	-.0922	.0042	.0073	.0091	.0105	.0089	.0105	.0165	.0163	.0027	.1066			
23		-.0761	-.0746	-.0759	-.0705	.0032	.0058	.0083	.0097	.0082	.0102	.0148	.0108	.0135				
24		-.0538	-.0524	-.0538	-.0488	.0029	.0052	.0078	.0096	.0082	.0106	.0104	.0051	.0382				
25		-.0331	-.0316	-.0330	-.0277	.0021	.0048	.0077	.0099	.0087	.0113	.0050	.0078	.0965				
26		-.0134	-.0121	-.0133	-.0081	.0016	.0043	.0079	.0101	.0092	.0114	.0099	.0187	.1368				
27		.0042	.0057	.0046	.0096	.0019	.0039	.0080	.0106	.0102	.0114	.0215	.0369					
28		.0199	.0214	.0203	.0254	.0024	.0044	.0085	.0119	.0116	.0088	.0409	.0829					
29		.0334	.0346	.0339	.0394	.0031	.0048	.0096	.0130	.0125	.0065	.0976	.1393					
30		.0450	.0462	.0457	.0513	.0045	.0058	.0109	.0148	.0138	.0098	.1363						
31		.0587	.0592	.0596	.0627	.0057	.0073	.0132	.0160	.0167	.0233							
32		.0666	.0675	.0686	.0747	.0078	.0090	.0148	.0173	.0159	.0427							
33		.0730	.0736	.0750	.0876	.0104	.0111	.0169	.0182	.0149	.0988							
34		.0776	.0791	.0823	.1067	.0121	.0133	.0185	.0183	.0176	.1444							
35		.0816	.0825	.0912	.1325	.0146	.0155	.0198	.0177	.0275								
36		.0842	.0863	.1032	.1701	.0176	.0179	.0194	.0201	.0483								
37		.0865	.0910	.1264	.2137	.0206	.0199	.0189	.0297	.1040								
38		.0885	.1001	.1638	.2597	.0237	.0216	.0213	.0504	.1550								
39		.0915	.1236	.2111	.3047	.0266	.0229	.0297	.1074									
40		.0970	.1605	.2605	.3484	.0296	.0235	.0502	.1606									
41		.1141	.2142	.3113	.3927	.0312	.0226	.1048										
42		.1542	.2725	.3562	.4324	.0336	.0248	.1639										
43		.2199	.3226	.3959	.4720	.0349	.0338											
44		.2915	.3660	.4353	.5047	.0350	.0547											
45		.3444	.3983	.4786	.5322	.0340	.1097											
46		.3793	.4324	.5134	.5528	.0367	.1674											
47		.4057	.4701	.5442	.5645	.0444												
48		.4360	.5129	.5740	.5682	.0653												
49		.4627	.5390	.5865	.5253	.1254												
50		.4983	.5681	.5782	.5255	.1774												
51		.5327	.5866	.5348	.6853													
52		.5595	.5812	.5214	.8839													
53		.5803	.5240	.6980														
54		.5694	.5127	.9239														
55		.4982	.7004															
56		.4930	.9606															
57		.7150																

Table II. Concluded

(c) $M_{\infty} = 2.86$

Orif	Loc	C_p for l/h of -								
		12	11	10.5	10	8	6	4	2	1
1	FP	.0009	.0031	.0023	.0040	.0030	.0020	.0034	.0010	.0027
2		-.0008	.0007	.0015	.0017	.0011	.0016	.0010	.0010	.0001
3		-.0009	-.0001	-.0004	.0021	.0011	.0011	.0020	.0012	.0007
4		-.0010	.0008	.0015	.0028	.0021	.0016	.0016	.0007	.0012
5	FF	-.1309	-.1290	-.1287	.0069	.0074	.0090	.0137	.0144	.0065
6		-.1325	-.1306	-.1305	.0059	.0076	.0088	.0146	.0123	.0059
7		-.1289	-.1269	-.1272	.0023	.0071	.009	.0133	.0104	.0122
62	RF	.6664	.7220	.7117	.0879	.0785	.0703	.0590	.0234	.0112
63		.5763	.6007	.6136	.0643	.0536	.0456	.0359	.0084	.0039
64		.7360	.8249	.8210	.0772	.0696	.0586	.0391	.0035	-.0037
65		.8805	.9595	.9937	.0975	.0948	.0805	.0558	.0080	-.0023
66		1.0317	1.1860	1.1944	.1333	.1387	.1168	.0799	.0287	.0070
67		1.1824	1.3475	1.3945	.1744	.1955	.1634	.1148	.0766	.0298
69	RP	.0467	.0424	.0424	-.0015	-.0011	-.0002	.0028	.0041	.0056
70		-.0159	-.0252	-.0264	-.0104	-.0102	-.0117	-.0095	-.0006	.0054
71		-.0573	-.0660	-.0671	-.0104	-.0100	-.0123	-.0097	-.0017	.0010
72		-.0830	-.0889	-.0887	-.0152	-.0096	-.0097	-.0077	-.0018	.0002
73	RF	.8363	.8409	.8561	.0809	.0508	.0325	.0210	.0173	.0031
74		1.3366	1.4297	1.4459	.1259	.0989	.0845	.0808	.0210	.0058
75		1.3441	1.3821	1.3905	.1304	.0962	.0859	.0783	.0190	.0054
76		.8434	.8082	.8172	.0837	.0421	.0281	.0215	.0160	.0023
77		.6911	.7163	.7193	.0846	.0666	.0564	.0439	.0206	.0093
78		.6328	.6615	.6813	.0803	.0675	.0569	.0460	.0230	.0101
79		.6308	.6639	.6359	.0823	.0628	.0572	.0467	.0196	.0093
80		.7101	.7310	.7383	.1667	.1490	.1426	.1313	.1159	.1096
11	FL	-.1326	-.1304	-.1310	.0008	.0060	.0085	.0112	.0099	.0082
13		-.1359	-.1337	-.1340	-.0012	.0031	.0009	.0044	.0048	.0165
14		-.1365	-.1342	-.1344	-.0015	.0039	-.0002	.0018	-.0025	.0141
15		-.1344	-.1323	-.1322	-.0010	.0031	-.0003	.0048	-.0040	
16		-.1275	-.1255	-.1255	-.0025	.0038	.0027	.0061	.0023	
17		-.1167	-.1148	-.1146	-.0029	.0035	.0035	.0073	.0292	
18		-.1029	-.1007	-.1009	-.0010	.0032	.0057	.0092	.0316	
19		-.0893	-.0874	-.0872	-.0020	.0021	.0046	.0088		
20		-.0735	-.0715	-.0719	-.0024	.0009	.0063	.0065		
22		-.0412	-.0420	-.0416	.0004	.0041	.0072	.0042		
23		-.0302	-.0312	-.0296	-.0019	.0020	.0074	.0078		
24		-.0181	-.0200	-.0192	-.0008	.0025	.0072	.0246		
25		-.0084	-.0096	-.0077	-.0002	.0028	.0078	.0625		
26		.0021	-.0003	.0015	-.0006	.0023	.0071	.0740		
27		.0101	.0072	.0082	-.0008	.0025	.0064			
28		.0160	.0170	.0163	-.0005	.0034	.0057			
29		.0230	.0218	.0212	.0005	.0030	.0041			
30		.0271	.0279	.0271	.0019	.0035	.0055			
31		.0303	.0305	.0293	.0038	.0050	.0109			
32		.0345	.0310	.0362	.0056	.0067	.0268			
33		.0361	.0343	.0363	.0085	.0088	.0659			
34		.0357	.0354	.0417	.0111	.0105	.0905			
35		.0372	.0358	.0517	.0123	.0105				
36		.0369	.0368	.0734	.0140	.0110				
37		.0342	.0459	.1150	.0149	.0110				
38		.0351	.0676	.1607	.0168	.0111				
39		.0345	.1160	.2044	.0188	.0156				
40		.0340	.1700	.2397	.0210	.0296				
41		.0348	.2187	.2762	.0225	.0693				
42		.0486	.2625	.3161	.0222	.0993				
43		.1005	.2981	.3485	.0237					
44		.1769	.3285	.3834	.0244					
45		.2399	.3634	.4205	.0250					
46		.2902	.3872	.4384	.0245					
47		.3213	.4161	.4468	.0282					
48		.3512	.4452	.4474	.0418					
49		.3725	.4478	.4255	.0804					
50		.3916	.4336	.4425	.1069					
51		.4157	.4118	.6663						
52		.4320	.4536	.8263						
53		.4335	.6623							
54		.4141	.8066							
55		.3892								
56		.4421								
57		.6389								

Table III. Pressure Coefficients for $h = 2.0$ in. and $w = 2.5$ in.

(a) $M_\infty = 1.50$

Orif	Loc	C_p for l/h of -							
		6	5	4.8	4	3	2	1.5	1
1	FP	.0052	.0065	.0029	.0034	.0029	.0079	.0019	.0044
2		.0065	.0092	.0068	.0048	.0056	.0102	.0036	.0076
3		.0098	.0161	.0111	.0075	.0098	.0139	.0083	.0112
4		.0136	.0175	.0141	.0095	.0144	.0175	.0097	.0147
5	FF	.0273	.0430	.0410	.0450	.0810	.0917	.0496	.0434
6		.0259	.0400	.0389	.0386	.0748	.0746	.0398	.0287
7		.0269	.0405	.0376	.0380	.0691	.0617	.0222	.0108
8		.0268	.0368	.0380	.0348	.0642	.0755	.0383	.0224
9		.0256	.0362	.0372	.0342	.0584	.0782	.0660	.0720
59	RF	.2719	.2678	.2670	.2520	.2682	.1896	.1269	.0647
60		.1883	.1685	.1729	.1539	.1397	.1023	.0632	.0476
61		.1765	.1487	.1538	.1263	.1037	.0388	.0212	.0153
62		.2747	.2738	.2709	.2407	.2506	.0927	.0182	.0174
64		.4459	.4381	.4252	.3807	.4232	.2619	.0944	.0406
65		.5055	.4875	.4832	.4444	.4940	.3410	.1466	.0571
66		.5705	.5516	.5529	.5253	.5813	.4461	.2487	.1093
67		.6210	.5961	.5997	.5809	.6393	.5321	.3752	.1980
69	RP	-.1049	-.1026	-.1010	-.1005	-.0932	-.0270	-.0211	-.0037
70		-.0665	-.0711	-.0675	-.0640	-.0696	-.0333	-.0119	-.0039
71		-.0204	-.0276	-.0257	-.0208	-.0303	-.0164	-.0006	-.0038
72		-.0003	-.0099	-.0094	-.0032	-.0076	-.0041	.0005	-.0002
73	RF	.2830	.2954	.3364	.3125	.3216	.2475	.1798	.1375
74		.4576	.4739	.4118	.4676	.5860	.3885	.2032	.1002
75		.4711	.5080	.4689	.5115	.6259	.4285	.1623	.1034
76		.2904	.2702	.2488	.2804	.3373	.2498	.0685	.1442
77		.2649	.2645	.2599	.2441	.2399	.0682	.0342	.0051
78		.2488	.2270	.2134	.1655	.1972	.0506	.0234	.0049
79		.2346	.2295	.2288	.1874	.2399	.0501	-.0034	.0061
80		.2664	.2709	.2763	.2415	.2587	.0708	.0017	.0097
81		.2754	.2677	.2579	.2687	.2592	.1345	.0633	.0311
82		.1995	.1910	.1868	.1778	.1737	.1078	.0500	.0333
83		.1951	.1942	.1908	.1777	.1781	.1103	.0550	.0350
84		.2834	.2690	.2639	.2627	.2600	.1389	.0372	.0339
11	FL	.0254	.0274	.0302	.0291	.0452	.0560	.0481	.0529
12		.0224	.0182	.0217	.0193	.0280	.0471	.0320	.0290
13		.0215	.0148	.0170	.0147	.0196	.0404	.0088	.0219
14		.0165	.0097	.0094	.0095	.0143	.0279	.0009	.0108
15		.0163	.0063	.0061	.0084	.0138	.0110	.0059	.0221
16		.0140	.0040	.0052	.0081	.0137	-.0070	.0095	.0519
17		.0145	.0067	.0032	.0081	.0189	-.0174	.0037	.0728
18		.0132	.0073	.0052	.0122	.0237	-.0271	.0035	.0716
19		.0121	.0106	.0093	.0135	.0253	-.0248	.0280	
20		.0114	.0131	.0115	.0155	.0198	-.0241	.0836	
21		.0103	.0153	.0125	.0191	.0147	-.0128	.1699	
22		.0175	.0216	.0191	.0234	.0076	.0192	.1455	
23		.0172	.0229	.0206	.0240	-.0008	.0678		
24		.0163	.0259	.0226	.0235	-.0047	.1456		
25		.0159	.0256	.0240	.0220	-.0087	.2511		
26		.0147	.0257	.0235	.0176	-.0098	.2314		
27		.0141	.0265	.0253	.0145	-.0078			
28		.0139	.0255	.0238	.0129	.0012			
29		.0129	.0223	.0230	.0085	.0138			
30		.0124	.0192	.0207	.0089	.0321			
31		.0115	.0173	.0126	.0106	.0672			
32		.0112	.0164	.0121	.0092	.1470			
33		.0117	.0185	.0123	.0151	.3356			
34		.0121	.0160	.0115	.0167	.3316			
35		.0102	.0167	.0130	.0221				
36		.0103	.0192	.0192	.0292				
37		.0110	.0196	.0219	.0394				
38		.0126	.0228	.0261	.0523				
39		.0146	.0233	.0313	.0753				
40		.0143	.0317	.0382	.1434				
41		.0177	.0321	.0411	.2955				
42		.0193	.0370	.0467	.3267				
43		.0234	.0420	.0558					
44		.0268	.0481	.0630					
45		.0309	.0542	.0779					
46		.0379	.0711	.1256					
47		.0423	.0947	.2357					
48		.0541	.1732	.3836					
49		.0510	.3090						
50		.0562	.3281						
51		.0639							
52		.0719							
53		.0759							
54		.0904							
55		.1128							
56		.1712							
57		.3148							

(b) $M_\infty = 2.16$

Orif	Loc	C_p for l/h of -							
		6	5	4.8	4	3	2	1.5	1
1	FP	.0049	.0051	.0046	.0047	.0042	.0062	.0059	.0046
2		.0051	.0051	.0042	.0049	.0042	.0054	.0064	.0043
3		.0034	.0042	.0029	.0031	.0031	.0037	.0056	.0028
4		.0068	.0074	.0055	.0059	.0061	.0067	.0090	.0058
5	FF	.0170	.0248	.0234	.0314	.0424	.0229	.0191	.0199
6		.0167	.0235	.0224	.0295	.0397	.0210	.0173	.0188
7		.0171	.0234	.0219	.0278	.0377	.0177	.0125	.0052
8		.0176	.0233	.0223	.0272	.0362	.0221	.0156	.0103
59	RF	.1349	.1564	.1445	.1416	.1313	.0474	.0313	.0327
60		.0779	.0890	.0809	.0736	.0675	.0298	.0181	.0293
61		.0578	.0664	.0559	.0473	.0288	.0156	.0063	.0098
62		.1021	.1122	.0987	.0874	.0509	.0157	.0096	.0191
64		.2038	.2324	.2206	.2218	.1669	.0356	.0177	.0244
65		.2510	.2920	.2836	.2895	.2387	.0534	.0279	.0412
66		.3259	.3732	.3695	.3859	.3425	.0990	.0645	.0748
67		.3992	.4524	.4548	.4790	.4710	.1716	.1368	.1368
69	RP	-.0298	-.0270	-.0250	-.0250	.0105	.0056	.0029	.0109
70		-.0362	-.0351	-.0326	-.0311	-.0061	.0002	-.0026	.0043
71		-.0351	-.0330	-.0311	-.0291	-.0166	-.0017	-.0040	.0007
72		-.0267	-.0253	-.0235	-.0214	-.0157	-.0012	-.0029	.0002
73	RF	.3133	.3641	.1506	.3258	.1996	.0972	.0543	.0718
74		.4128	.5074	.2266	.5683	.3536	.0959	.0525	.0661
75		.2218	.2296	.4881	.2933	.3237	.0956	.0357	.0679
76		.1524	.1462	.3383	.3408	.2124	.1055	.0209	.0742
77		.1014	.1580	.1476	.1418	.0609	.0153	.0132	.0081
78		.0702	.1568	.1460	.0781	.0392	.0127	.0090	.0104
79		.0673	.0644	.0596	.0547	.0408	.0143	.0044	.0113
80		.1326	.1576	.1053	.1571	.0620	.0182	.0052	.0082
81		.1232	.1343	.1317	.1300	.0960	.0352	.0222	.0256
82		.0868	.1011	.0952	.0924	.0712	.0310	.0199	.0273
83		.0871	.1020	.0982	.0927	.0731	.0326	.0171	.0291
84		.1147	.1502	.1528	.1305	.0954	.0361	.0054	.0259
11	FL	.0157	.0185	.0190	.0215	.0278	.0169	.0148	.0256
12		.0139	.0146	.0147	.0154	.0216	.0151	.0123	.0198
13		.0117	.0111	.0114	.0115	.0157	.0143	.0068	.0091
14		.0091	.0070	.0073	.0077	.0119	.0104	.0007	.0075
15		.0067	.0036	.0044	.0051	.0094	.0054	-.0022	.0160
16		.0043	.0022	.0034	.0042	.0104	.0009	-.0025	.0308
17		.0043	.0010	.0024	.0047	.0136	-.0018	.0001	.0397
18		.0037	.0006	.0036	.0053	.0173	-.0038	.0035	.0392
19		.0032	.0021	.0037	.0068	.0209	-.0022	.0136	
20		.0033	.0036	.0052	.0084	.0226	-.0014	.0293	
21		.0042	.0056	.0072	.0101	.0200	.0016	.0446	
22		.0039	.0127	.0129	.0159	.0174	.0120	.0402	
23		.0053	.0140	.0141	.0177	.0073	.0246		
24		.0053	.0162	.0158	.0196	-.0011	.0462		
25		.0062	.0175	.0160	.0208	-.0078	.0667		
26		.0063	.0191	.0164	.0217	-.0122	.0594		
27		.0063	.0193	.0170	.0215	-.0127			
28		.0064	.0187	.0158	.0196	-.0076			
29		.0059	.0173	.0153	.0160	.0037			
30		.0068	.0171	.0147	.0104	.0212			
31		.0111	.0133	.0131	.0066	.0447			
32		.0115	.0128	.0126	.0019	.0889			
33		.0115	.0138	.0125	.0024	.1728			
34		.0119	.0139	.0118	.0016	.1587			
35		.0115	.0161	.0115	.0047				
36		.0117	.0189	.0142	.0112				
37		.0100	.0166	.0095	.0112				
38		.0088	.0169	.0089	.0181				
39		.0090	.0154	.0077	.0328				
40		.0084	.0146	.0089	.0826				
41		.0082	.0126	.0112	.1884				
42		.0087	.0133	.0156	.1932				
43		.0104	.0168	.0206					
44		.0118	.0209	.0275					
45		.0110	.0261	.0375					
46		.0131	.0343	.0701					
47		.0116	.0501	.1472					
48		.0134	.0981	.2174					
49		.0115	.1952						
50		.0124	.1961						
51		.0137							
52		.0159							
53		.0207							
54		.0290							
55		.0450							
56		.0841							
57		.1709							

Table IV. Pressure Coefficients for $h = 2.5$ in. and $w = 2.5$ in.

(a) $M_\infty = 1.50$

Orif	Loc	C_p for l/h of -					
		4.8	4	3	2	1.5	1
1	FP	.0030	.0058	.0057	.0064	.0052	.0070
2		.0049	.0085	.0082	.0093	.0080	.0098
3		.0075	.0112	.0105	.0106	.0099	.0113
4		.0074	.0103	.0144	.0158	.0099	.0122
5	FF	.0300	.0424	.0734	.1238	.0474	.0430
6		.0285	.0398	.0634	.0996	.0407	.0334
7		.0288	.0388	.0571	.0725	.0265	.0176
8		.0272	.0370	.0502	.0849	.0237	.0128
9		.0279	.0352	.0476	.1305	.0421	.0241
10		.0276	.0323	.0422	.1213	.0497	.0545
58	RF	.2973	.2913	.2883	.2431	.0810	.0775
59		.1939	.1708	.1349	.0915	.0288	.0230
60		.1951	.1662	.1233	.0368	.0089	.0137
61		.2178	.1781	.1359	.0201	.0023	.0109
63		.2827	.2473	.2299	.1033	.0129	.0139
62		.3328	.3090	.3047	.2096	.0254	.0224
64		.4293	.4074	.4269	.3876	.0497	.0503
65		.4701	.4521	.4857	.4876	.0741	.0856
66		.5211	.5129	.5520	.5730	.1282	.1584
67		.5604	.5397	.6088	.6465	.2143	.2623
69	RP	-.1095	-.1050	-.1034	-.0473	-.0095	-.0132
70		-.0751	-.0733	-.0714	-.0458	-.0168	-.0129
71		-.0308	-.0335	-.0295	-.0210	-.0069	-.0065
72		-.0096	-.0142	-.0092	-.0102	.0025	-.0033
73	RF	.3412	.4291	.2404	.2780	.2586	.1218
74		.6081	.6596	.3231	.5215	.1877	.1517
75		.4768	.3892	.6224	.5753	.1760	.1537
76		.3932	.4000	.5269	.3458	.2649	.1319
77		.3406	.2817	.2508	.1064	.0315	.0215
78		.3358	.3200	.2591	.1490	.0428	.0184
79		.3172	.3011	.3390	.0935	.0189	.0124
81		.2633	.2667	.2523	.0899	.0221	.0104
82		.2357	.1758	.1876	.0394	.0134	.0082
83		.2217	.2050	.1815	.0359	.0125	.0091
84		.2810	.2887	.2384	.0641	.0222	.0103
11	FL	.0249	.0296	.0363	.0886	.0400	.0423
12		.0233	.0220	.0209	.0779	.0368	.0200
13		.0208	.0152	.0133	.0672	.0262	.0099
14		.0185	.0159	.0084	.0480	.0114	.0095
15		.0191	.0137	.0083	.0299	-.0004	.0138
16		.0175	.0117	.0080	.0138	-.0102	.0229
17		.0169	.0111	.0058	-.0070	-.0161	.0459
18		.0169	.0135	.0096	-.0201	-.0167	.0842
19		.0169	.0137	.0119	-.0269	-.0113	.1140
20		.0161	.0142	.0165	-.0352	-.0049	.0956
21		.0148	.0142	.0216	-.0393	.0160	
22		.0131	.0202	.0290	-.0383	.0510	
23		.0143	.0204	.0298	-.0328	.0978	
24		.0131	.0213	.0289	-.0224	.1174	
25		.0124	.0211	.0228	-.0003	.1020	
26		.0135	.0224	.0172	.0476		
27		.0138	.0233	.0122	.1245		
28		.0137	.0232	.0070	.2186		
29		.0137	.0224	.0059	.2935		
30		.0160	.0207	.0091	.2651		
31		.0156	.0188	.0149			
32		.0161	.0153	.0240			
33		.0162	.0159	.0403			
34		.0159	.0128	.0500			
35		.0153	.0124	.0668			
36		.0123	.0144	.0868			
37		.0125	.0158	.1178			
38		.0122	.0209	.1975			
39		.0124	.0263	.3215			
40		.0119	.0336	.3268			
41		.0142	.0396				
42		.0158	.0522				
43		.0208	.0706				
44		.0260	.0836				
45		.0301	.0955				
46		.0362	.1159				
47		.0476	.1408				
48		.0632	.2208				
49		.0650	.3131				
50		.0793	.3224				
51		.0942					
52		.1043					
53		.1121					
54		.1282					
55		.1522					
56		.2088					
57		.3269					

(b) $M_\infty = 2.16$

Orif	Loc	C_p for l/h of -					
		4.8	4	3	2	1.5	1
1	FP	.0030	.0036	.0036	.0034	.0028	.0033
2		.0025	.0034	.0032	.0032	.0026	.0029
3		.0018	.0026	.0024	.0029	.0024	.0026
4		.0036	.0045	.0041	.0040	.0041	.0033
5	FF	.0219	.0313	.0406	.0247	.0178	.0166
6		.0217	.0296	.0379	.0217	.0156	.0131
7		.0216	.0287	.0362	.0188	.0108	.0056
8		.0215	.0279	.0345	.0212	.0092	.0008
9		.0215	.0280	.0314	.0243	.0170	.0094
10		.0207	.0256	.0291	.0214	.0193	.0255
58	RF	.1690	.1705	.1424	.0549	.0341	.0329
59		.0744	.0683	.0430	.0226	.0161	.0209
60		.0646	.0586	.0254	.0231	.0078	.0034
61		.0688	.0588	.0240	.0217	.0042	.0031
63		.1266	.1169	.0706	.0160	.0070	.0091
62		.1853	.1753	.1229	.0283	.0106	.0082
64		.3018	.3176	.2522	.0632	.0237	.0341
65		.3692	.4038	.3350	.0963	.0406	.0504
66		.4579	.5096	.4457	.1568	.0773	.0853
67		.5290	.5845	.5615	.2357	.1445	.1454
69	RP	-.0283	-.0310	.0119	.0072	.0041	.0081
70		-.0339	-.0366	-.0120	-.0040	.0018	.0001
71		-.0330	-.0368	-.0241	-.0088	.0003	-.0042
72		-.0263	-.0304	-.0216	-.0075	.0007	-.0032
73	RF	.2962	.3632	.2176	.1505	.0757	.0720
74		.3816	.4018	.4186	.1558	.0744	.0834
75		.4540	.4435	.4781	.1557	.0739	.0861
76		.2352	.3560	.3244	.1529	.0750	.0812
77		.1408	.1382	.0783	.0226	.0070	.0104
78		.1665	.1557	.0921	.0331	.0139	.0132
79		.1813	.1957	.0803	.0138	.0061	.0078
81		.1170	.1226	.0680	.0260	.0099	.0049
82		.0731	.0709	.0332	.0202	.0075	.0019
83		.0805	.0756	.0275	.0208	.0081	.0020
84		.1041	.1123	.0493	.0253	.0097	.0052
11	FL	.0189	.0225	.0259	.0180	.0153	.0193
12		.0169	.0184	.0196	.0161	.0135	.0133
13		.0143	.0157	.0145	.0158	.0104	.0102
14		.0123	.0117	.0121	.0146	.0052	-.0003
15		.0102	.0099	.0087	.0112	-.0009	.0010
16		.0095	.0092	.0077	.0062	-.0051	.0106
17		.0086	.0078	.0093	.0041	-.0078	.0234
18		.0090	.0084	.0117	.0035	-.0082	.0405
19		.0089	.0089	.0141	-.0013	-.0061	.0460
20		.0085	.0098	.0167	-.0048	-.0018	.0420
21		.0098	.0111	.0193	-.0030	.0060	
22		.0117	.0140	.0264	.0078	.0235	
23		.0115	.0140	.0267	.0085	.0375	
24		.0118	.0135	.0248	.0069	.0449	
25		.0118	.0136	.0216	.0077	.0404	
26		.0121	.0138	.0142	.0187		
27		.0127	.0132	.0062	.0363		
28		.0127	.0134	-.0017	.0602		
29		.0125	.0145	-.0081	.0784		
30		.0121	.0159	-.0113	.0700		
31		.0143	.0201	-.0114			
32		.0124	.0205	-.0110			
33		.0105	.0207	-.0033			
34		.0094	.0190	.0055			
35		.0091	.0156	.0196			
36		.0099	.0117	.0412			
37		.0096	.0031	.0644			
38		.0113	-.0001	.1155			
39		.0134	-.0034	.1800			
40		.0167	-.0006	.1658			
41		.0187	.0026				
42		.0183	.0114				
43		.0197	.0189				
44		.0155	.0291				
45		.0110	.0360				
46		.0077	.0487				
47		.0039	.0679				
48		.0042	.1321				
49		.0063	.2092				
50		.0118	.2006				
51		.0172					
52		.0301					
53		.0411					
54		.0524					
55		.0731					
56		.1218					
57		.2068					

Table V. Pressure Coefficients for Range of Cavity Widths

(a) $h = 0.5$ in., $l/h = 12$

Orif	Loc	$M_\infty = 1.50$, C_p for w of -				$M_\infty = 2.16$, C_p for w of -			
		2.0	1.5	1.0	0.5	2.0	1.5	1.0	0.5
1	FP	.0022	.0005	.0010	.0043	.0008	-.0000	.0050	.0065
2		.0052	.0043	.0049	.0063	.0002	-.0008	.0040	.0057
3		.0119	.0093	.0132	.0127	.0003	-.0010	.0041	.0052
4		.0130	.0121	.0127	.0145	.0025	.0013	.0063	.0075
5	FF	-.0225	-.1287	-.1390	-.1071	-.0176	-.1481	-.1358	-.0897
6	FF	-.0251	-.1288	-.1384	-.1084	-.0193	-.1437	-.1338	-.0915
64	RF	.2585	.4853	.4926	.3986	.1693	.4863	.4835	.3411
65		.2283	.4595	.4629	.3910	.1494	.4352	.4396	.3316
66		.2276	.4792	.5092	.4599	.1475	.4664	.5334	.3855
67		.2521	.5160	.5910	.5794	.1723	.5710	.7298	.4985
68		.2721	.5099	.6302	.6974	.2131	.6856	.9109	.6278
69	RP	-.0929	-.2263	-.2884	-.1641	-.0202	-.0577	-.1335	-.1124
70		-.0739	-.1607	-.0986	-.0517	-.0392	-.1098	-.1213	-.0418
71		-.0367	-.0631	-.0501	-.0230	-.0331	-.1034	-.0464	-.0262
72		-.0192	-.0382	-.0285	-.0078	-.0236	-.0509	-.0249	-.0168
74	RF	.2688	.5529			.1688	.4992		
75	RF	.2782	.5221			.1654	.4690		
11	FL	-.0338	-.1478	-.1489	-.1141	-.0251	-.1559	-.1453	-.0920
13		-.0404	-.1515	-.1504	-.1172	-.0307	-.1616	-.1474	-.0950
14		-.0417	-.1517	-.1527	-.1156	-.0321	-.1462	-.1347	-.0894
15		-.0435	-.1478	-.1443	-.1070	-.0334	-.1184	-.1049	-.0731
16		-.0435	-.1306	-.1167	-.0788	-.0324	-.0874	-.0702	-.0480
17		-.0406	-.1009	-.0751	-.0341	-.0297	-.0559	-.0357	-.0181
18		-.0335	-.0620	-.0298	.0182	-.0238	-.0271	-.0049	.0105
20		-.0102	.0191	.0529	.0859	-.0067	.0210	.0407	.0544
22		.0293	.0978	.1072	.1087	.0186	.0686	.0732	.0776
23		.0466	.1319	.1244	.1037	.0291	.0951	.0806	.0778
24		.0660	.1655	.1447	.1008	.0409	.1252	.0897	.0762
25		.0835	.2020	.1724	.1070	.0517	.1588	.1146	.0790
26		.1003	.2341	.2133	.1306	.0620	.1913	.1682	.1003
27		.1165	.2669	.2649	.1818	.0727	.2265	.2328	.1531
28		.1321	.3025	.3125	.2442	.0821	.2635	.2847	.2072
29		.1448	.3401	.3535	.2897	.0893	.3010	.3251	.2442
32		.1672	.4038	.4158	.3395	.0990	.3547	.3751	.2846
33		.1851	.4051	.4090	.3478	.1167	.3598	.3492	.2938
34		.2748	.5192	.5223	.4306	.1812	.5320	.5452	.3751

(b) $h = 0.5$ in., $l/h = 6$

Orif	Loc	$M_\infty = 1.50$, C_p for w of -				$M_\infty = 2.16$, C_p for w of -			
		2.0	1.5	1.0	0.5	2.0	1.5	1.0	0.5
1	FP	.0029	.0014	.0014	.0011	.0035	.0036	.0005	.0027
2		.0057	.0041	.0053	.0048	.0029	.0025	-.0003	.0018
3		.0120	.0117	.0115	.0109	.0035	.0031	-.0007	.0025
4		.0136	.0134	.0127	.0115	.0058	.0055	.0022	.0054
5	FF	.0282	.0260	.0230	.0200	.0187	.0159	.0136	.0141
6	FF	.0273	.0249	.0242	.0191	.0185	.0156	.0133	.0132
64	RF	.1700	.1750	.1345	.1054	.1137	.1218	.0802	.0619
65		.1417	.1348	.0874	.0671	.0949	.0950	.0517	.0424
66		.1302	.1390	.0974	.0657	.0839	.0959	.0589	.0357
67		.1606	.1914	.1714	.1200	.1163	.1424	.1198	.0695
68		.2238	.2626	.2914	.2321	.1986	.2125	.2384	.1594
69	RP	-.0278	-.0394	-.0135	.0005	-.0050	-.0218	-.0118	.0003
70		-.0184	-.0163	-.0005	.0045	-.0100	-.0130	-.0023	.0049
71		-.0026	-.0023	.0064	.0077	-.0044	-.0031	.0016	.0069
72		.0028	.0015	.0068	.0072	-.0001	.0011	.0029	.0071
74	RF	.1410	.0837			.0842	.0449		
75	RF	.1336	.0815			.0781	.0451		
11	FL	.0238	.0158	.0204	.0177	.0161	.0091	.0115	.0123
13		.0229	.0156	.0177	.0150	.0140	.0091	.0093	.0102
14		.0220	.0171	.0164	.0132	.0124	.0123	.0077	.0088
15		.0205	.0164	.0133	.0092	.0107	.0125	.0064	.0071
16		.0195	.0169	.0117	.0068	.0085	.0124	.0041	.0060
17		.0195	.0201	.0083	.0068	.0079	.0139	.0017	.0050
18		.0231	.0232	.0055	.0051	.0081	.0161	-.0003	.0021
20		.0386	.0391	.0057	-.0007	.0190	.0266	-.0027	-.0043
22		.1867	.2005	.1632	.1225	.1242	.1403	.1008	.0730

ORIGINAL PAGE IS
OF POOR QUALITY

Table V. Concluded

(c) $h = 1.0$ in., $l/h = 12$

Orif	Loc	M_∞ = 1.50				M_∞ = 2.16			
		C_p for w of -				C_p for w of -			
		2.0	1.5	1.0	0.5	2.0	1.5	1.0	0.5
1	FP	.0041	.0058	.0055	.0057	.0005	.0033	.0013	.0004
2		.0079	.0108	.0073	.0063	.0009	.0046	.0003	-.0011
3		.0102	.0120	.0120	.0114	-.0006	.0028	.0009	-.0002
4		.0084	.0112	.0099	.0119	.0023	.0053	.0036	.0014
5	FF	-.1566	-.1355	-.1168	-.0798	-.1546	-.1316	-.1055	-.0737
6		-.1553	-.1349	-.1173	-.0798	-.1543	-.1314	-.1064	-.0741
7		-.1558	-.1361	-.1162	-.0795	-.1492	-.1285	-.1062	-.0738
62	RF	.6075	.5619	.5127	.4083	.6610	.5800	.4896	.3434
63		.6050	.5577	.5354	.4234	.6242	.5519	.4921	.3441
64		.6970	.6349	.6238	.5772	.8131	.6838	.5833	.5156
65		.7434	.6840	.6784	.6799	.9464	.7792	.6503	.6601
66		.7968	.7303	.7296	.7695	1.0656	.8902	.7154	.7998
67		.8149	.7556	.7674	.8125	1.1958	.9960	.7893	.8997
69	RP	-.3705	-.3954	-.3645	-.2004	-.1100	-.1549	-.1929	-.1568
70		-.3342	-.2553	-.1768	-.0678	-.1455	-.1779	-.1375	-.0628
71		-.1908	-.1302	-.0709	-.0417	-.1679	-.1493	-.0772	-.0571
72		-.1053	-.0727	-.0399	-.0192	-.1626	-.0962	-.0410	-.0483
74	RF	.7792	.7374			1.0190	.8712		
75		.7180	.6718			.9475	.7726		
78		.5949	.5758			.6434	.6060		
79		.5768	.5751			.6255	.6025		
11	FL	-.1644	-.1407	-.1182	-.0815	-.1598	-.1375	-.1073	-.0750
13		-.1717	-.1457	-.1200	-.0834	-.1655	-.1424	-.1091	-.0759
14		-.1704	-.1465	-.1200	-.0828	-.1652	-.1413	-.1099	-.0770
15		-.1694	-.1474	-.1205	-.0854	-.1649	-.1408	-.1105	-.0783
16		-.1683	-.1465	-.1224	-.0869	-.1654	-.1408	-.1115	-.0800
17		-.1686	-.1466	-.1227	-.0888	-.1641	-.1408	-.1110	-.0799
18		-.1705	-.1465	-.1232	-.0882	-.1585	-.1384	-.1090	-.0775
19		-.1700	-.1457	-.1212	-.0842	-.1480	-.1316	-.1054	-.0725
20		-.1680	-.1434	-.1191	-.0807	-.1343	-.1219	-.1002	-.0667
22		-.1472	-.1255	-.1020	-.0591	-.0994	-.0908	-.0795	-.0523
23		-.1314	-.1101	-.0898	-.0469	-.0798	-.0727	-.0666	-.0416
24		-.1112	-.0923	-.0734	-.0306	-.0594	-.0533	-.0508	-.0275
25		-.0865	-.0684	-.0527	-.0087	-.0382	-.0332	-.0327	-.0132
26		-.0595	-.0421	-.0273	.0121	-.0194	-.0135	-.0145	.0027
27		-.0298	-.0138	-.0004	.0352	-.0003	.0057	.0038	.0182
28		-.0026	.0130	.0273	.0576	.0163	.0235	.0220	.0340
29		.0260	.0412	.0545	.0797	.0308	.0401	.0389	.0486
30		.0525	.0650	.0780	.0982	.0436	.0550	.0551	.0606
31		.0772	.0883	.0994	.1100	.0578	.0712	.0683	.0764
32		.0986	.1097	.1175	.1169	.0682	.0826	.0804	.0849
33		.1150	.1214	.1259	.1181	.0767	.0915	.0896	.0910
34		.1300	.1330	.1312	.1188	.0858	.0997	.0979	.0933
35		.1408	.1402	.1343	.1144	.0912	.1054	.1036	.0937
36		.1531	.1453	.1332	.1087	.0990	.1107	.1071	.0929
37		.1608	.1471	.1303	.0994	.1026	.1135	.1091	.0901
38		.1674	.1479	.1253	.0916	.1051	.1136	.1085	.0853
39		.1793	.1499	.1201	.0848	.1075	.1138	.1076	.0800
40		.1959	.1550	.1143	.0767	.1141	.1135	.1033	.0725
41		.2160	.1685	.1158	.0720	.1319	.1138	.0997	.0663
42		.2453	.1911	.1251	.0721	.1695	.1212	.0989	.0604
43		.2766	.2194	.1488	.0751	.2167	.1429	.1054	.0557
44		.3127	.2566	.1861	.0894	.2690	.1956	.1258	.0578
45		.3511	.2968	.2295	.1151	.3155	.2532	.1721	.0792
46		.3833	.3303	.2773	.1509	.3449	.3047	.2321	.1201
47		.4125	.3657	.3154	.1942	.3657	.3372	.2809	.1666
48		.4405	.3990	.3568	.2393	.3931	.3694	.3190	.2069
49		.4558	.4186	.3837	.2750	.4115	.3929	.3450	.2351
50		.4733	.4424	.4077	.3072	.4403	.4201	.3699	.2606
51		.4882	.4581	.4261	.3374	.4628	.4441	.3868	.2805
52		.5016	.4821	.4338	.3632	.4840	.4636	.3979	.2944
53		.5098	.4945	.4404	.3779	.5012	.4796	.4047	.3026
54		.5205	.5035	.4520	.3823	.5107	.4867	.4192	.3043
55		.5322	.5052	.4592	.3841	.4955	.4786	.4253	.3032
56		.5111	.4936	.4662	.3843	.4620	.4673	.4279	.3108
57		.5443	.5148	.4660	.3989	.5676	.5154	.4450	.3276

(d) $h = 1.0$ in., $l/h = 6$

Orif	Loc	M_∞ = 1.50				M_∞ = 2.16			
		C_p for w of -				C_p for w of -			
		2.0	1.5	1.0	0.5	2.0	1.5	1.0	0.5
1	FP	.0038	.0030	.0053	.0039	-.0004	.0001	.0031	.0007
2		.0047	.0060	.0046	.0037	-.0019	-.0013	.0024	-.0011
3		.0109	.0104	.0114	.0111	-.0008	-.0009	.0030	-.0003
4		.0109	.0120	.0111	.0100	.0017	.0013	.0050	.0022
5	FF	.0255	.0246	.0167	.0143	.0122	.0094	.0136	.0057
6		.0256	.0253	.0165	.0145	.0122	.0091	.0130	.0061
7		.0259	.0235	.0170	.0147	.0121	.0088	.0131	.0054
62	RF	.2395	.2116	.1846	.1316	.0843	.0762	.0661	.0585
63		.1590	.1358	.1259	.0868	.0418	.0377	.0256	.0232
64		.2333	.2093	.1764	.1227	.0665	.0494	.0280	.0243
65		.3072	.2820	.2256	.1700	.0996	.0703	.0458	.0436
66		.4069	.3893	.3074	.2426	.1599	.1177	.0871	.0890
67		.5020	.5040	.4041	.3399	.2415	.1846	.1500	.1568
69	RP	-.0639	-.0662	-.0544	-.0018	-.0198	-.0250	-.0067	-.0033
47		-.0375	-.0111	-.0041	.0094	-.0179	-.0177	.0027	.0014
71		-.0070	.0069	.0044	.0151	-.0105	-.0081	.0062	.0031
72		.0047	.0106	.0095	.0179	-.0062	-.0040	.0068	.0031
74	RF	.2489	.1843			.1043	.1428		
75		.2312	.1782			.0687	.0383		
78		.2136	.2408			.0816	.0976		
79		.2055	.2262			.0745	.0747		
11	FL	.0246	.0200	.0145	.0150	.0113	.0054	.0136	.0056
13		.0200	.0121	.0099	.0146	.0096	-.0012	.0127	.0053
14		.0183	.0125	.0109	.0141	.0090	-.0018	.0122	.0050
15		.0173	.0154	.0095	.0136	.0082	.0000	.0115	.0052
16		.0147	.0158	.0096	.0139	.0074	.0021	.0114	.0049
17		.0146	.0153	.0062	.0137	.0067	.0040	.0108	.0040
18		.0136	.0143	.0069	.0129	.0061	.0046	.0099	.0036
19		.0129	.0132	.0052	.0116	.0055	.0042	.0090	.0026
20		.0120	.0104	.0035	.0094	.0046	.0041	.0079	.0022
22		.0166	.0119	.0066	.0084	.0042	.0048	.0093	.0054
23		.0158	.0121	.0062	.0088	.0027	.0038	.0076	.0051
24		.0145	.0106	.0094	.0111	.0015	.0026	.0053	.0047
25		.0148	.0116	.0100	.0092	-.0005	.0012	.0014	.0020
26		.0143	.0124	.0112	.0092	-.0029	-.0005	-.0025	-.0016
27		.0156	.0131	.0126	.0049	-.0056	-.0021	-.0073	-.0035
28		.0186	.0147	.0212	-.0007	-.0081	-.0023	-.0110	-.0067
29		.0179	.0188	.0239	-.0031	-.0105	-.0020	-.0138	-.0137
30		.0206	.0219	.0367	-.0001	-.0112	-.0014	-.0147	-.0207
31		.0352	.0250	.0547	.0176	-.0050	.0040	-.0088	-.0144
32		.0663	.0455	.0692	.0494	.0090	.0137	.0108	.0067
33		.1737	.1346	.1265	.1064	.0612	.0538	.0596	.0496
34		.3209	.2947	.2446	.1533	.1181	.1057	.0871	.0719

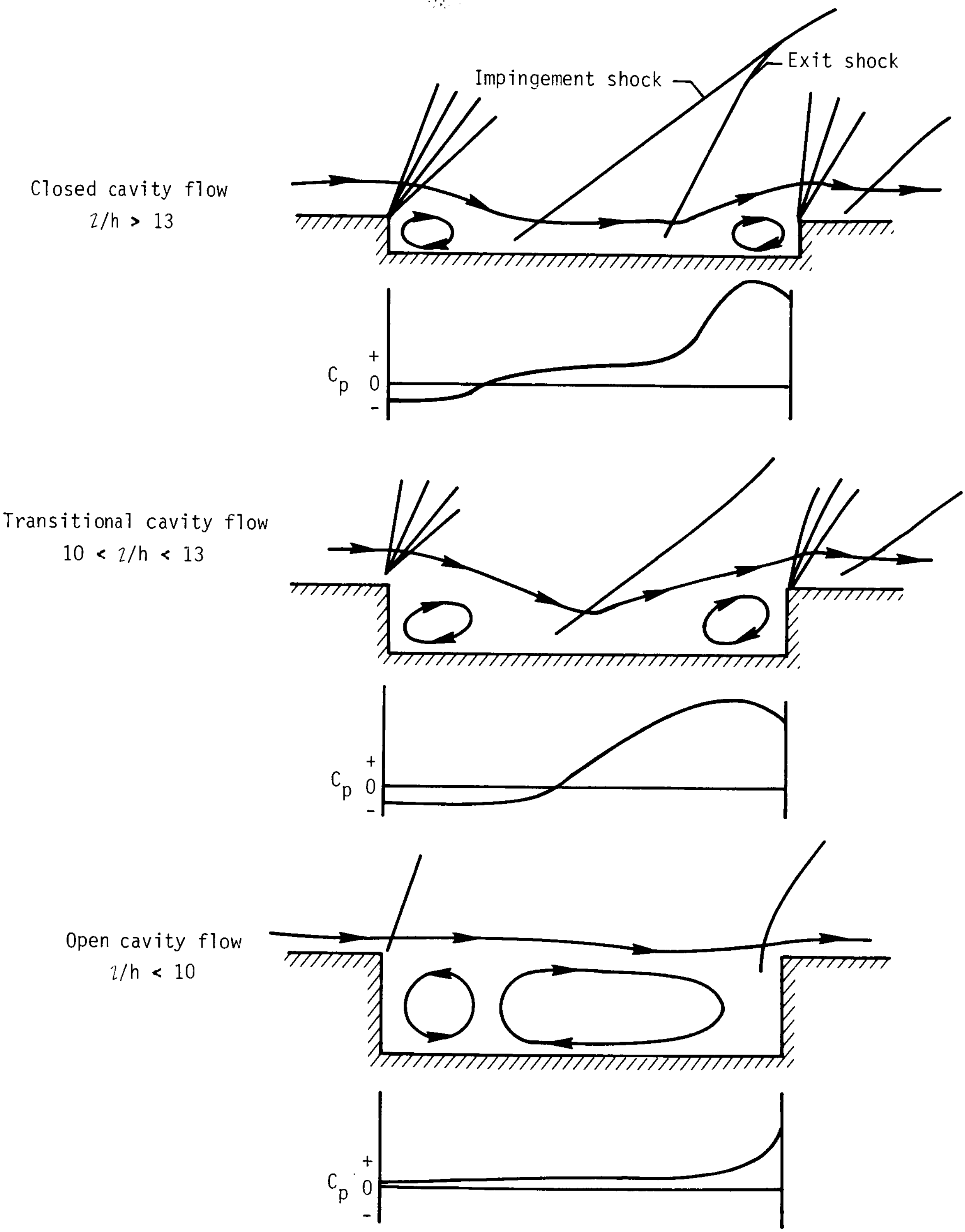

Figure 1. Sketches of cavity flow field models.

ORIGINAL PAGE IS
OF POOR QUALITY

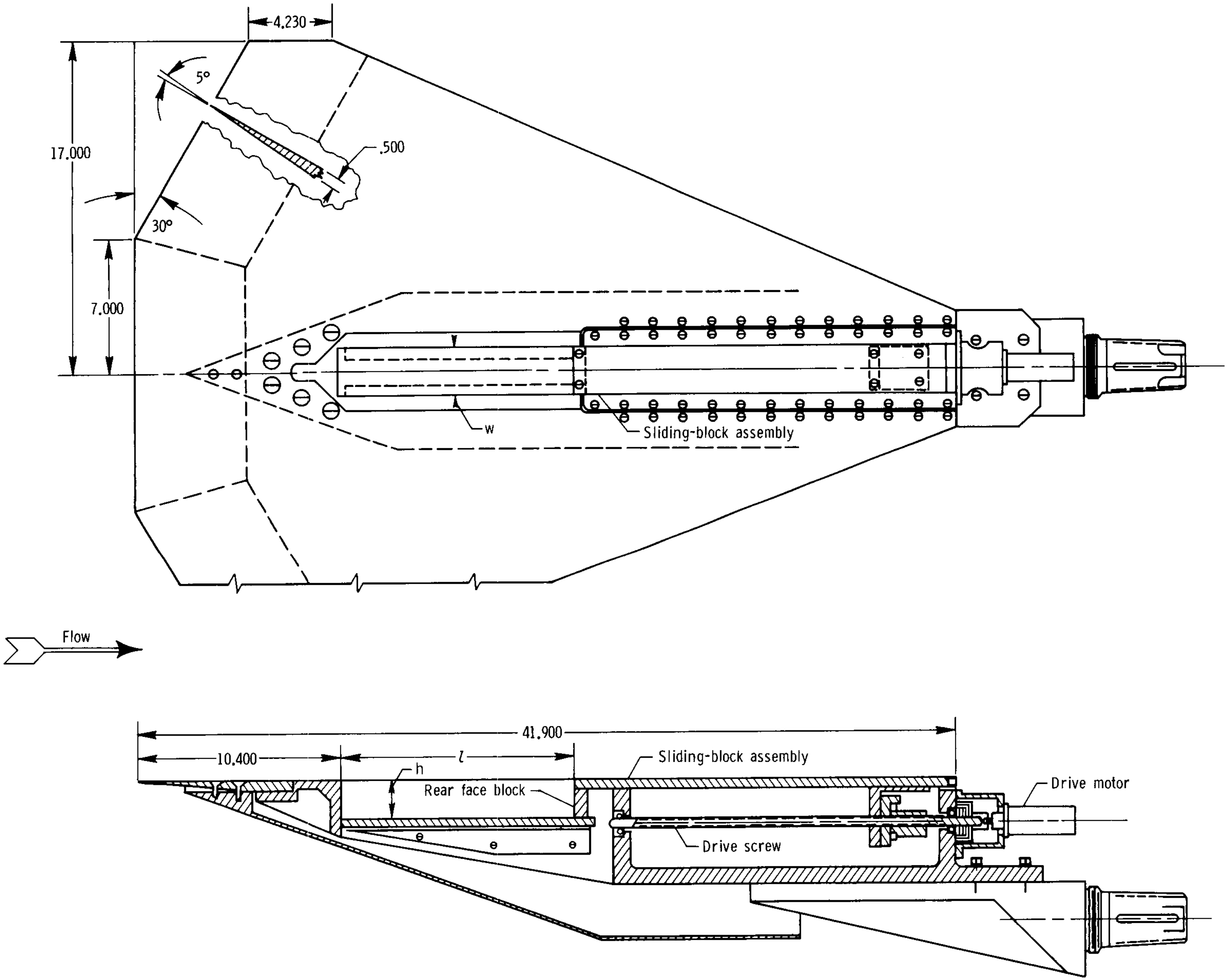

(a) Plate drawing.

Figure 2. Model description. Linear dimensions are in inches.

ORIGINAL PAGE IS
OF POOR QUALITY

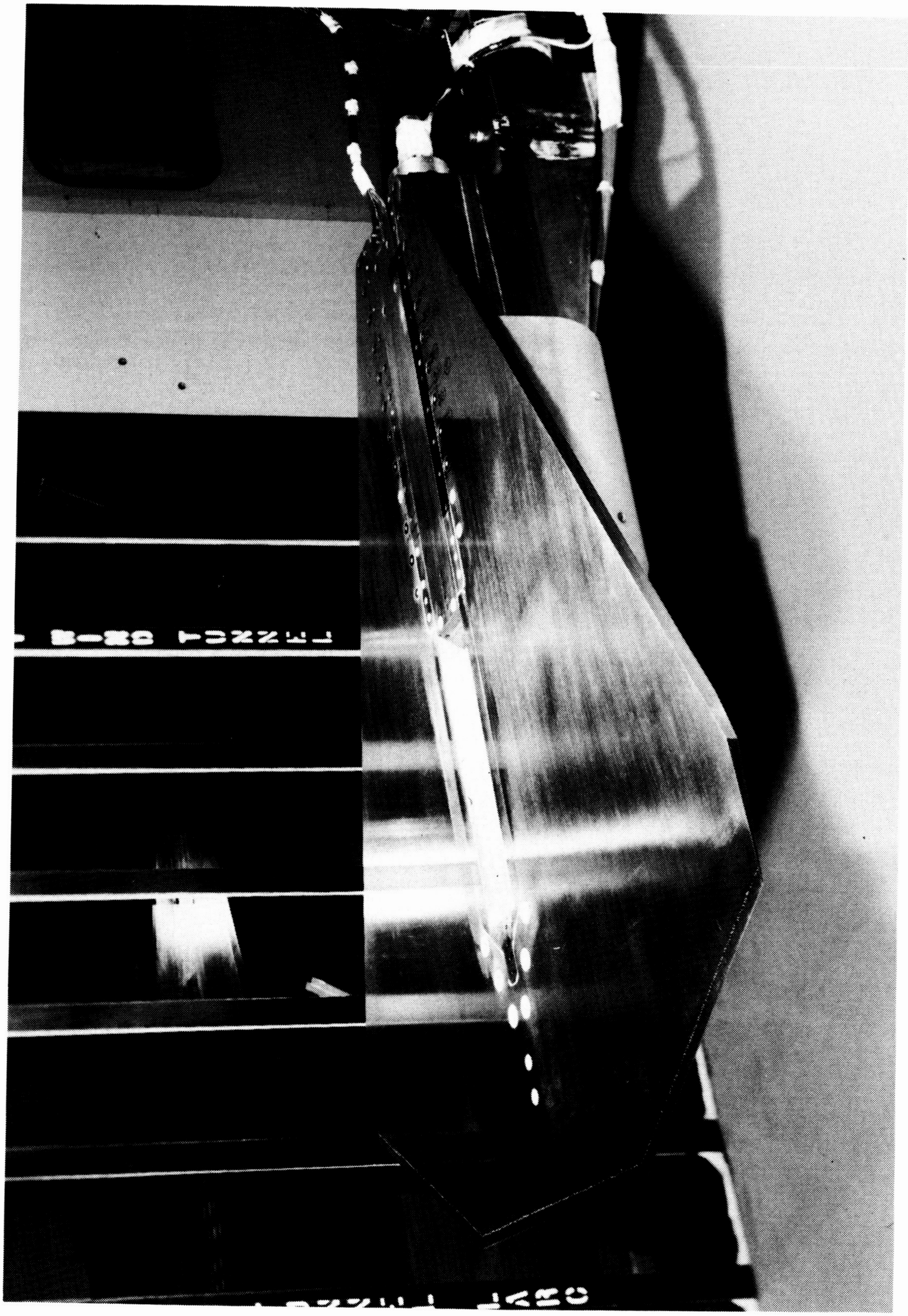

L-84-1089

(b) Photograph of model installed in tunnel. $h = 1.0$ in.; $w = 2.5$ in.

Figure 2. Continued.

ORIGINAL PAGE IS
OF POOR QUALITY

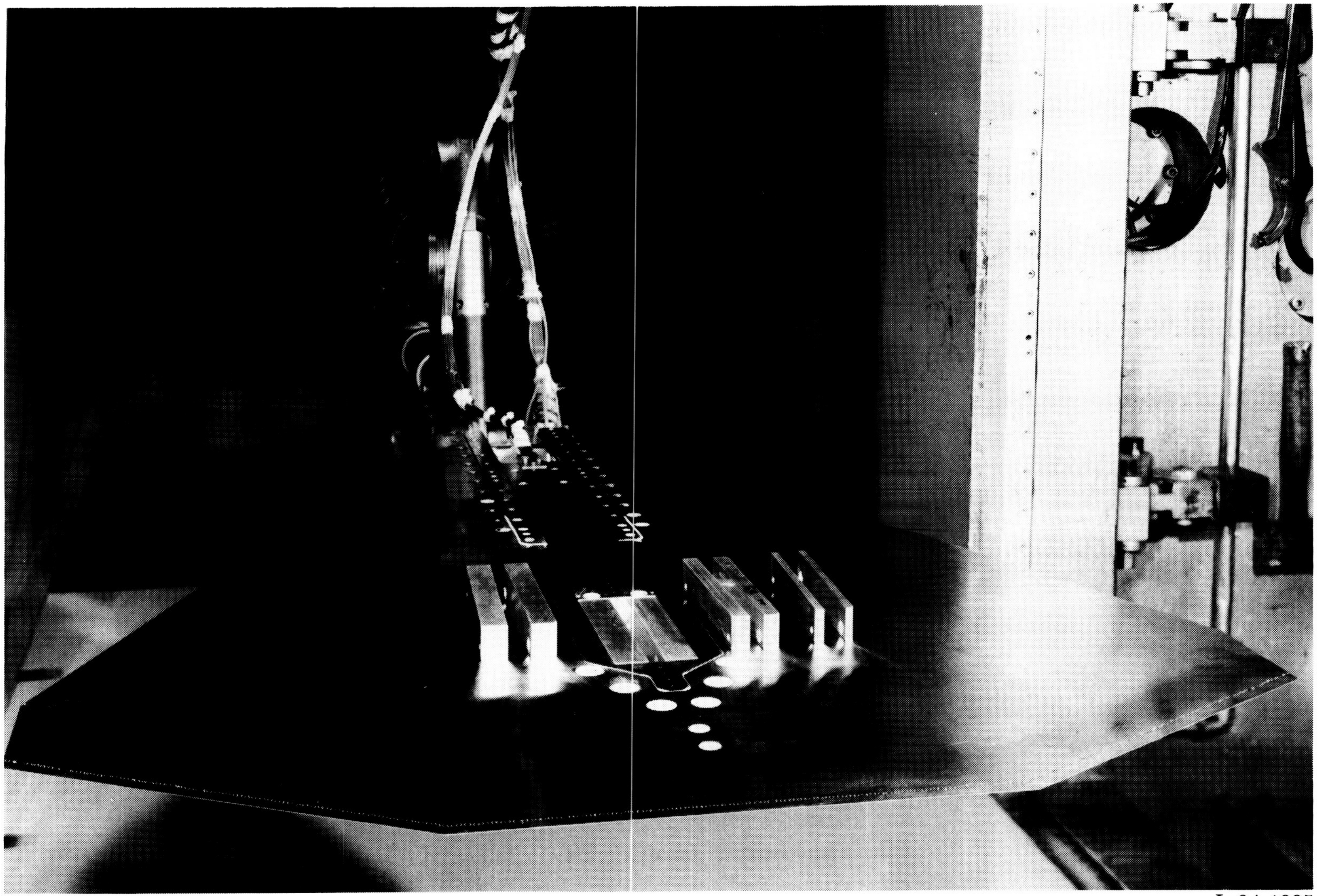

L-84-1095

(c) Photograph of typical block inserts for varying cavity width. $h = 1.0$ in.

Figure 2. Concluded.

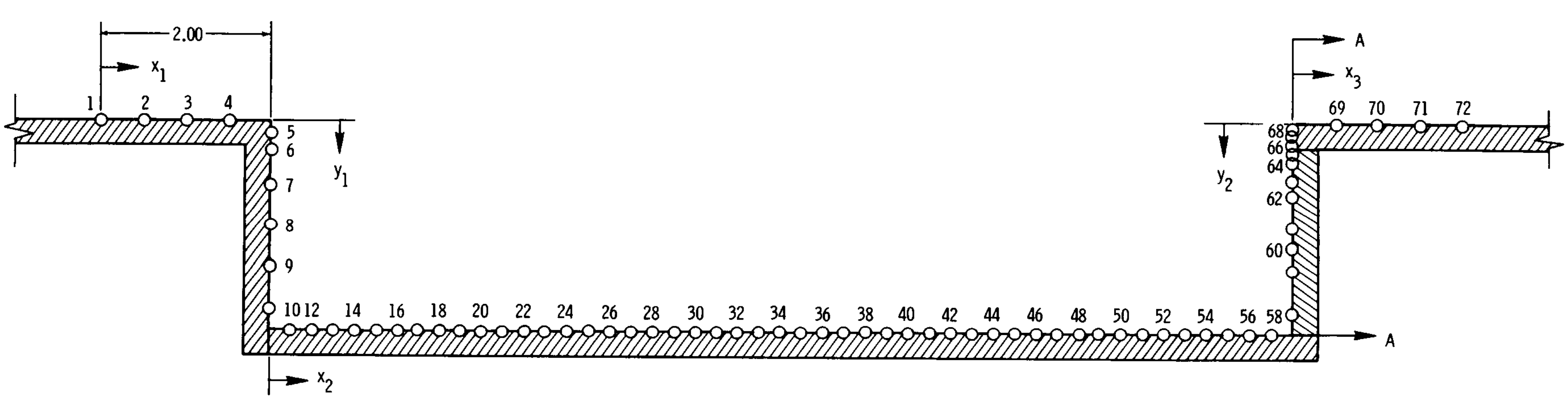

Orif	Loc.	x_1, in.	y_1, in.	x_2, in.	z, in.
1	FP	0.00			0.00
2		0.50			
3		1.00			
4		1.50			
5	FF		0.15		
6			0.35		
7			0.75		
8			1.25		
9			1.75		
10			2.25		
11	FL			0.25	
12				0.50	
13				0.75	
14				1.00	
15				1.25	
16				1.50	
17				1.75	
18				2.00	
19				2.25	
20				2.50	
21				2.75	
22				3.00	
23				3.25	
24				3.50	
25				3.75	
26				4.00	
27				4.25	
28				4.50	

Orif.	Loc	x_2, in.	z, in.
29	FL	4.75	0 .00
30		5.00	
31		5.25	
32		5.50	
33		5.75	
34		6.00	
35		6.25	
36		6.50	
37		6.75	
38		7.00	
39		7.25	
40		7.50	
41		7.75	
42		8.00	
43		8.25	
44		8.50	
45		8.75	
46		9.00	
47		9.25	
48		9.50	
49		9.75	
50		10.00	
51		10.25	
52		10.50	
53		10.75	
54		11.00	
55		11.25	
56		11.50	
57		11.75	

Orif.	Loc	y_2, in.	x_3, in.	z, in.
58	RF	2.25		0.00
59		1.75		
60		1.50		
61		1.25		
62		0.85		
63		0.65		
64		0.45		
65		0.35		
66		0.25		
67		0.15		
68		0.05		
69	RP		0.50	
70			1.00	
71			1.50	
72			1.75	
73	RF	0.25		-1.00
74				-0.50
75				0.50
76				1.00
77		0.85		-1.00
78				-0.50
79				0.50
80				1.00
81		1.50		-1.00
82				-0.50
83				0.50
84				1.00

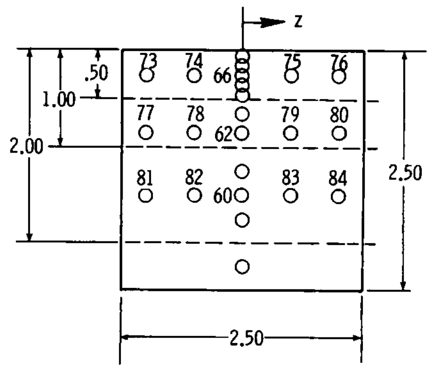

Section A-A

Figure 3. Pressure orifice locations. Linear dimensions are in inches.

ORIGINAL PAGE IS
OF POOR QUALITY

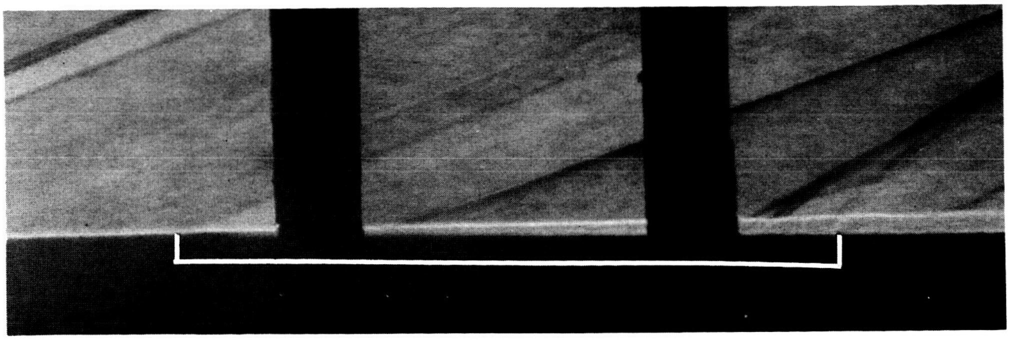

(a) $l/h = 24.0$.

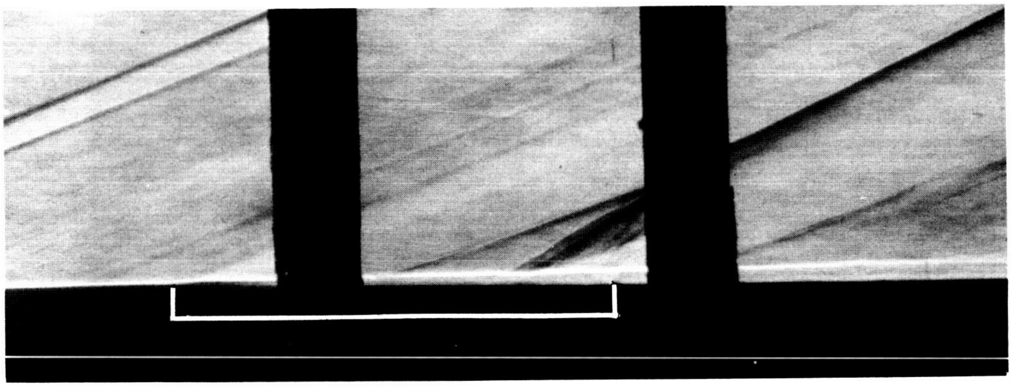

(b) $l/h = 16.0$.

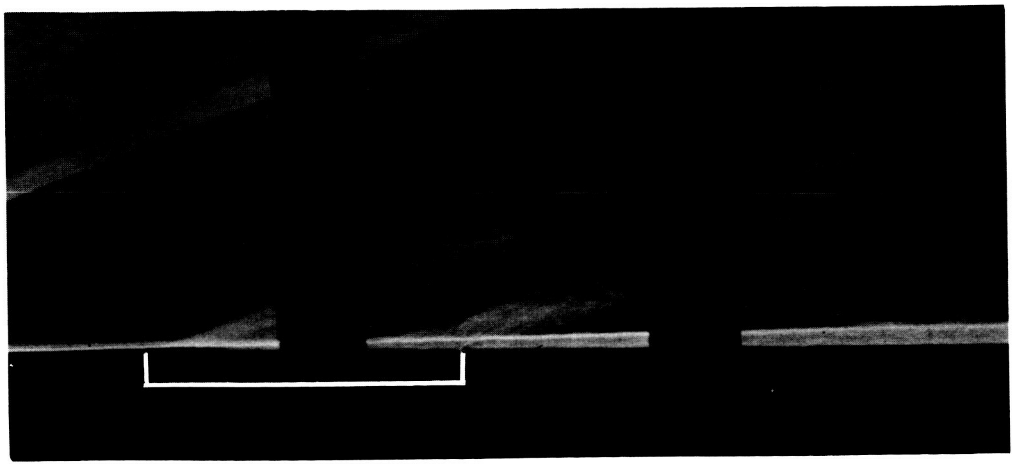

(c) $l/h = 11.6$.

L-87-569

Figure 4. Schlieren photographs of cavity flow field for $h = 0.5$ in. and $M_{\infty} = 2.86$.

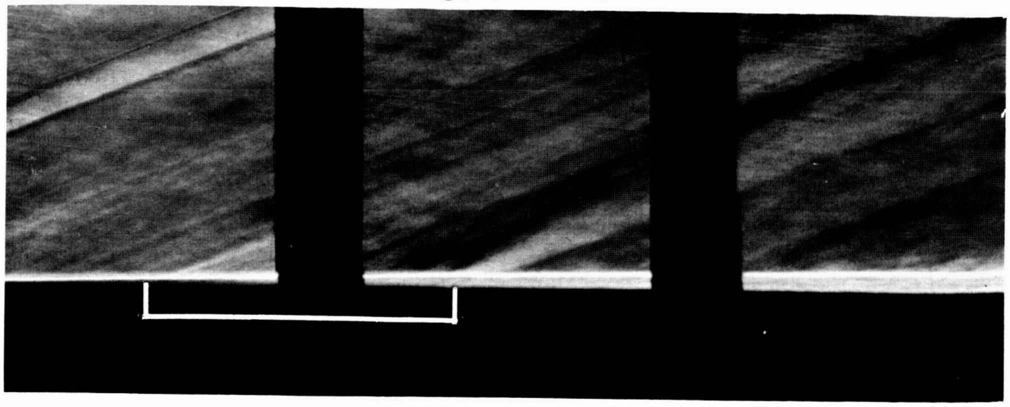

(d) $l/h = 11.2$.

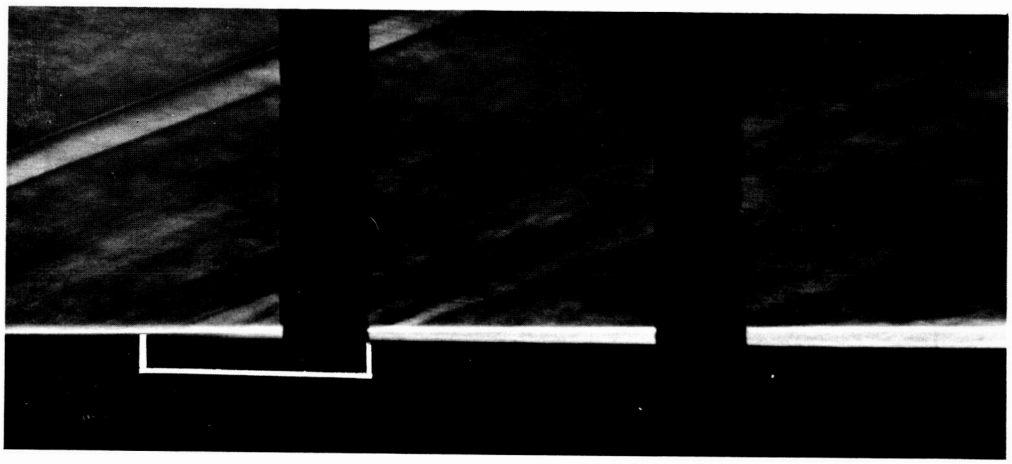

(e) $l/h = 8.0$.

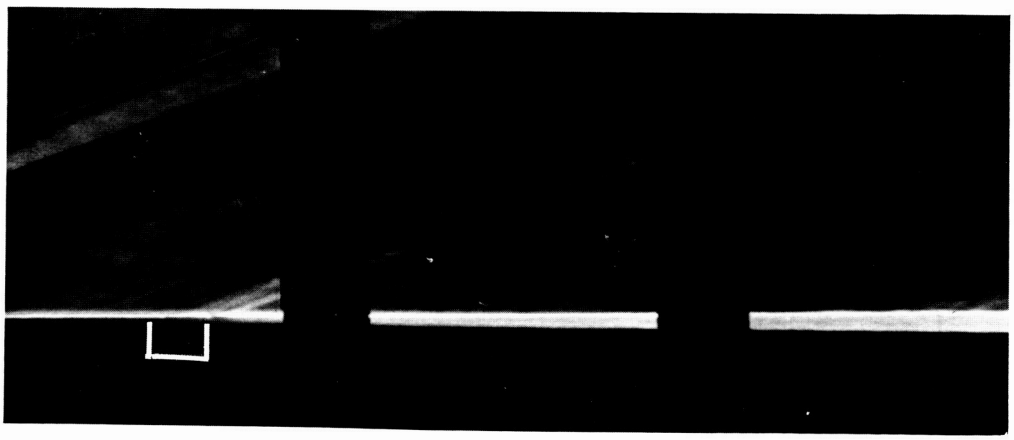

(f) $l/h = 2.0$.

L-87-570

Figure 4. Concluded.

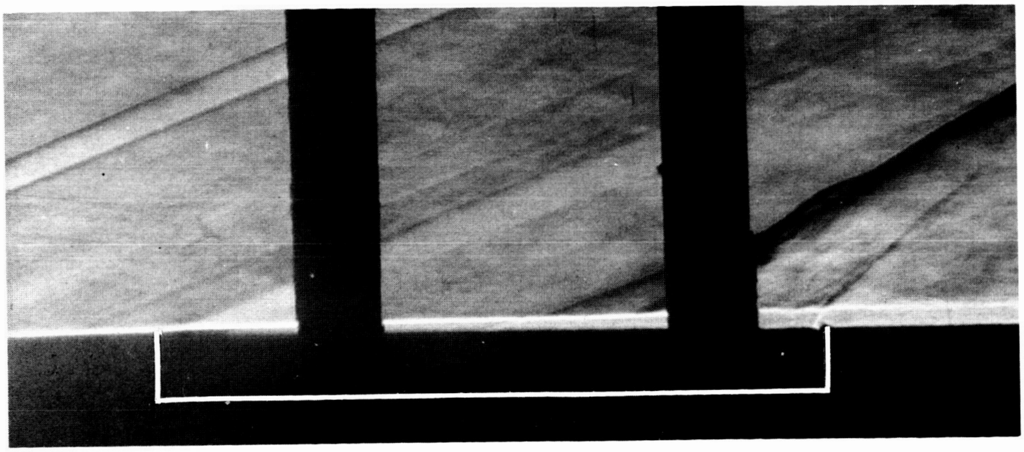

(a) $l/h = 12.0$.

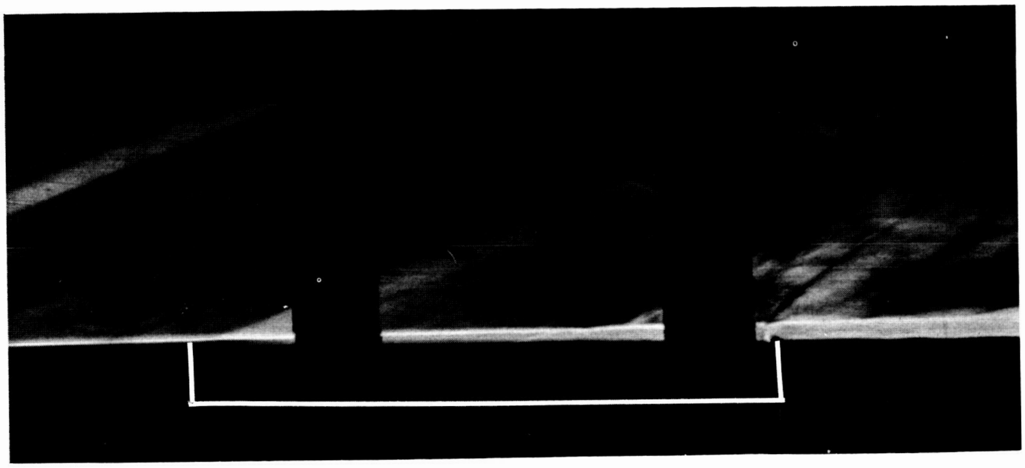

(b) $l/h = 10.5$.

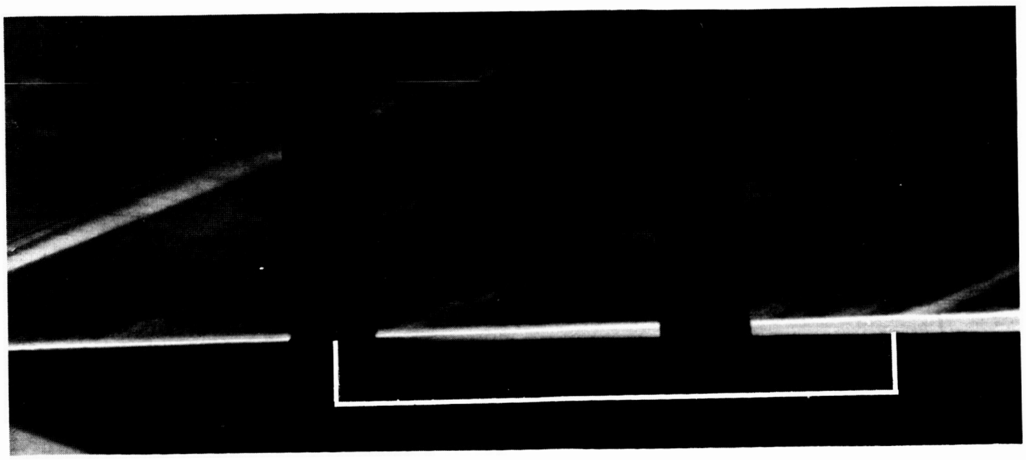

(c) $l/h = 10.0$.

L-87-571

Figure 5. Schlieren photographs of cavity flow field for $h = 1.0$ in. and $M_\infty = 2.86$.

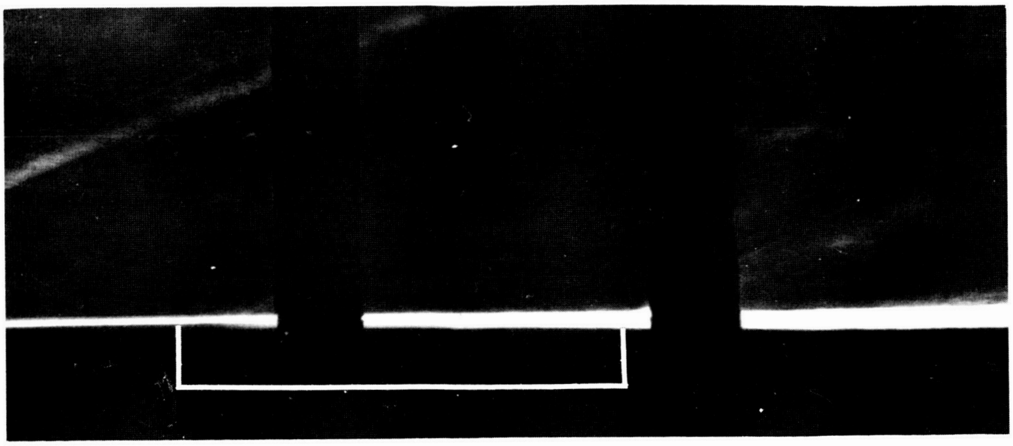

(d) $l/h = 8.0$.

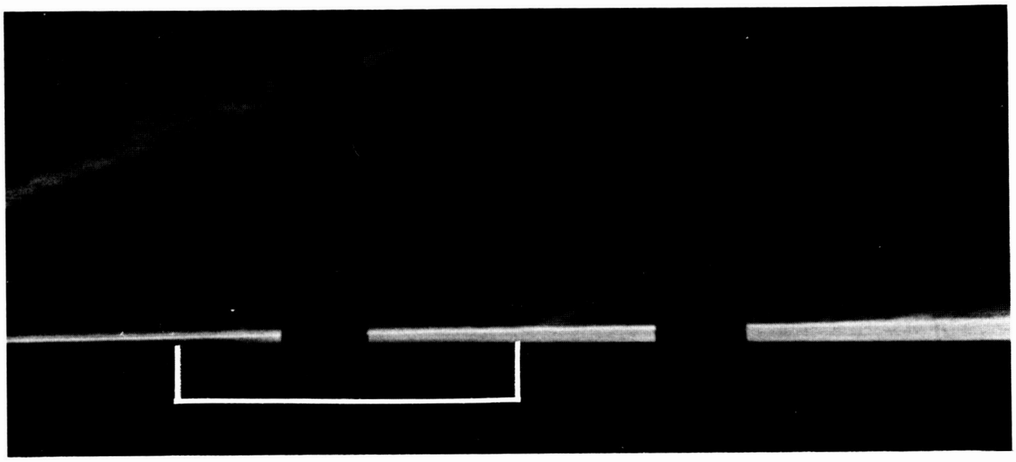

(e) $l/h = 6.0$.

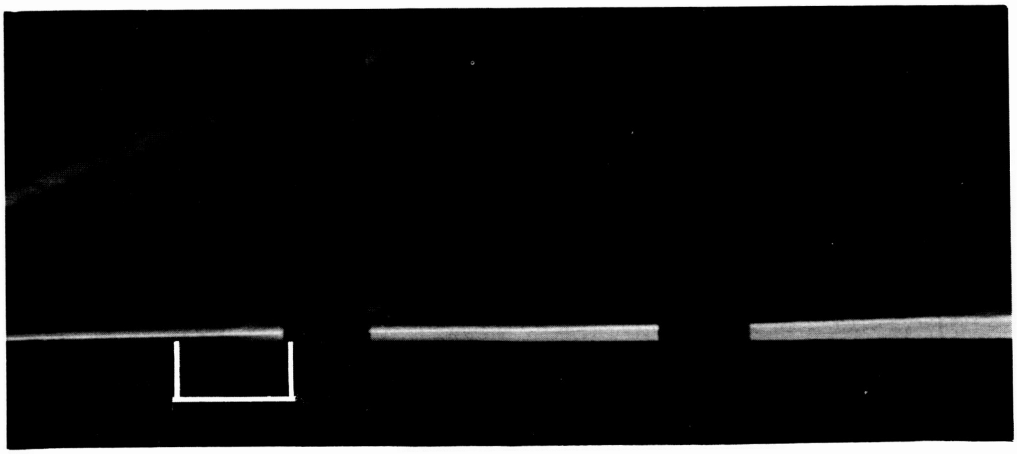

(f) $l/h = 2.0$.

L-87-572

Figure 5. Concluded.

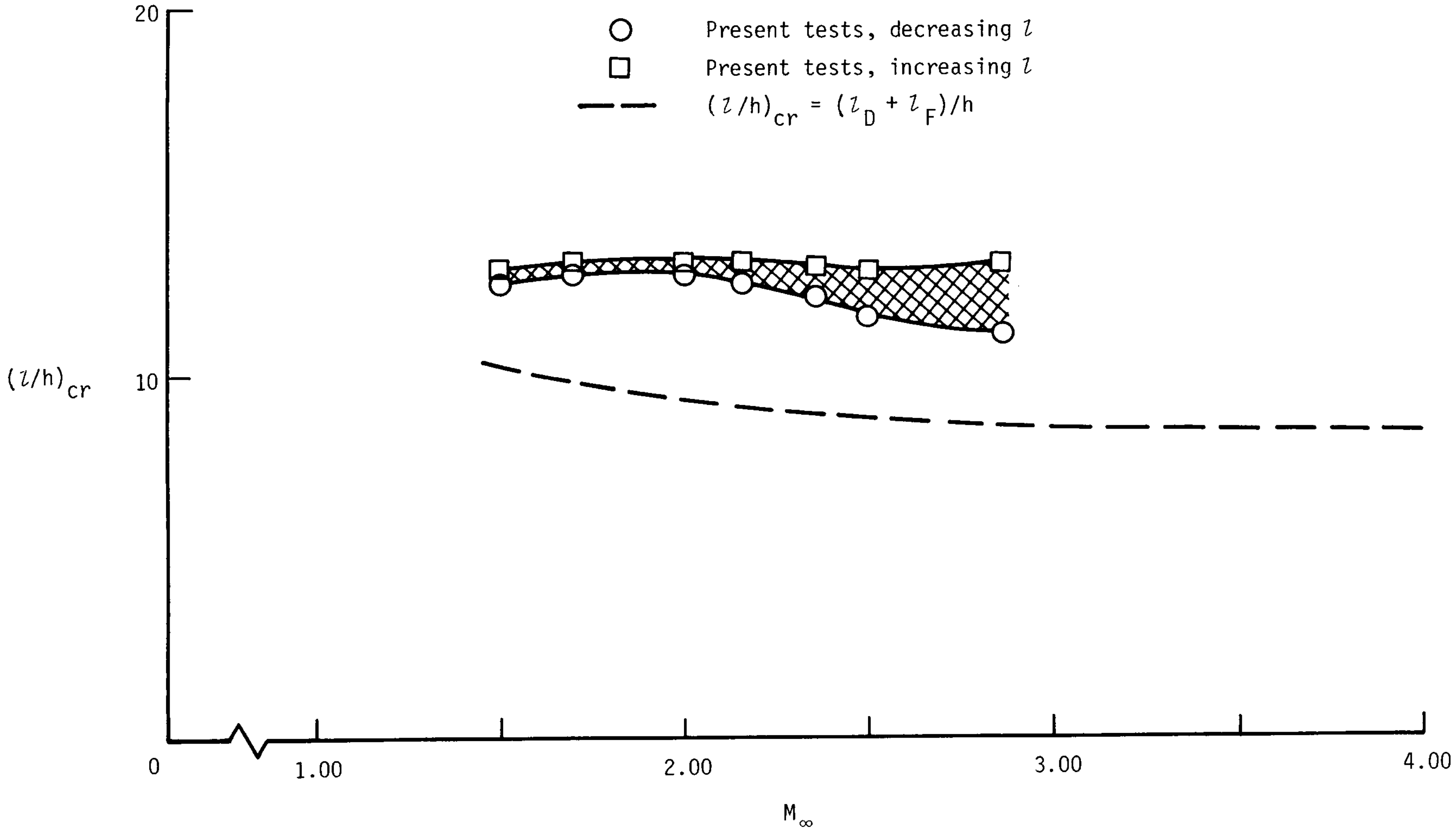

Figure 6. Variation with Mach number of critical length-to-depth ratios. $h = 0.5$ in.; $w = 2.5$ in.

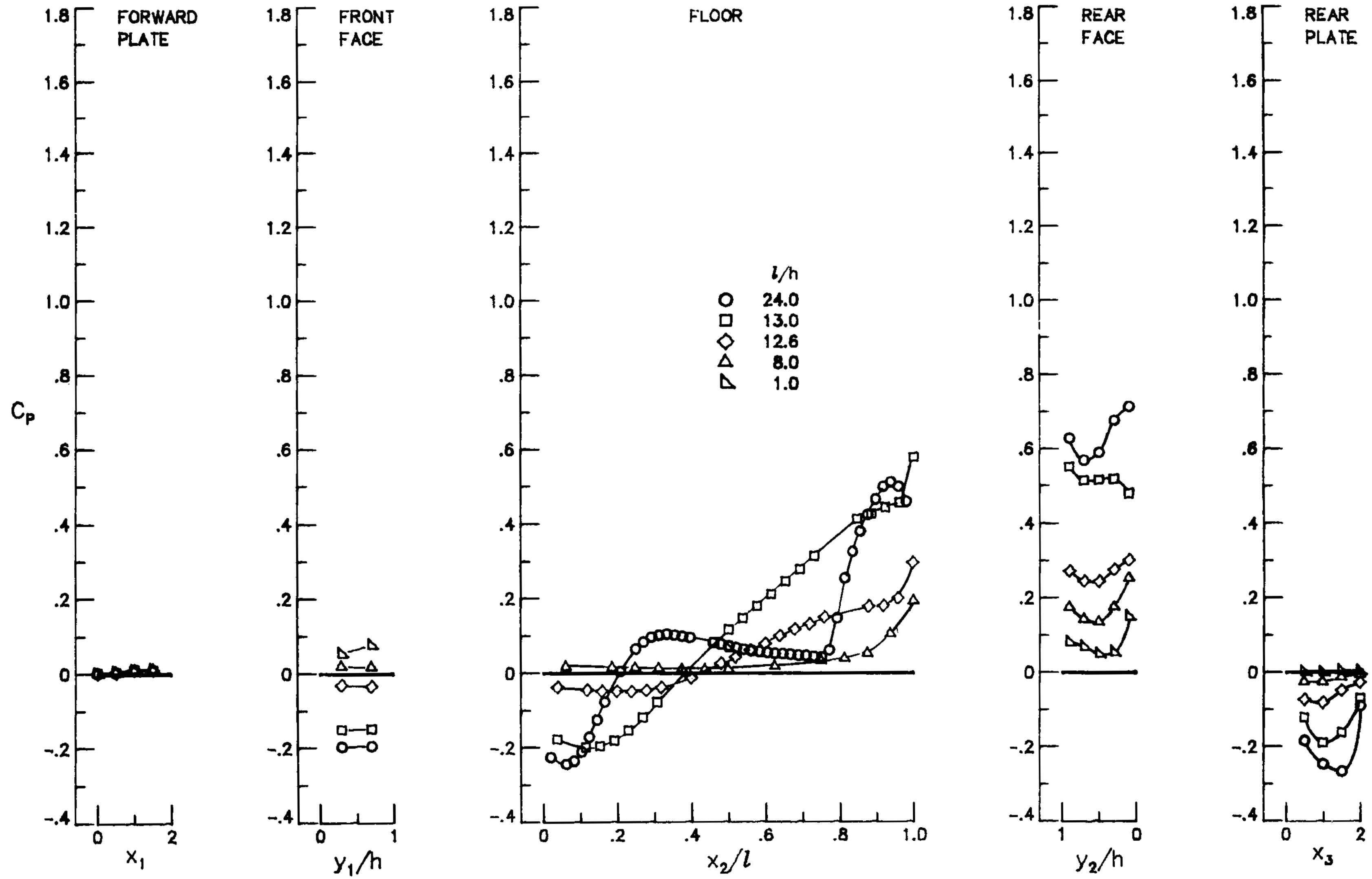

(a) $M_\infty = 1.50$; $h = 0.5$ in.

Figure 7. Effect of cavity length-to-depth ratio on cavity centerline pressure distributions. $w = 2.5$ in.

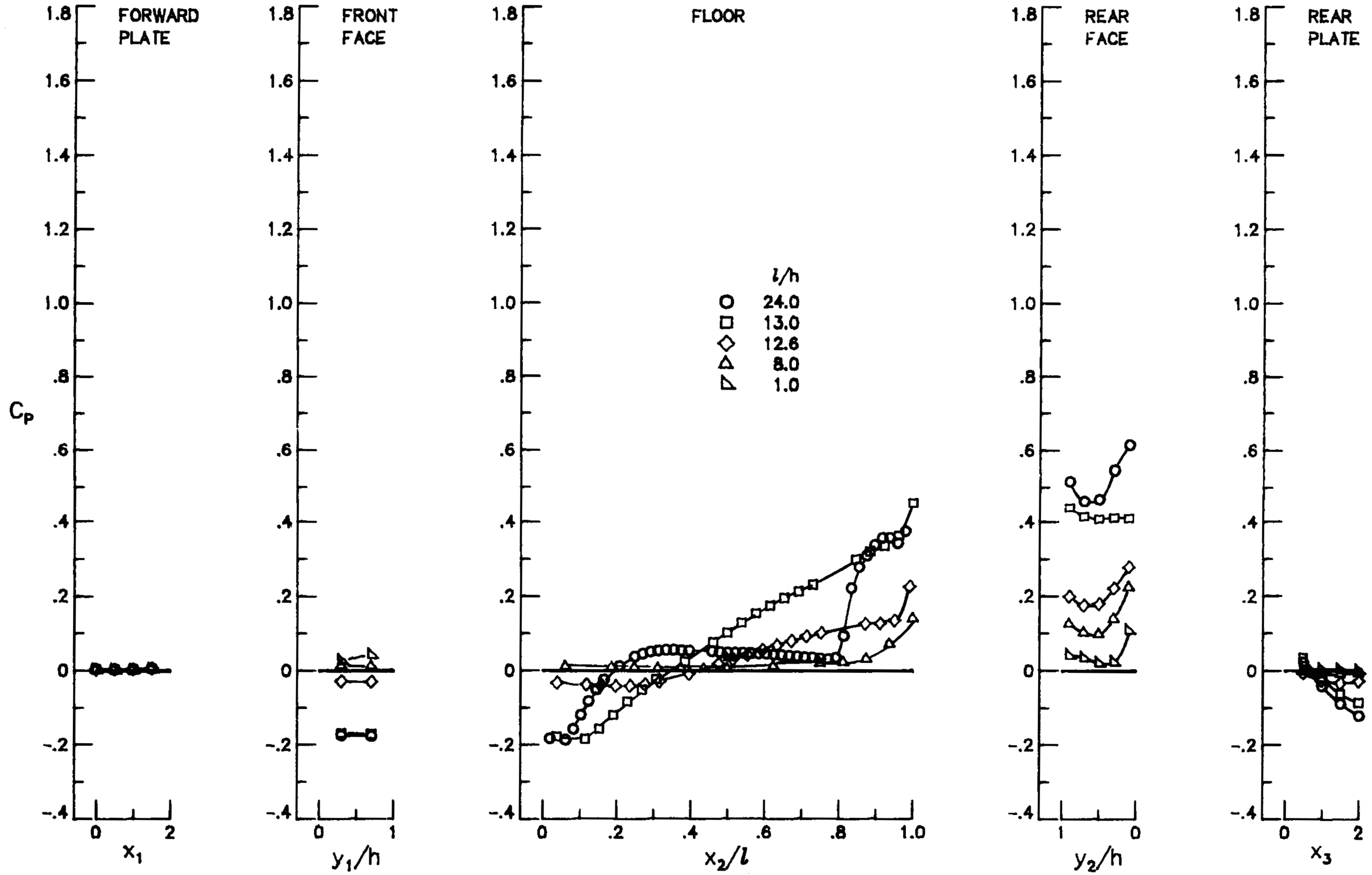

(b) $M_\infty = 2.16$; $h = 0.5$ in.

Figure 7. Continued.

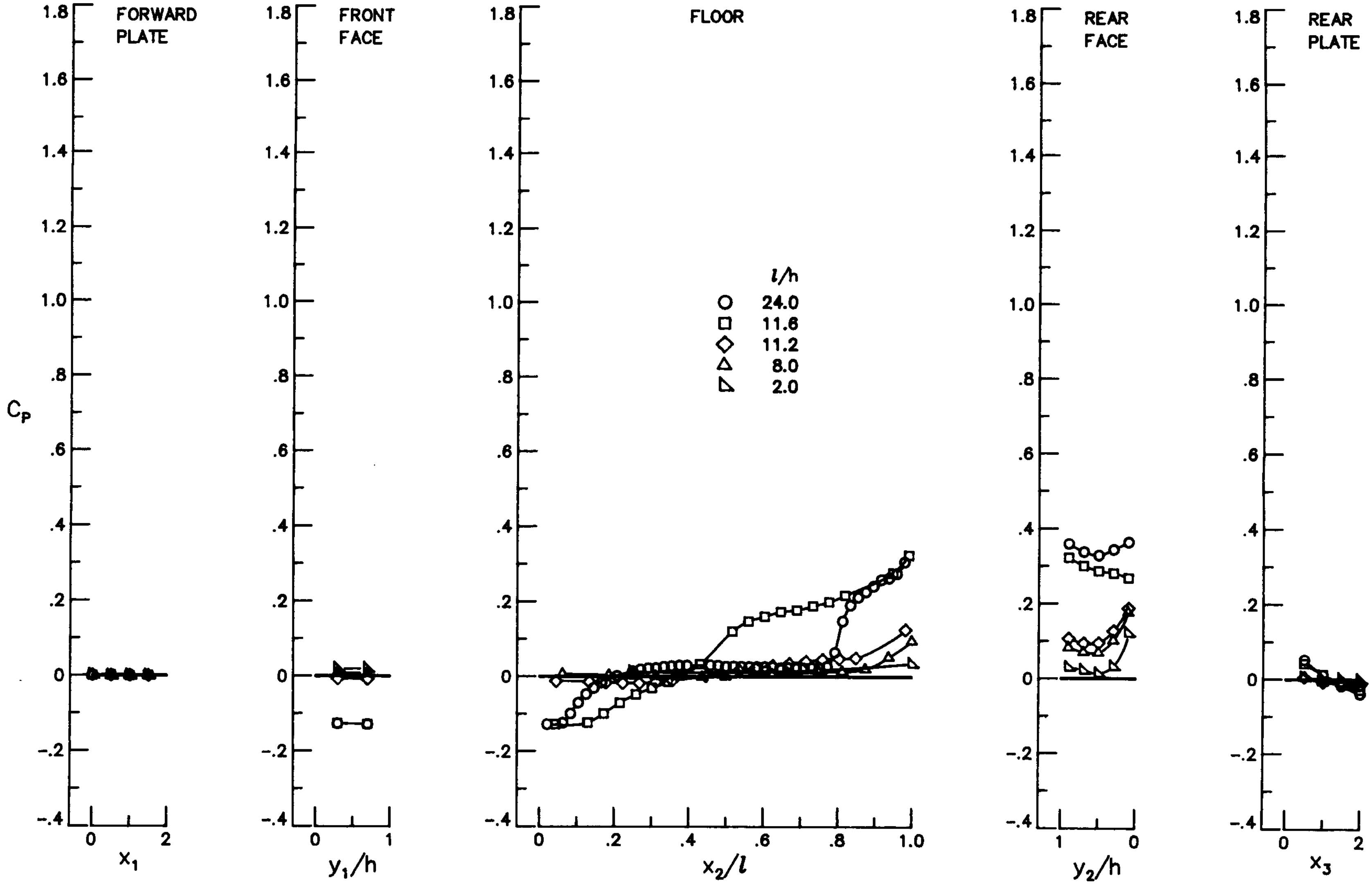

(c) $M_\infty = 2.86$; $h = 0.5$ in.

Figure 7. Continued.

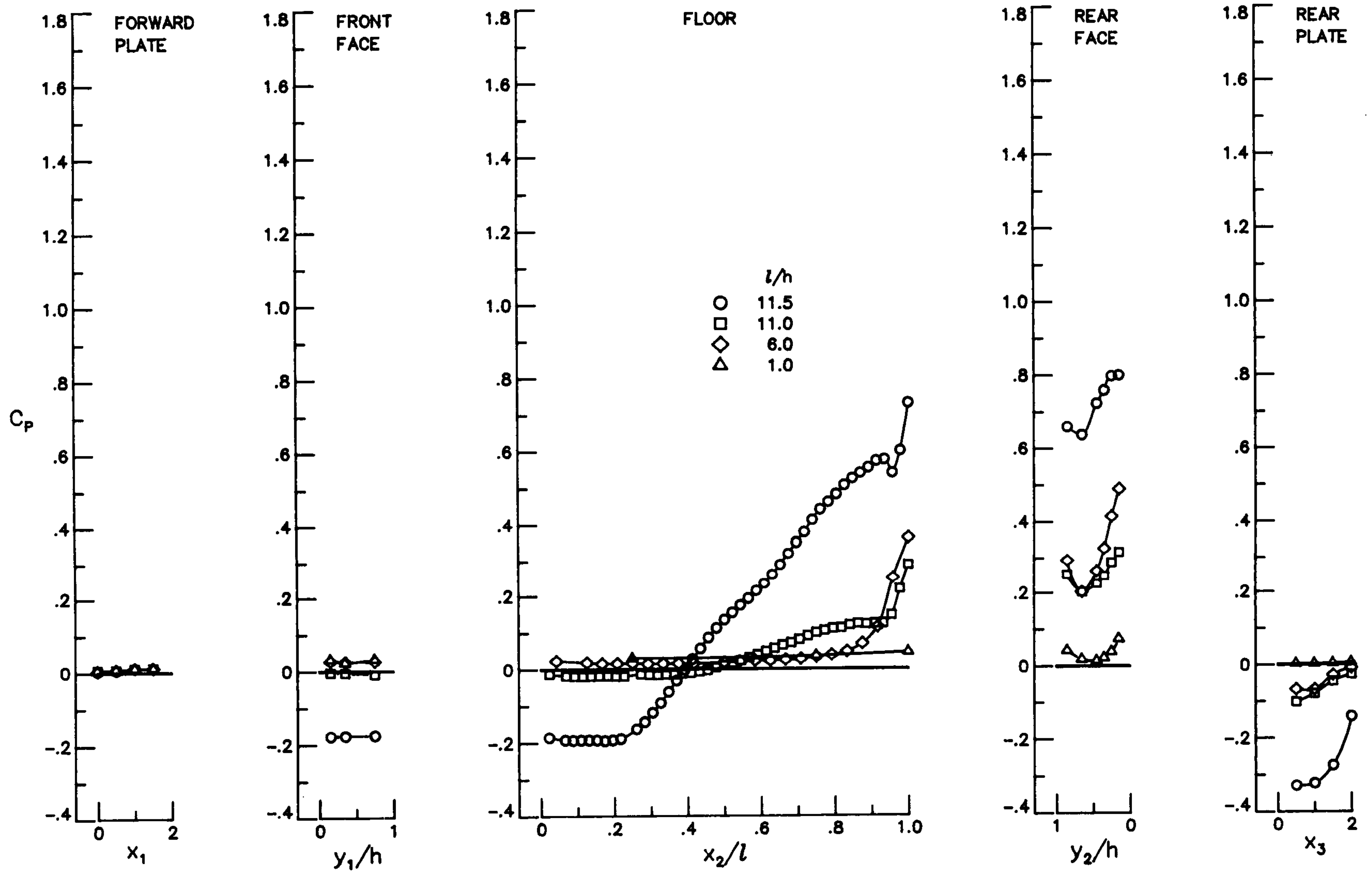

(d) $M_\infty = 1.50$; $h = 1.0$ in.

Figure 7. Continued.

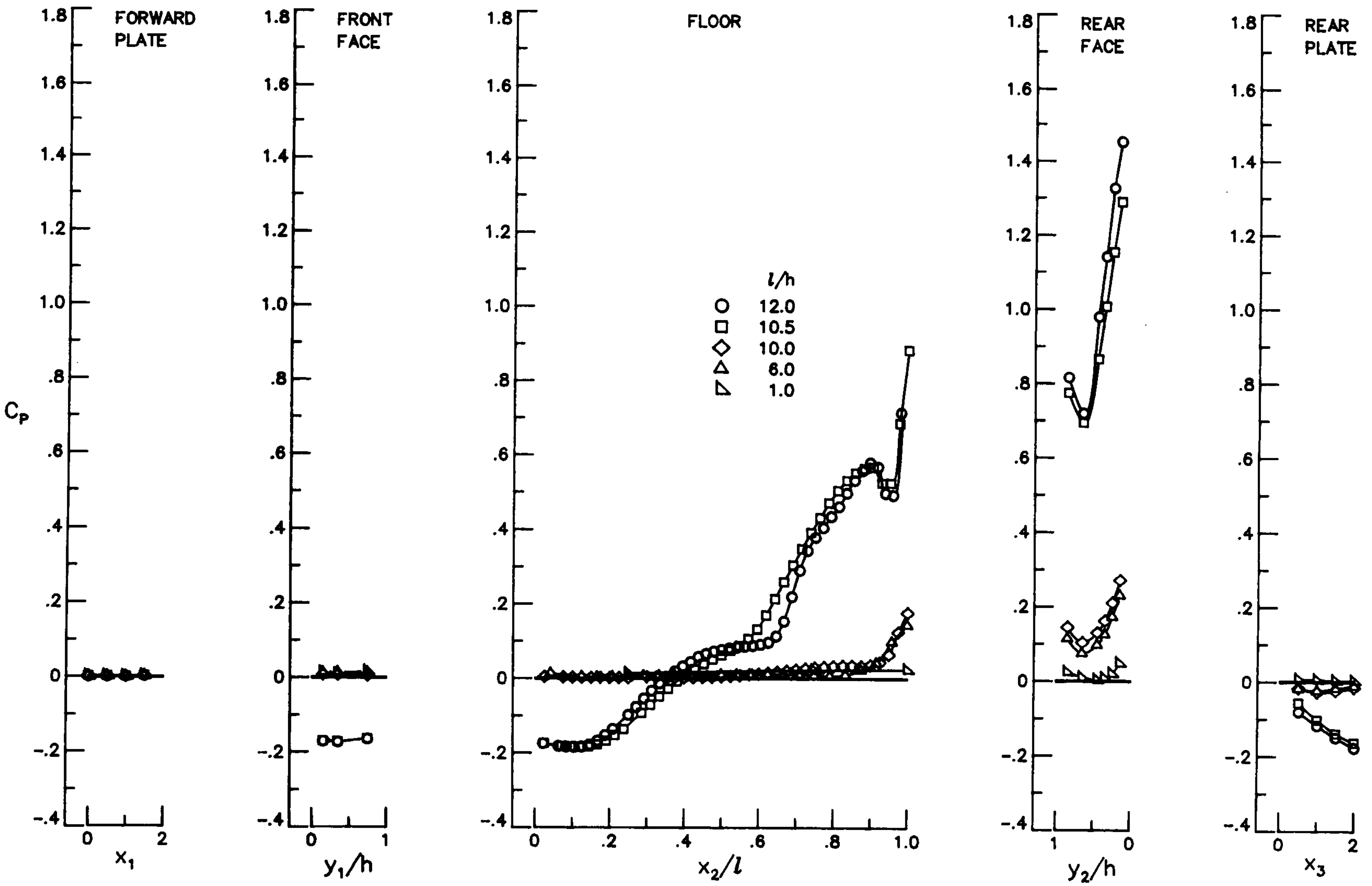

(e) $M_\infty = 2.16$; $h = 1.0$ in.

Figure 7. Continued.

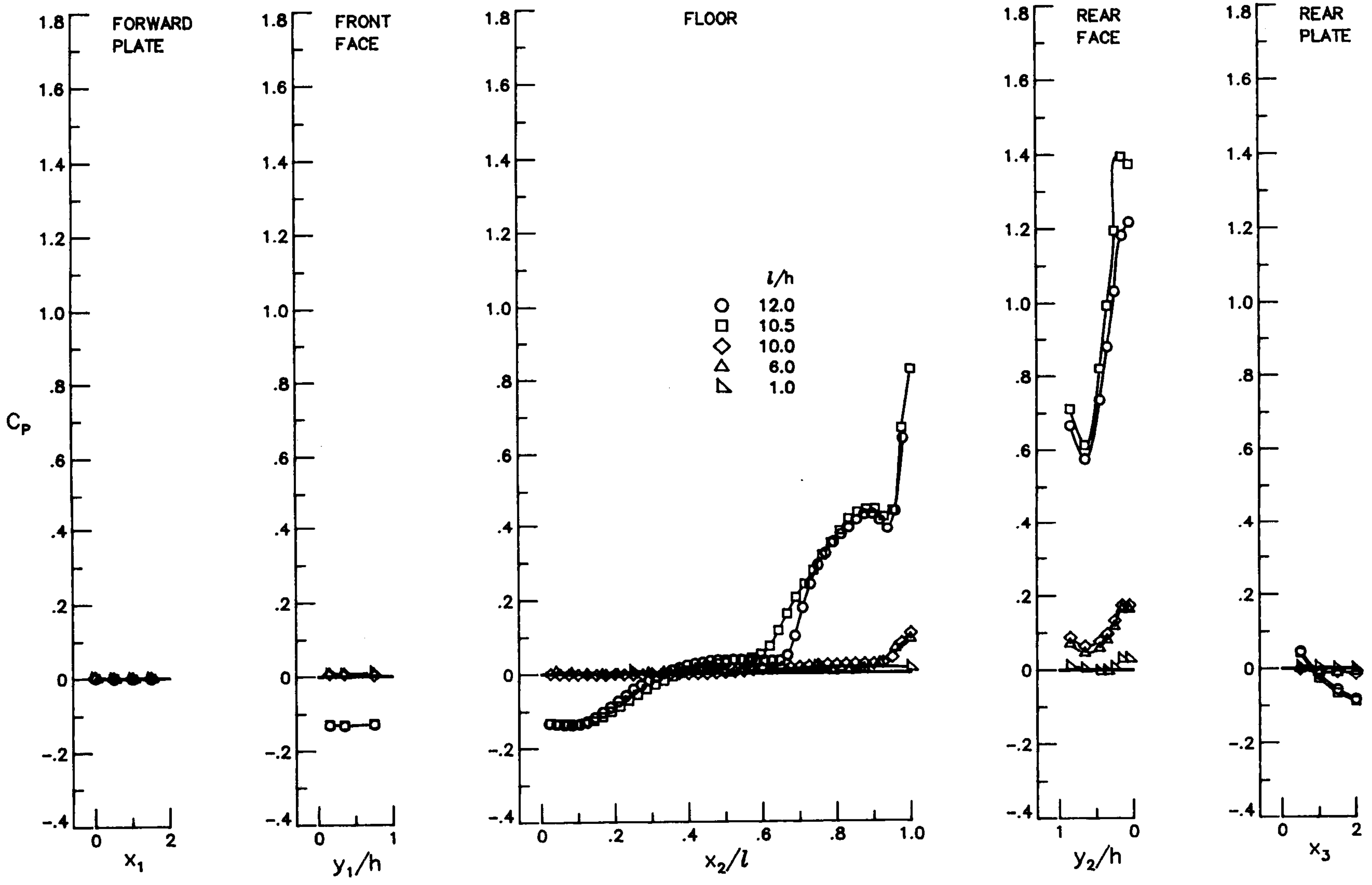

(f) $M_\infty = 2.86$; $h = 1.0$ in.

Figure 7. Continued.

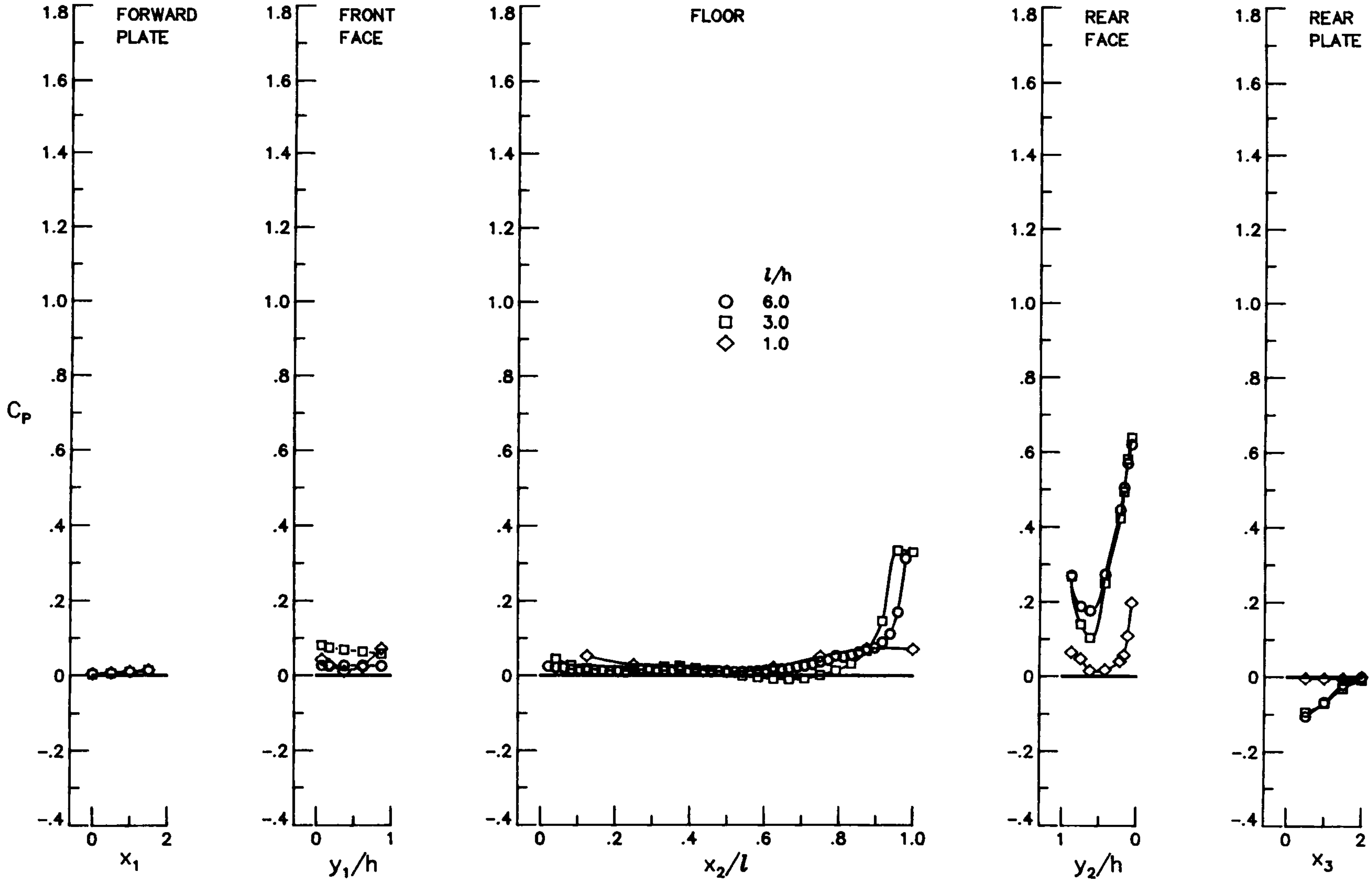

(g) $M_\infty = 1.50$; $h = 2.0$ in.

Figure 7. Continued.

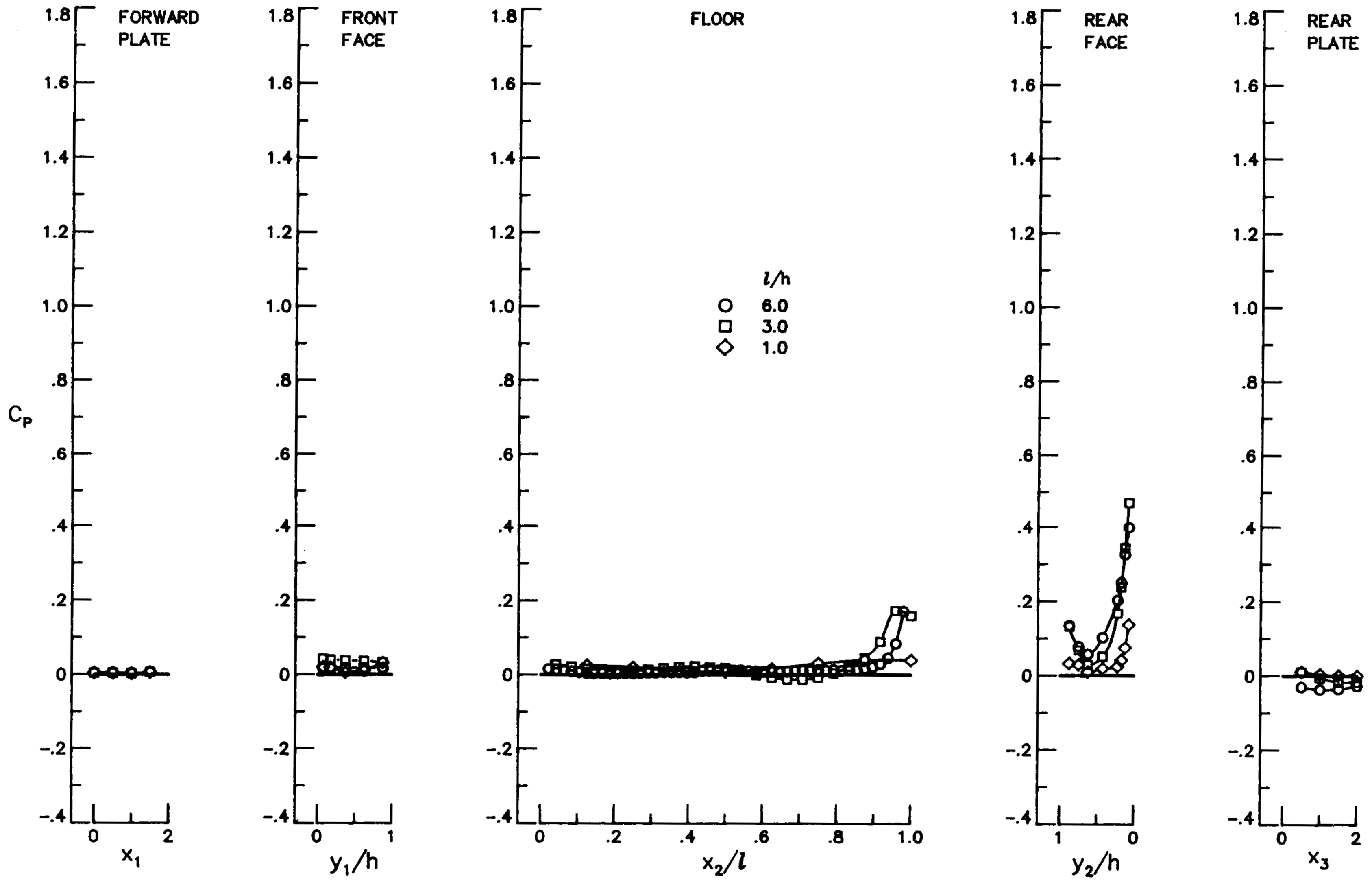

(h) $M_\infty = 2.16$; $h = 2.0$ in.

Figure 7. Continued.

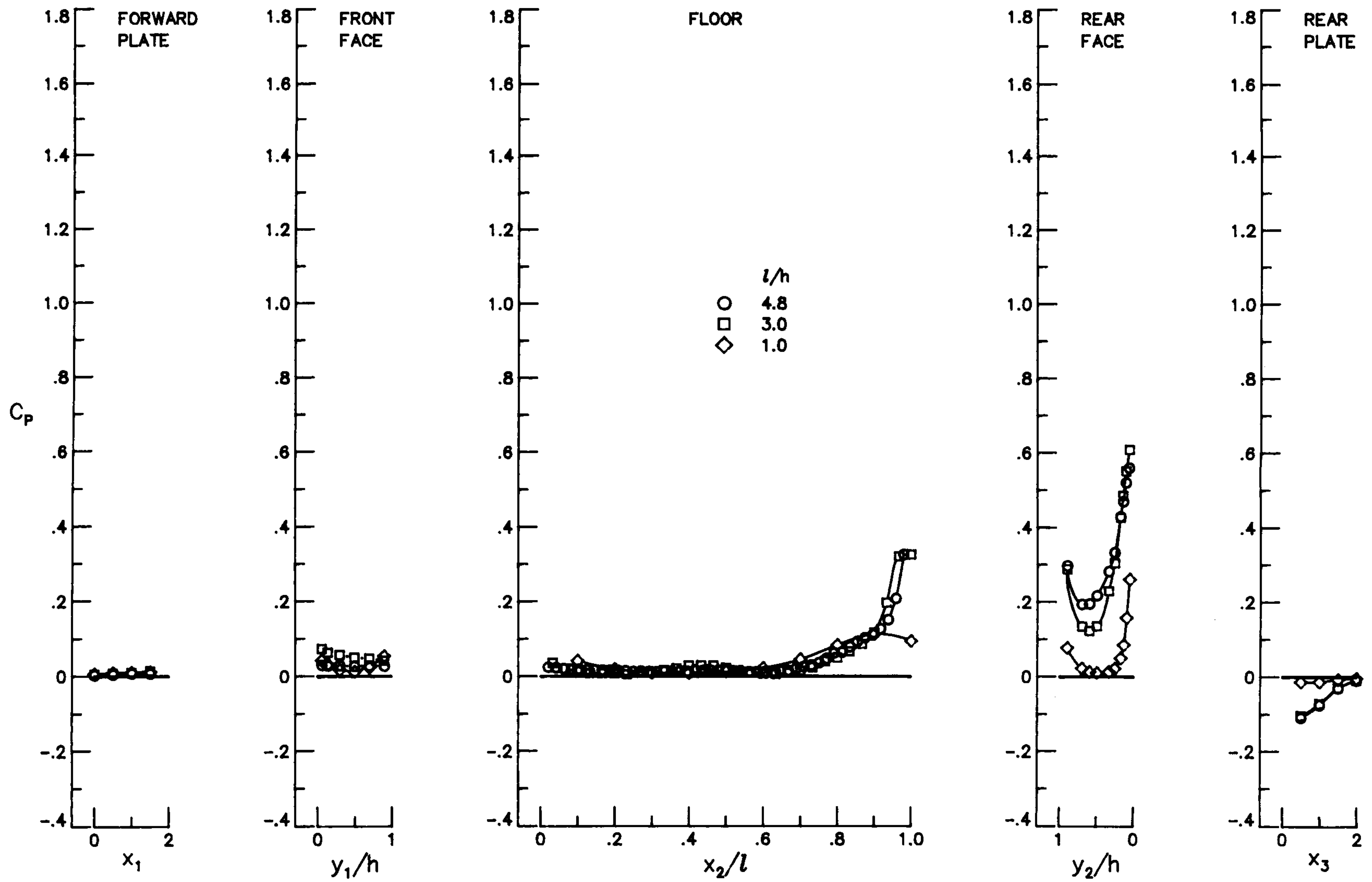

(i) $M_\infty = 1.50$; $h = 2.5$ in.

Figure 7. Continued.

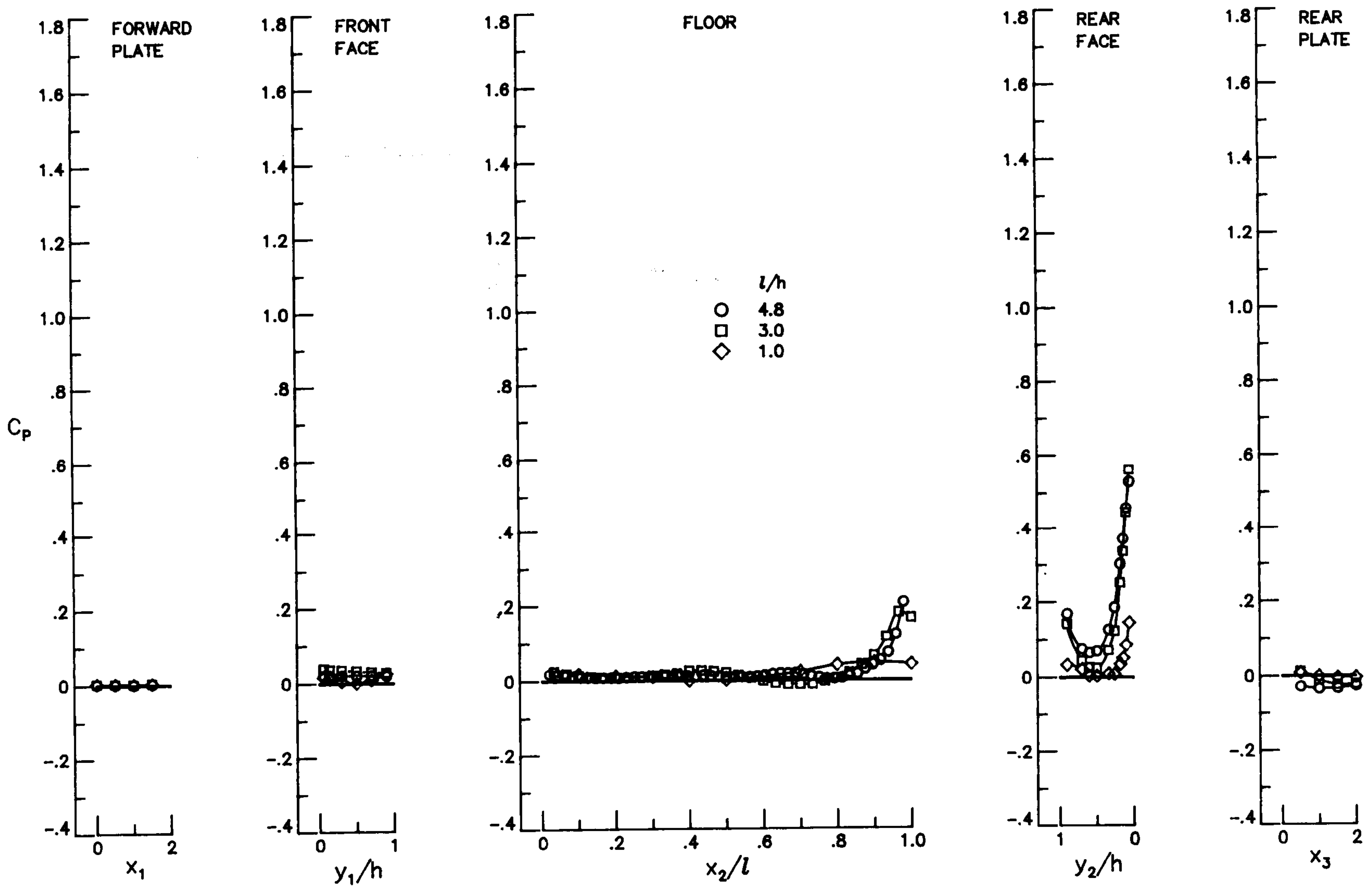

(j) $M_\infty = 2.16$; $h = 2.5$ in.

Figure 7. Concluded.

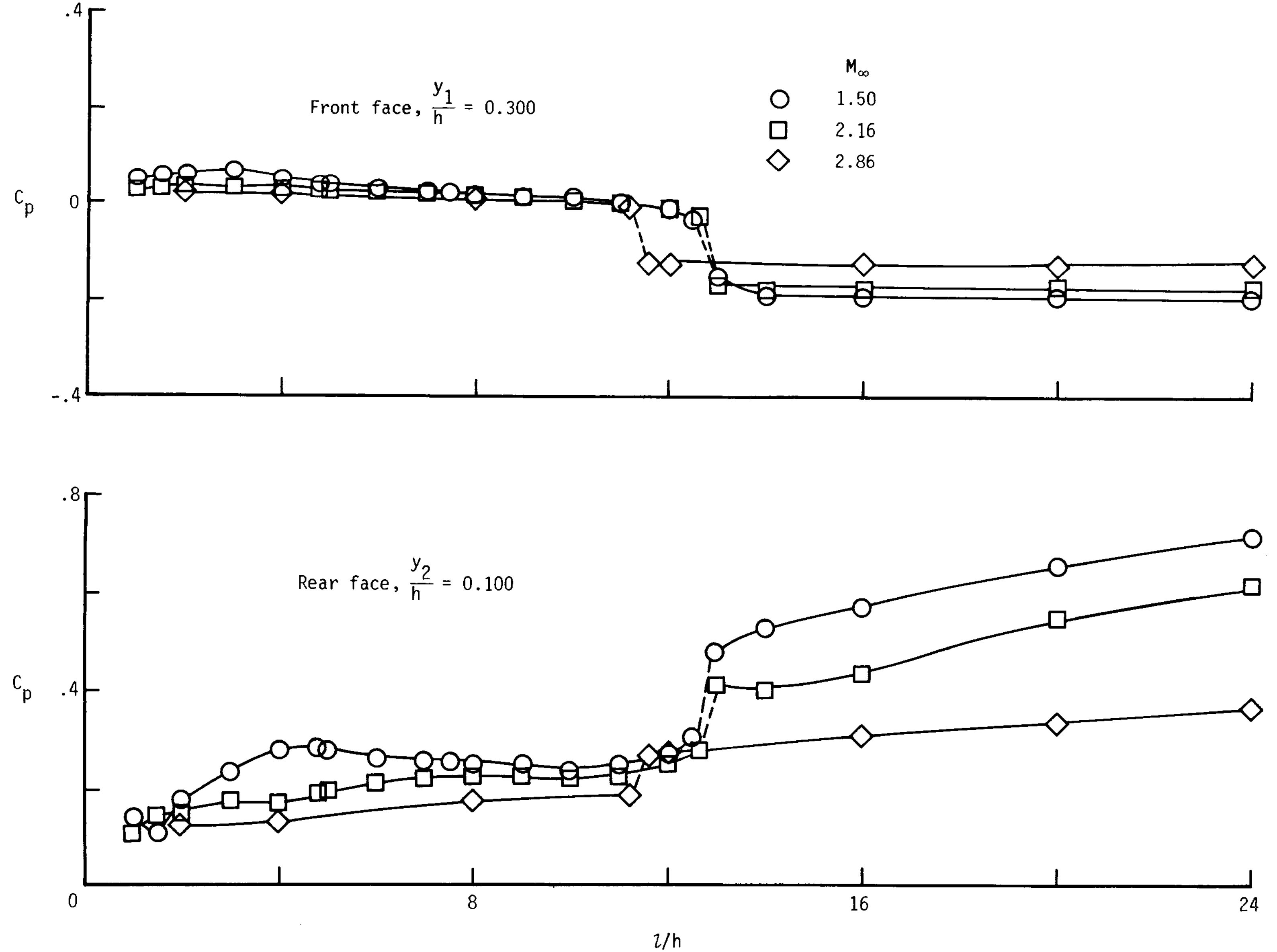

(a) $h = 0.5$ in.

Figure 8. Variation of C_p with l/h at outer-edge region of cavity front and rear faces. $w = 2.5$ in.

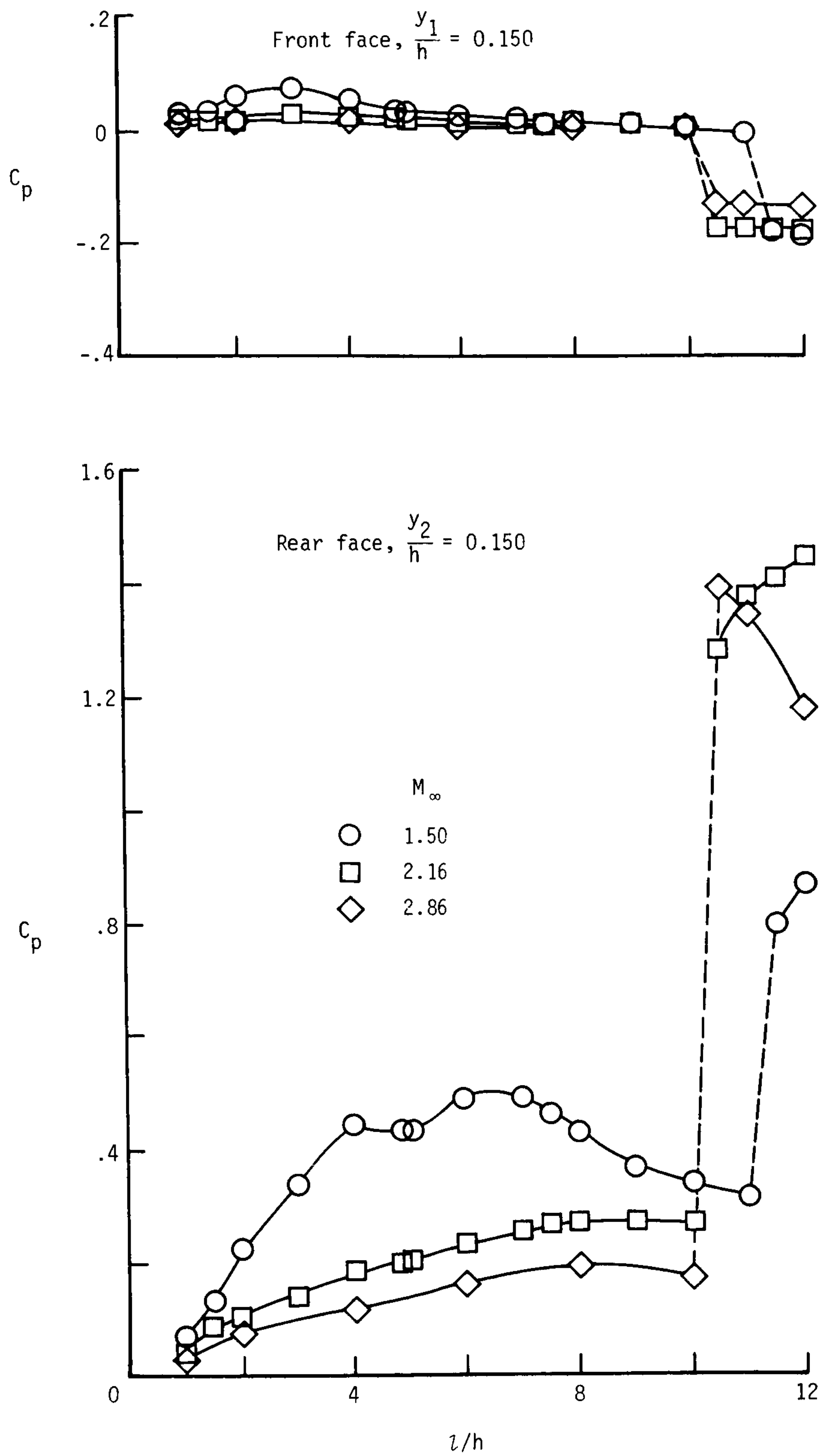

(b) $h = 1.0$ in.

Figure 8. Continued.

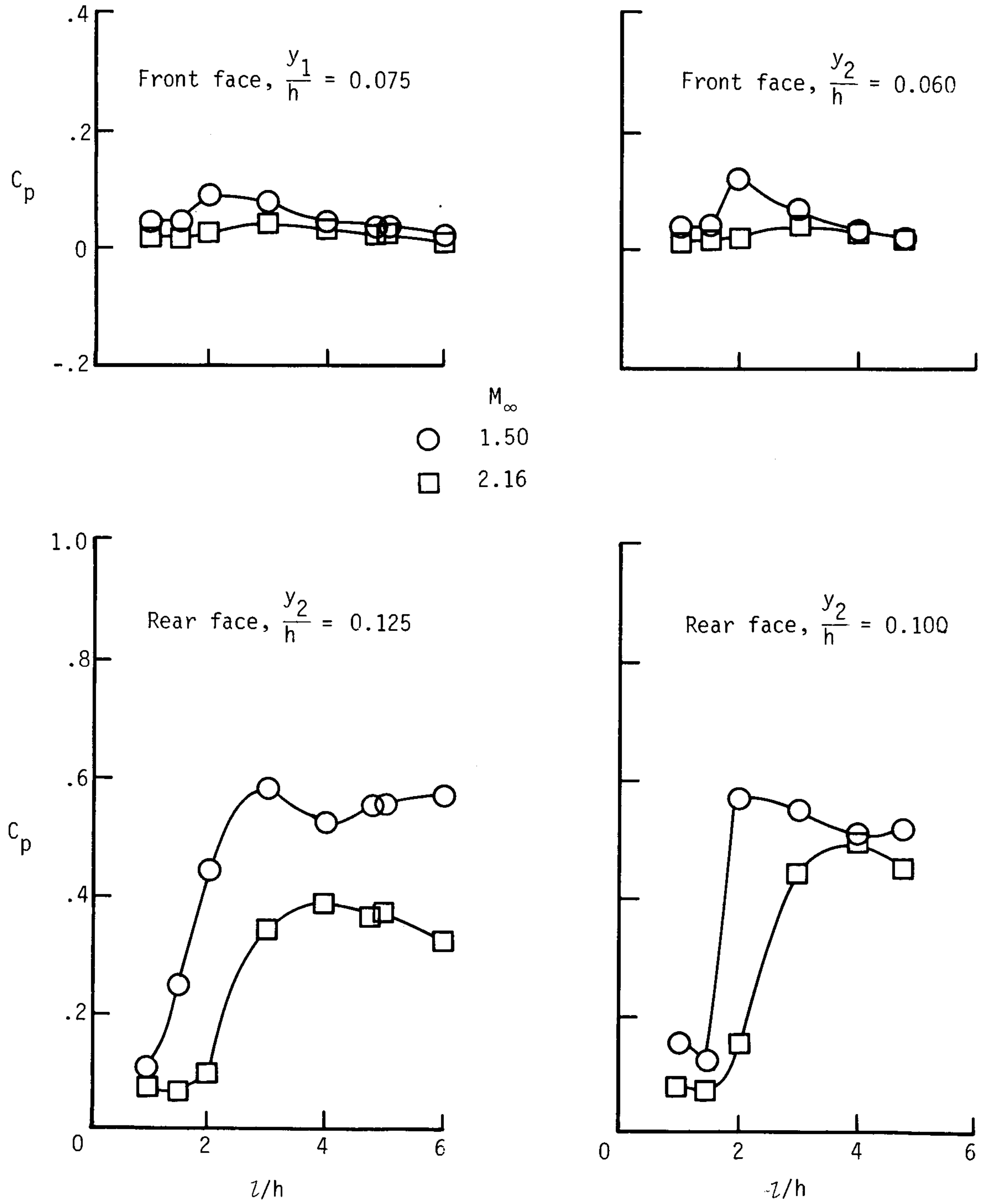

(c) $h = 2.0$ in.

(d) $h = 2.5$ in.

Figure 8. Concluded.

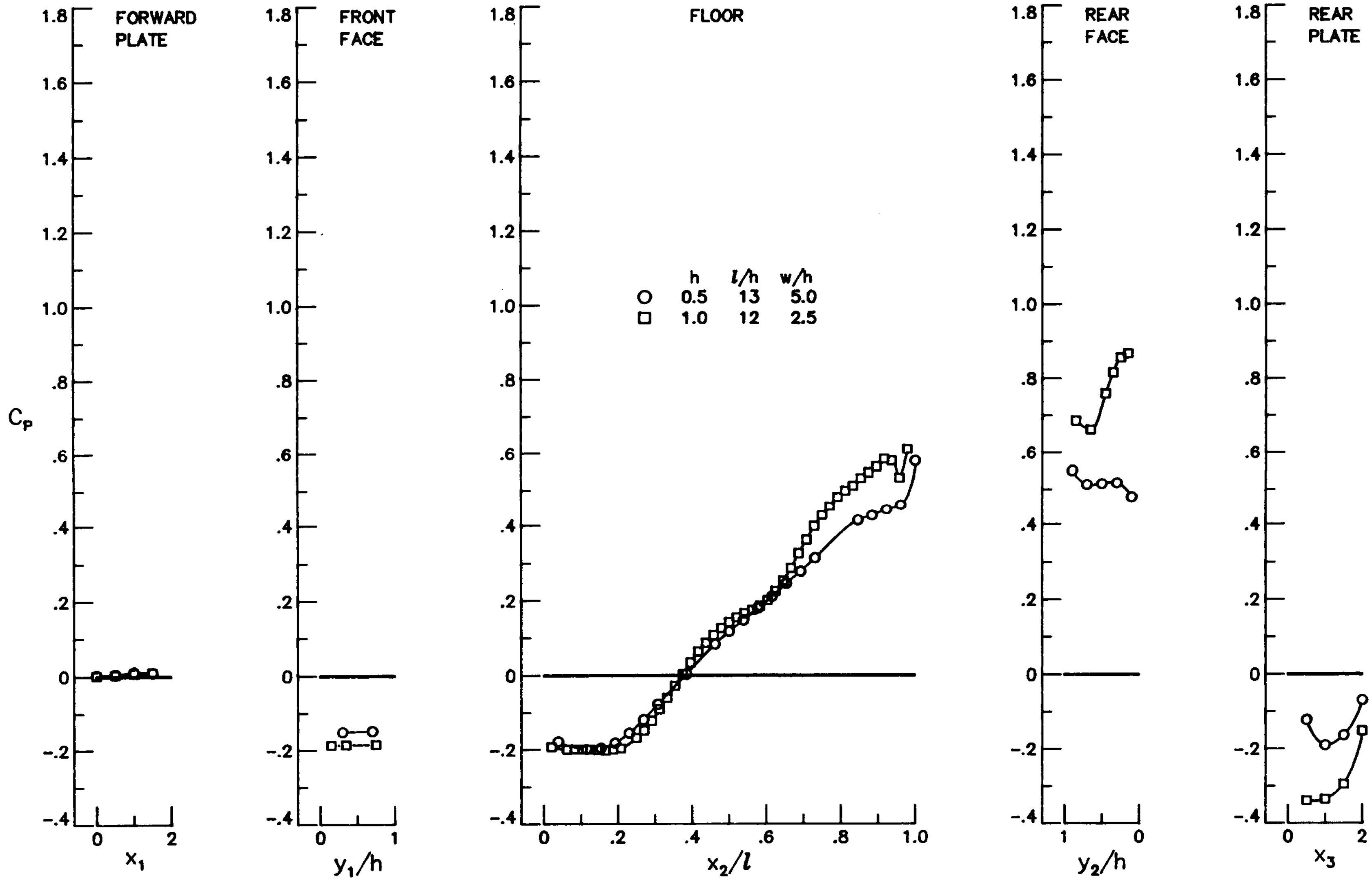

(a) $M_\infty = 1.50$; $l/h \approx 12$.

Figure 9. Effect of cavity depth on cavity centerline pressure distributions. $w = 2.5$ in.

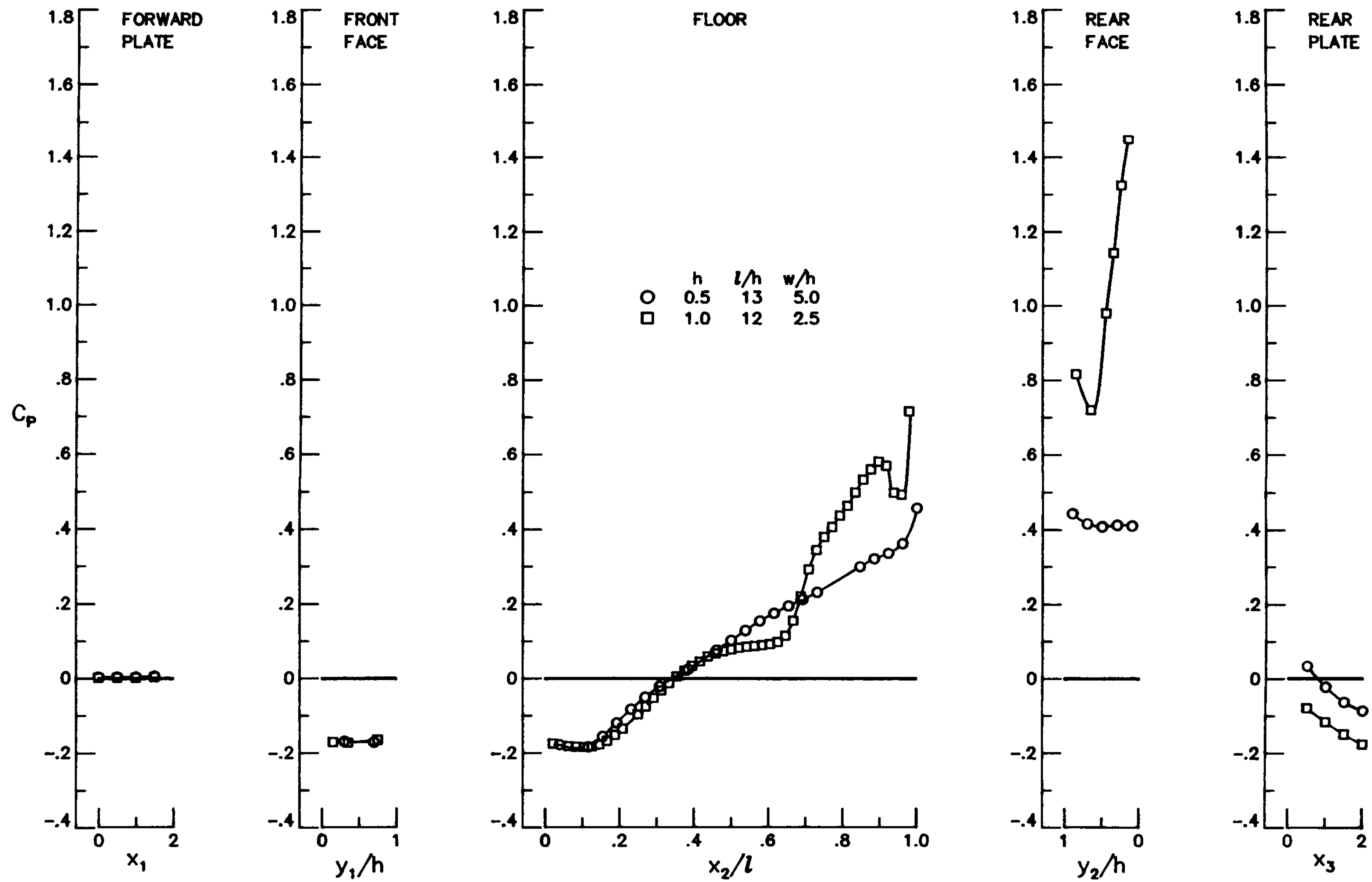

(b) $M_\infty = 2.16$; $l/h \approx 12$.

Figure 9. Continued.

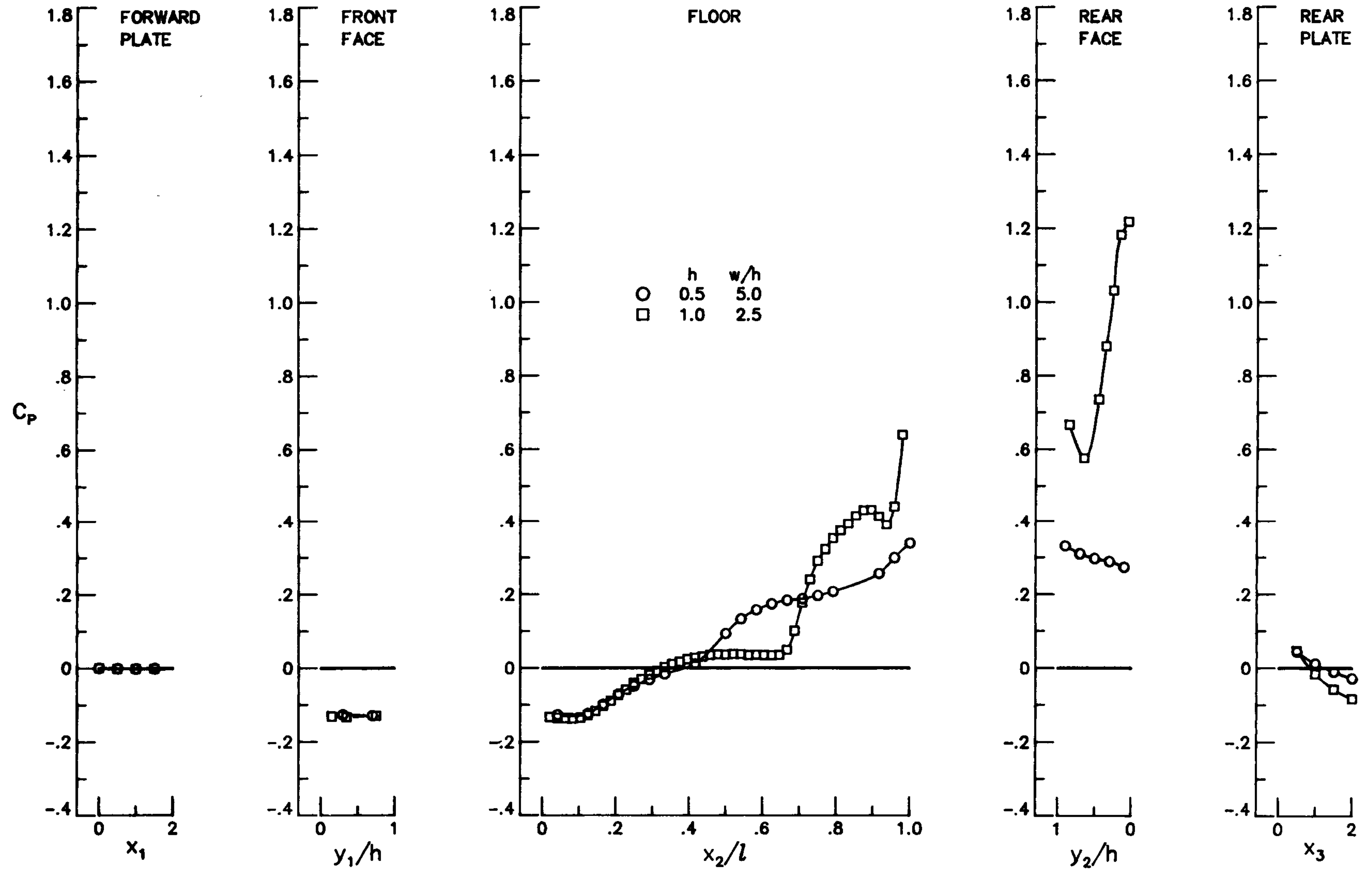

(c) $M_\infty = 2.86; l/h = 12$.

Figure 9. Continued.

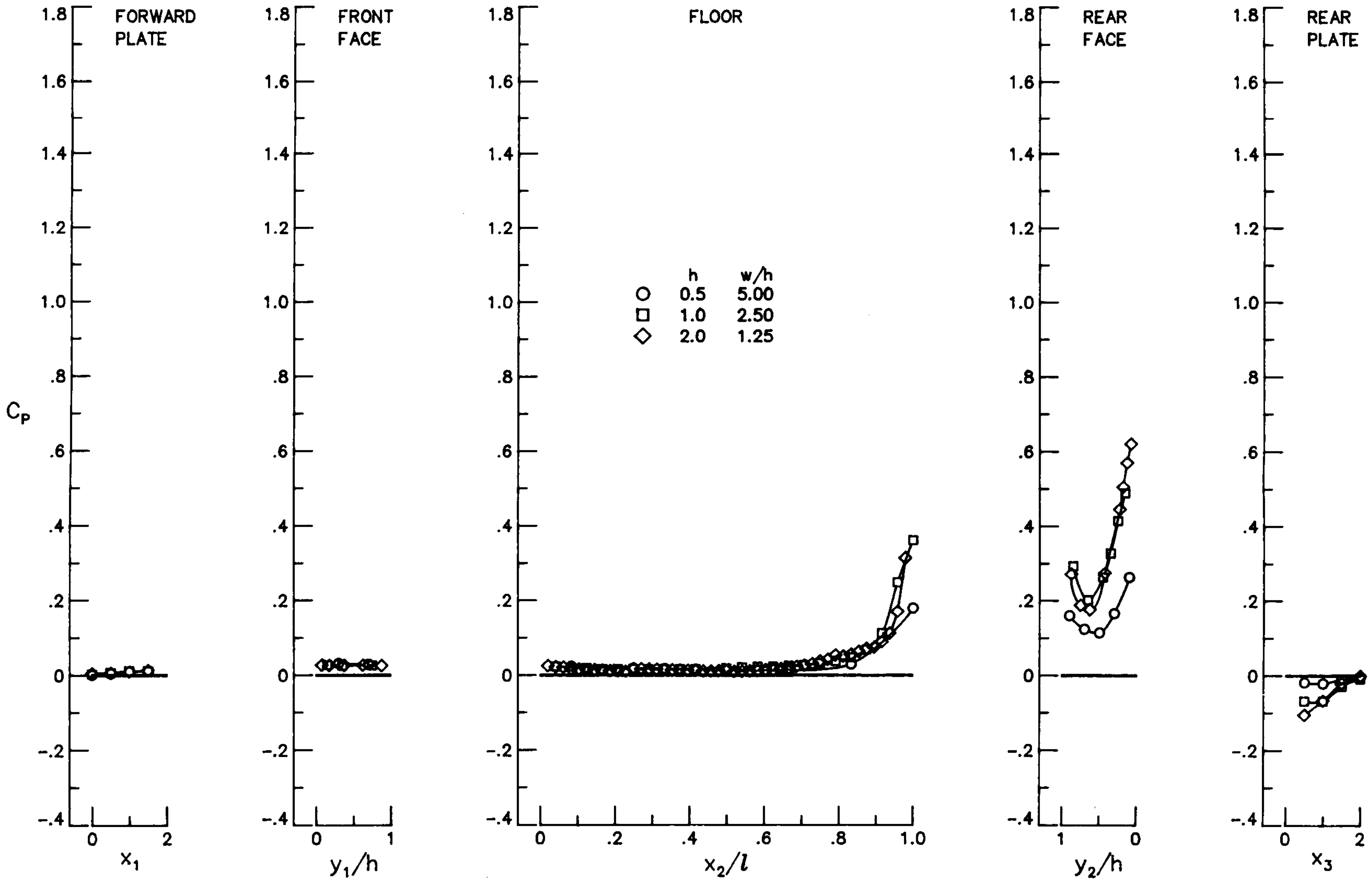

(d) $M_\infty = 1.50$; $l/h = 6$.

Figure 9. Continued.

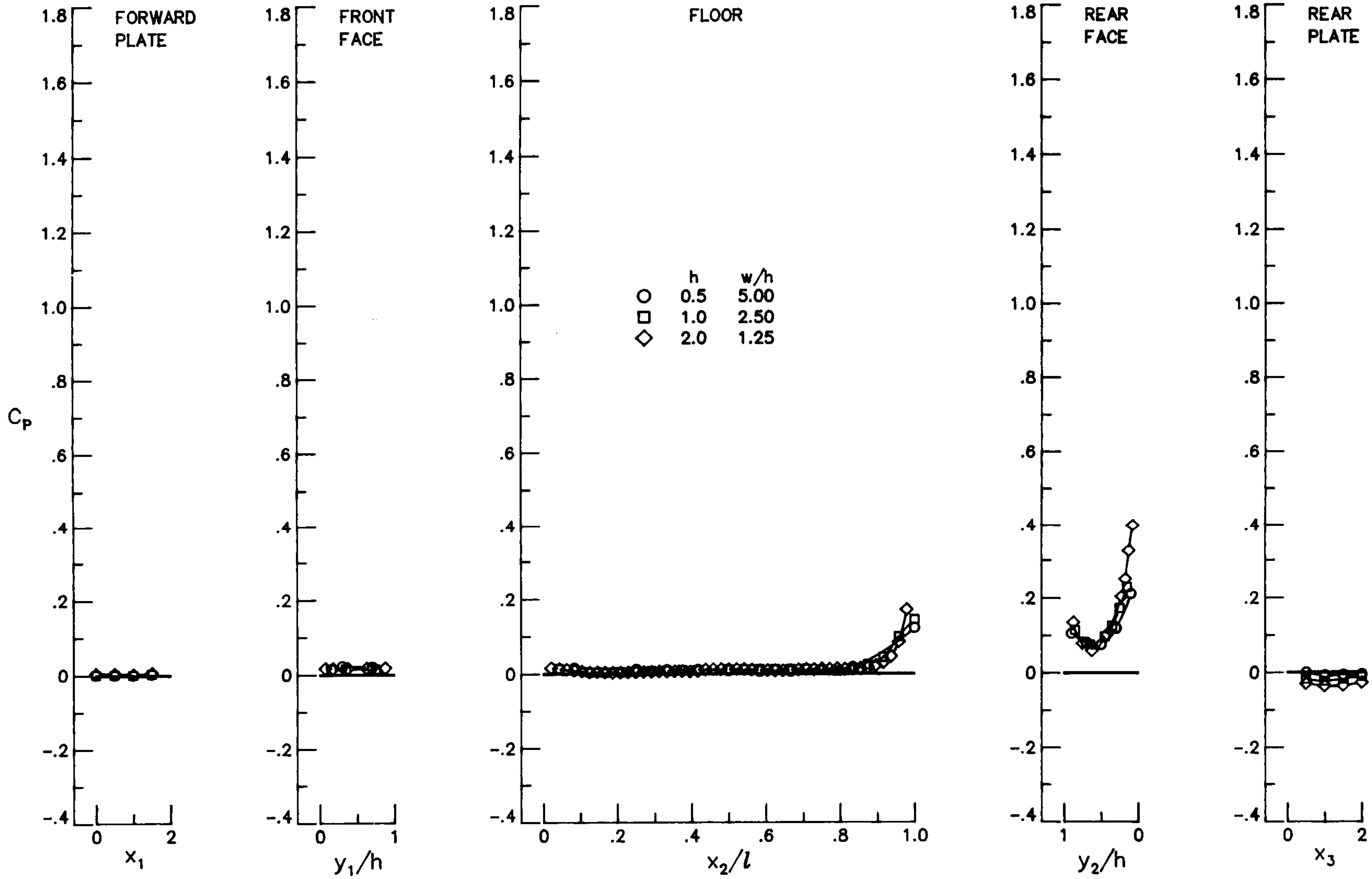

(e) $M_\infty = 2.16$; $l/h = 6$.

Figure 9. Continued.

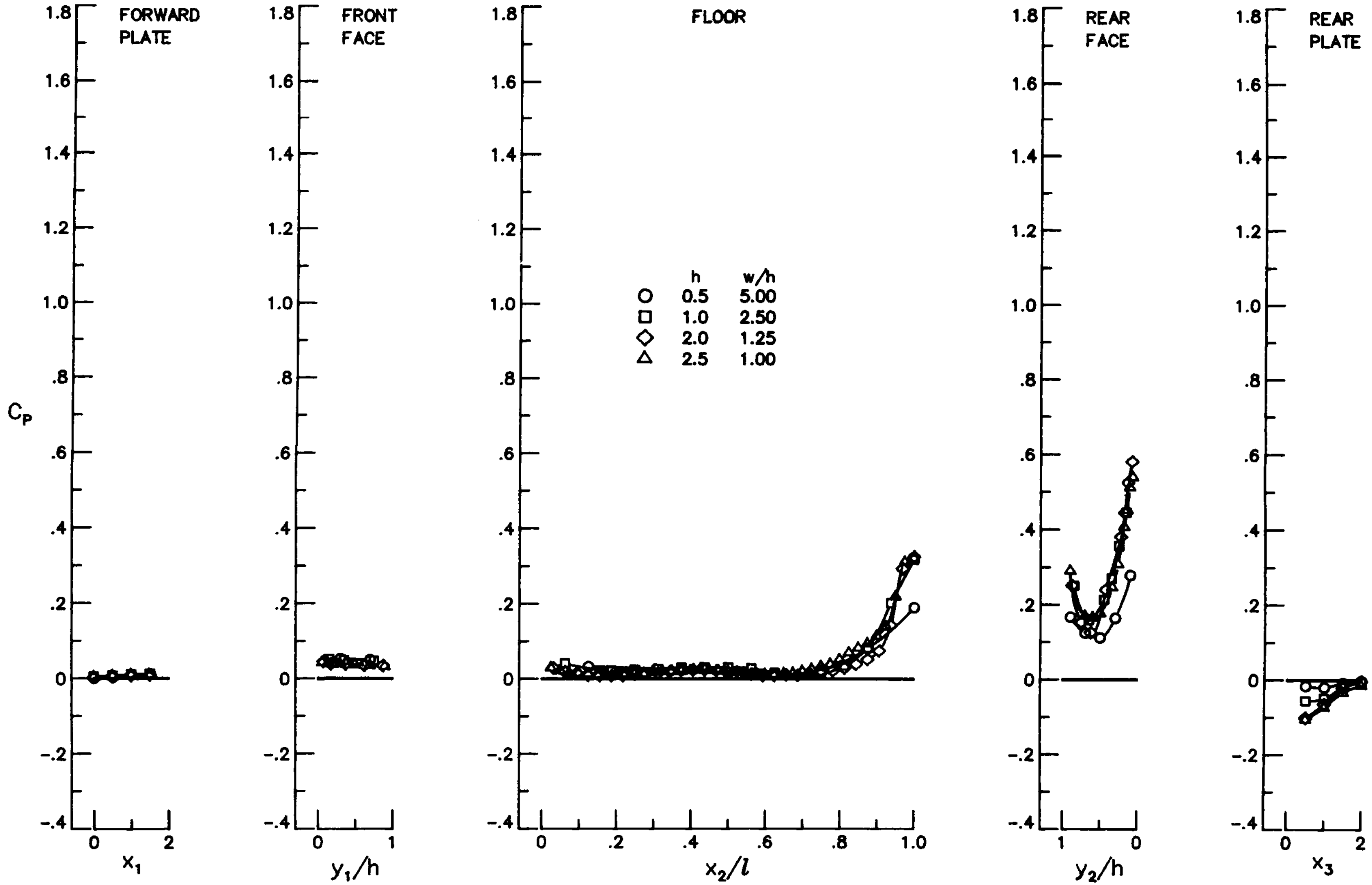

(f) $M_\infty = 1.50$; $l/h = 4$.

Figure 9. Continued.

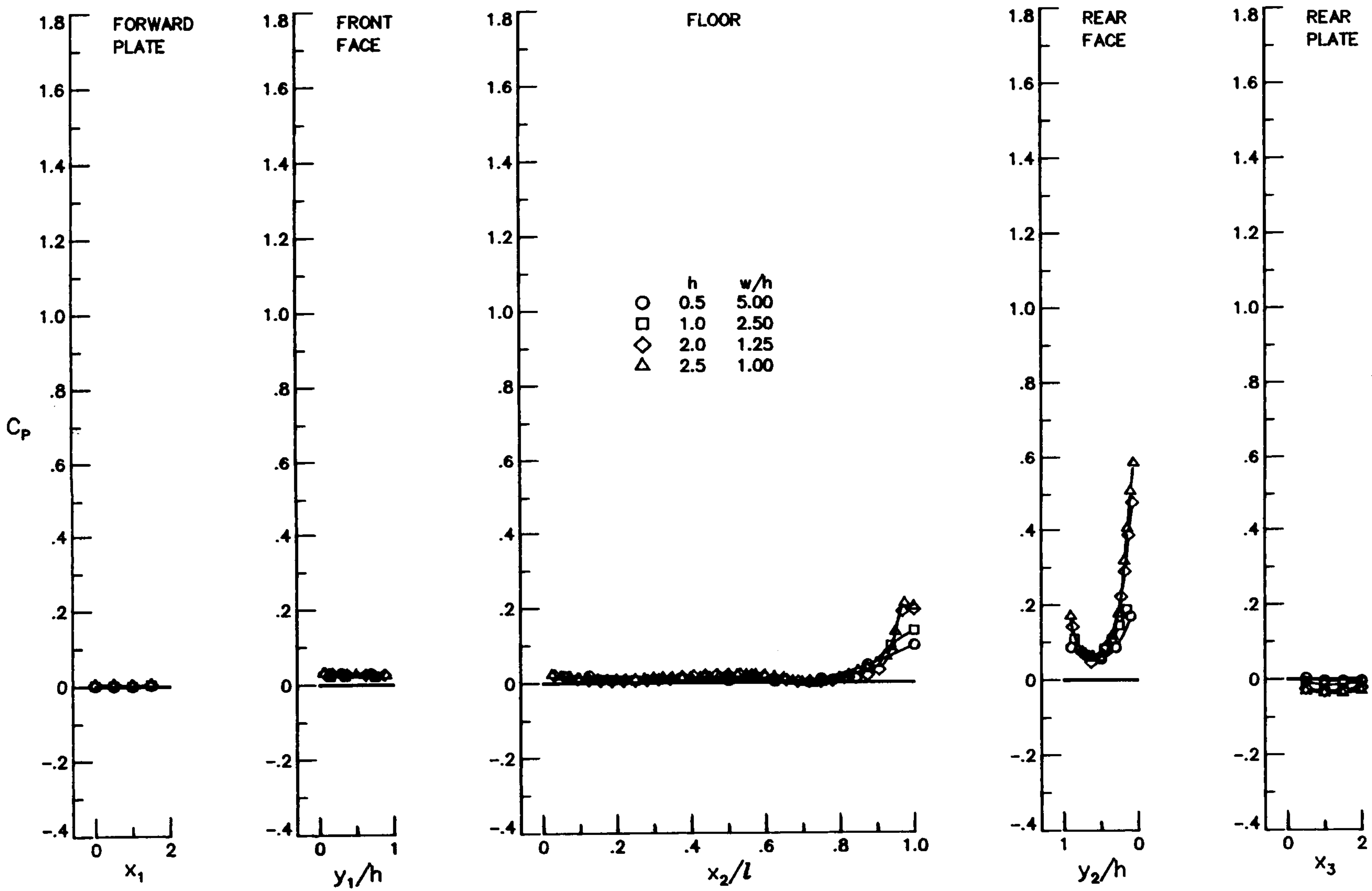

(g) $M_\infty = 2.16$; $l/h = 4$.

Figure 9. Continued.

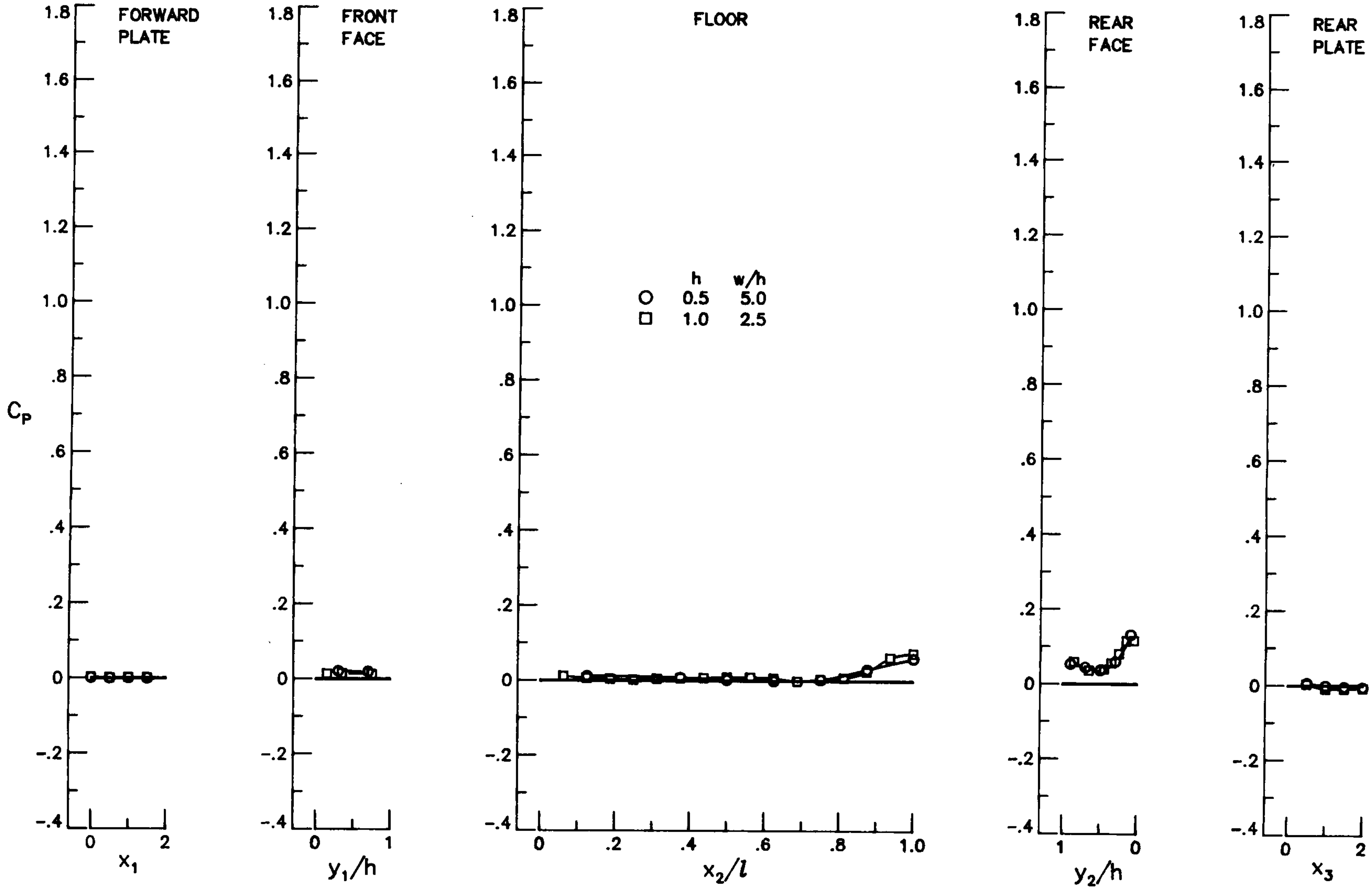

(h) $M_\infty = 2.86$; $l/h = 4$.

Figure 9. Continued.

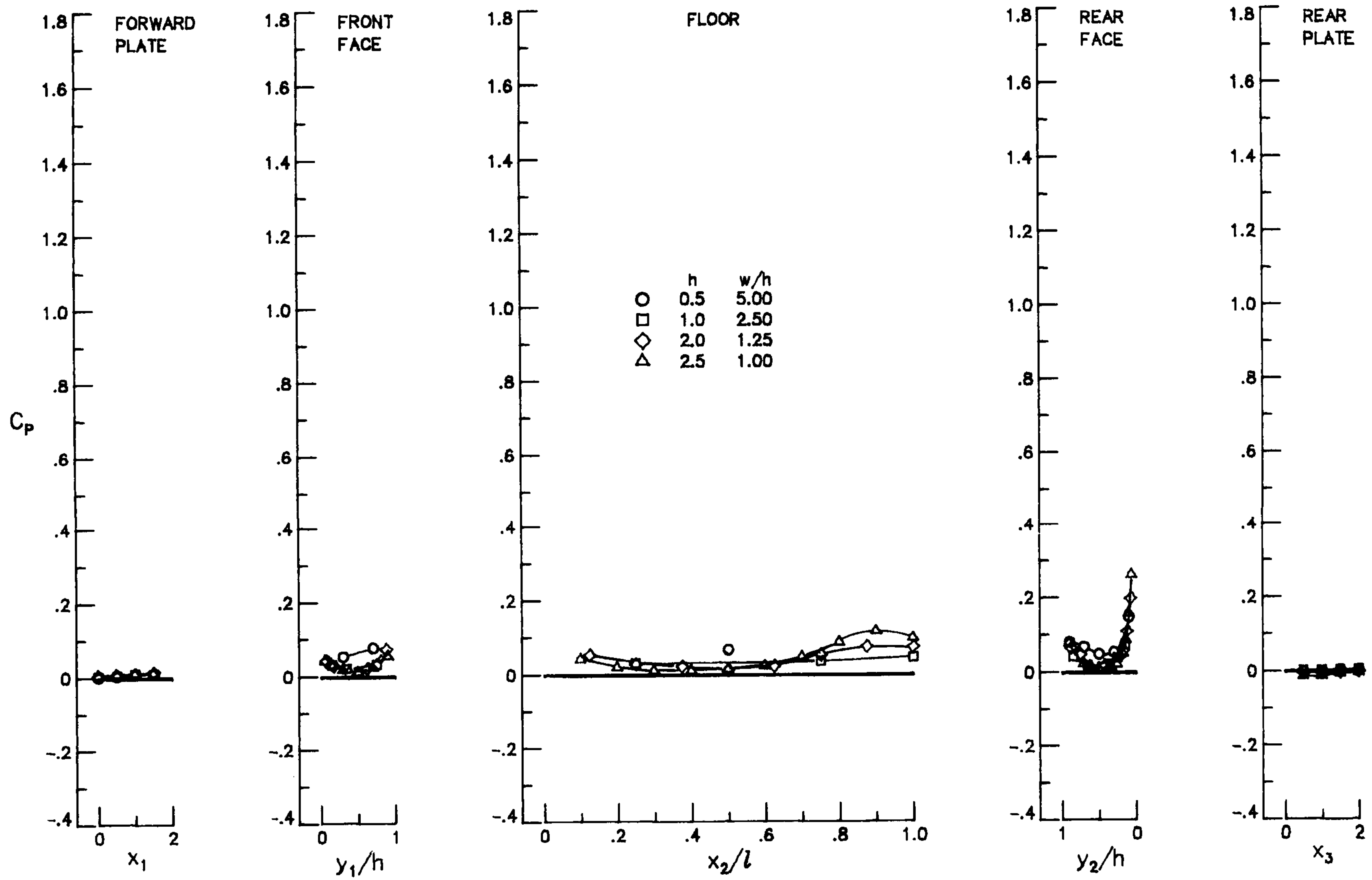

(i) $M_\infty = 1.50$; $l/h = 1$.

Figure 9. Continued.

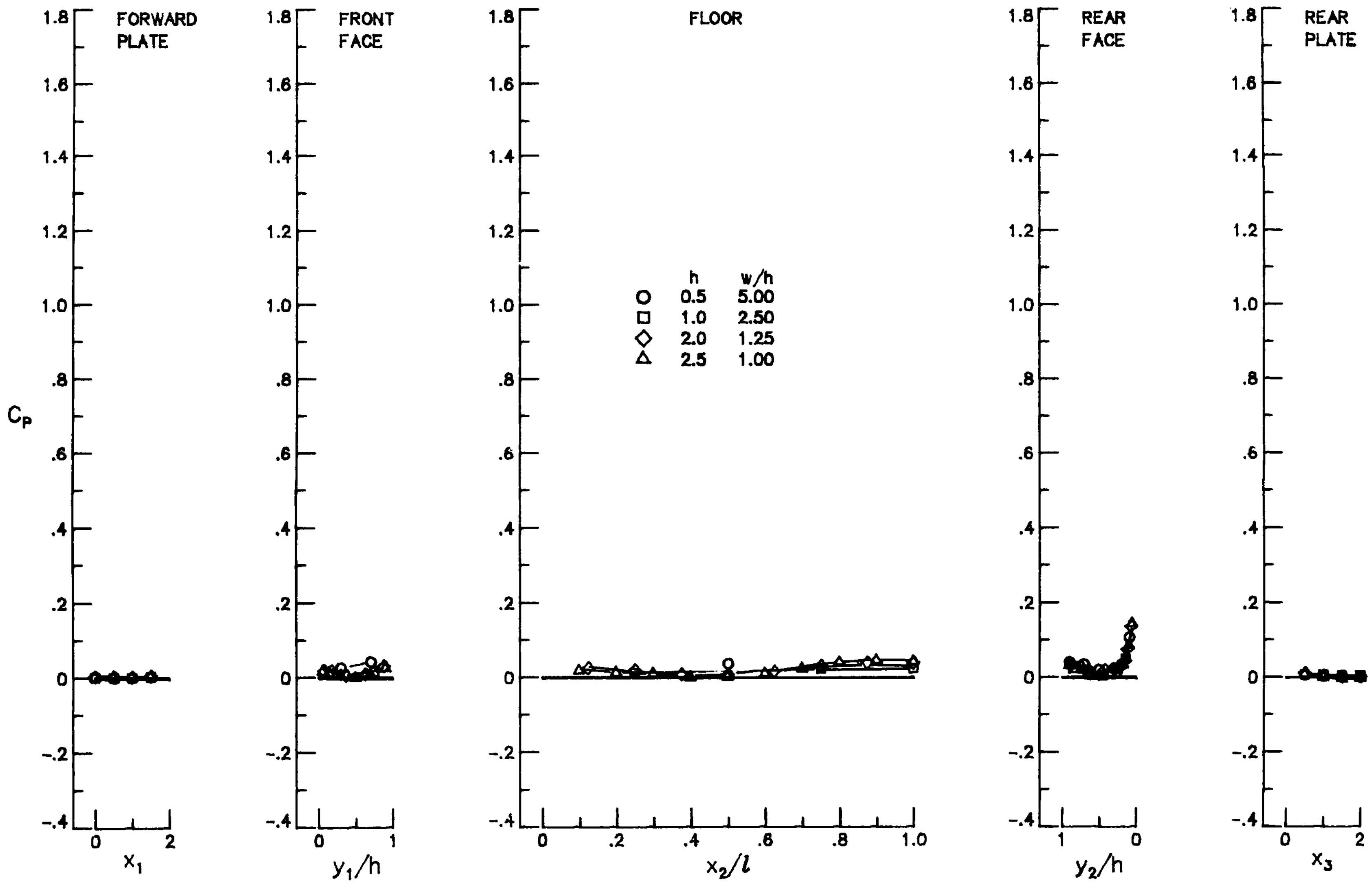

(j) $M_\infty = 2.16$; $l/h = 1$.

Figure 9. Concluded.

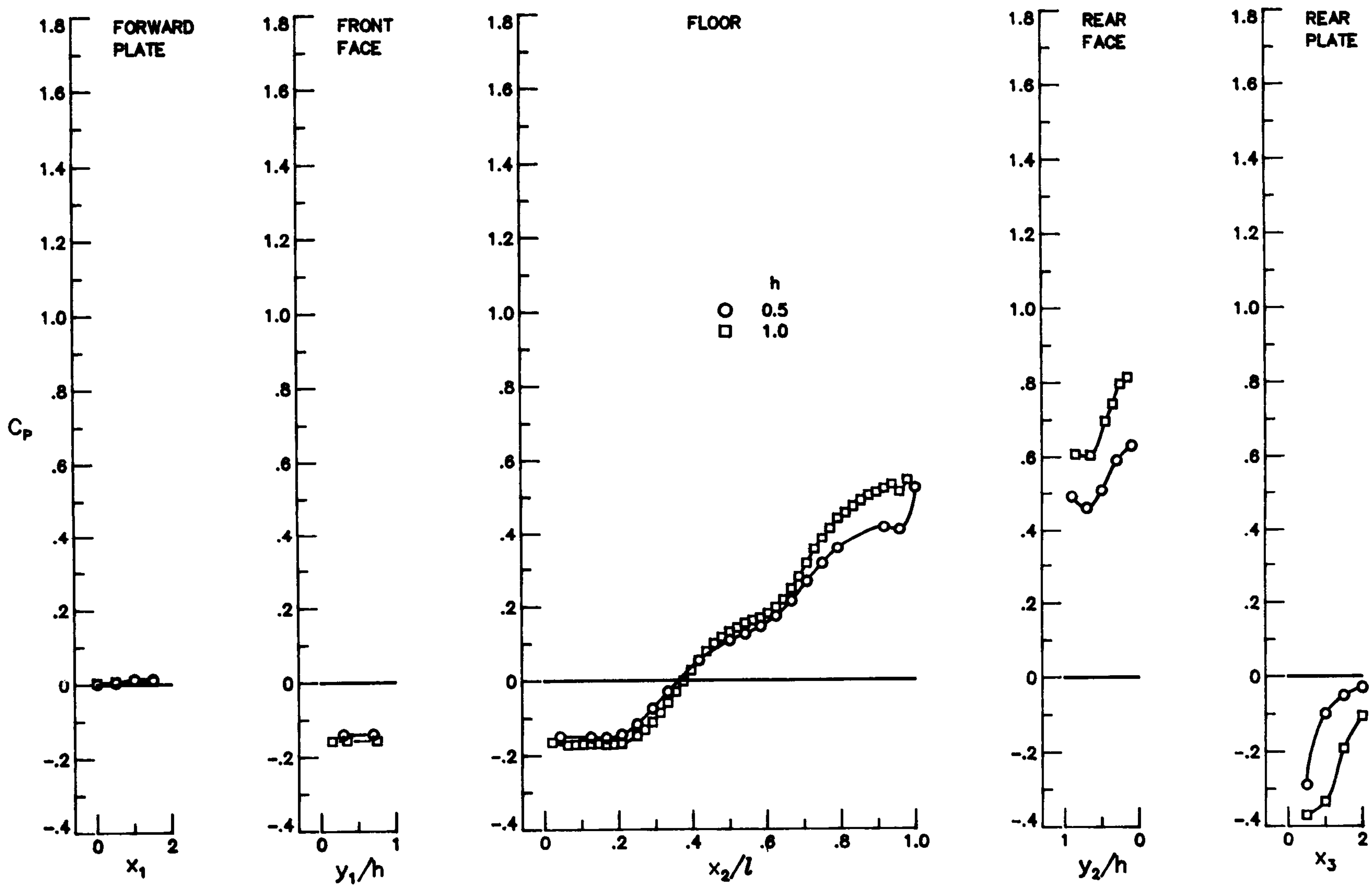

(a) $M_\infty = 1.50$; $l/h = 12$.

Figure 10. Correlation of cavity pressure distributions based on l/h and w/h. $w/h = 2.0$.

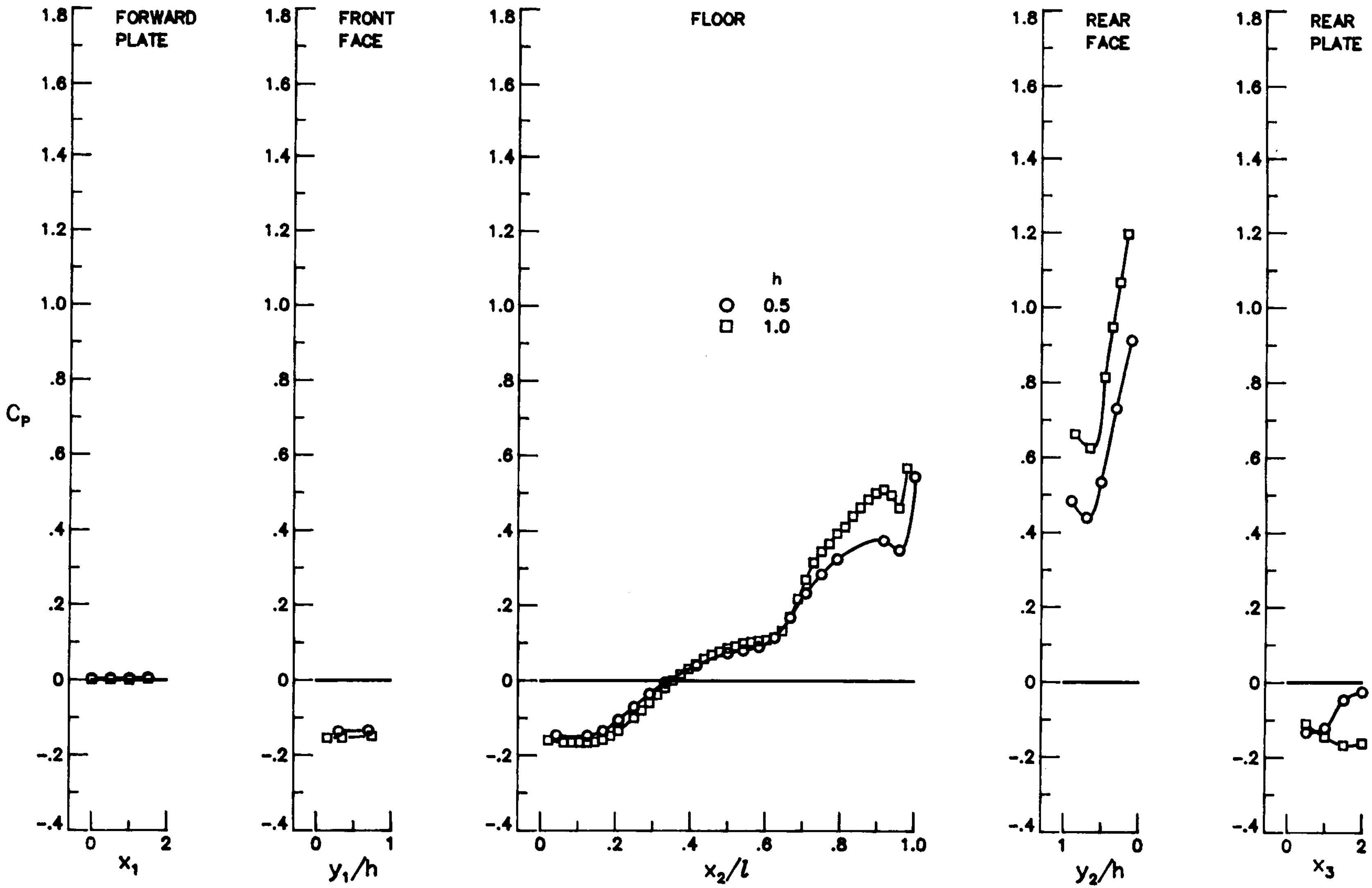

(b) $M_\infty = 2.16$; $l/h = 12$.

Figure 10. Continued.

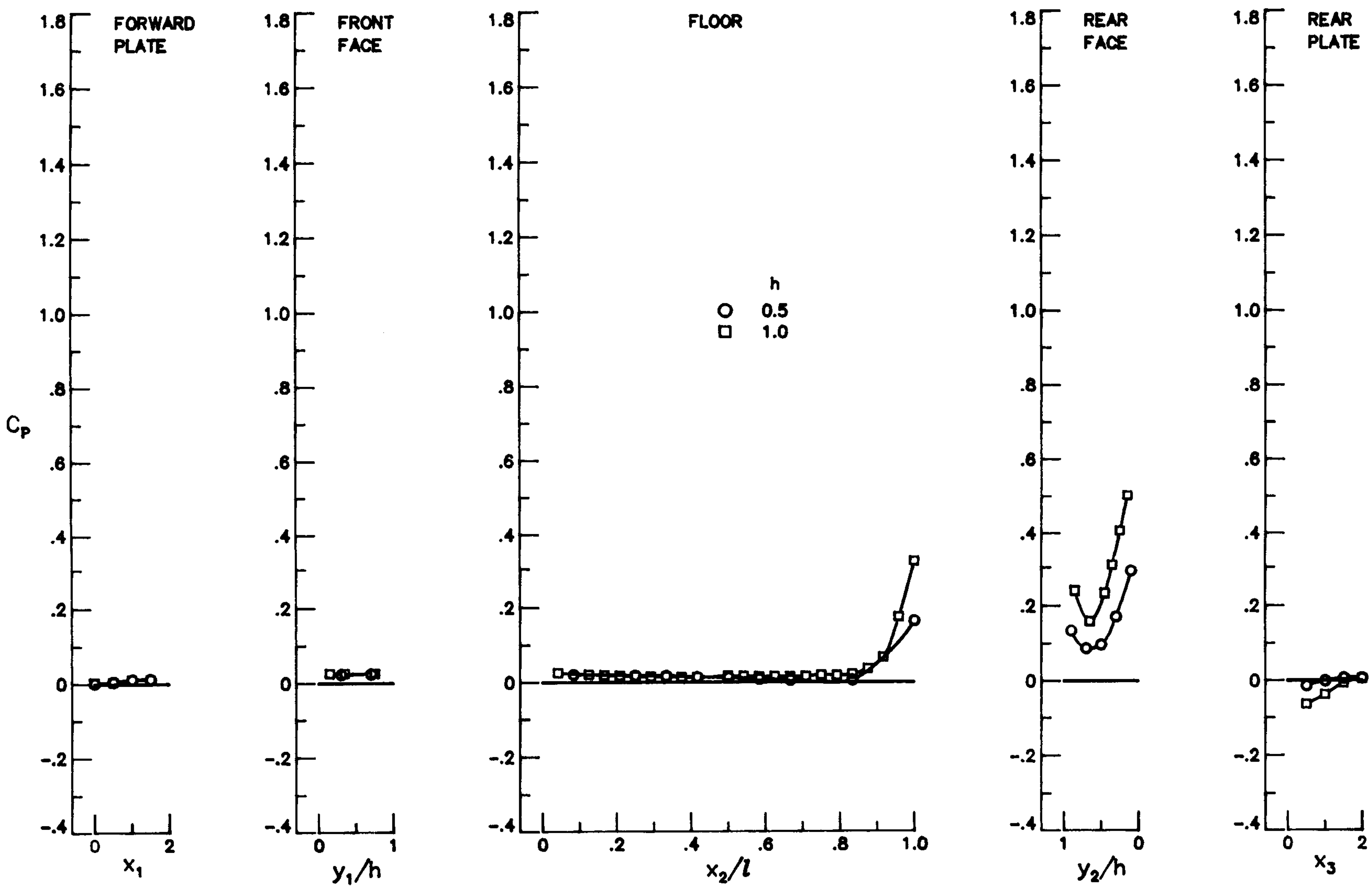

(c) $M_\infty = 1.50$; $l/h = 6$.

Figure 10. Continued.

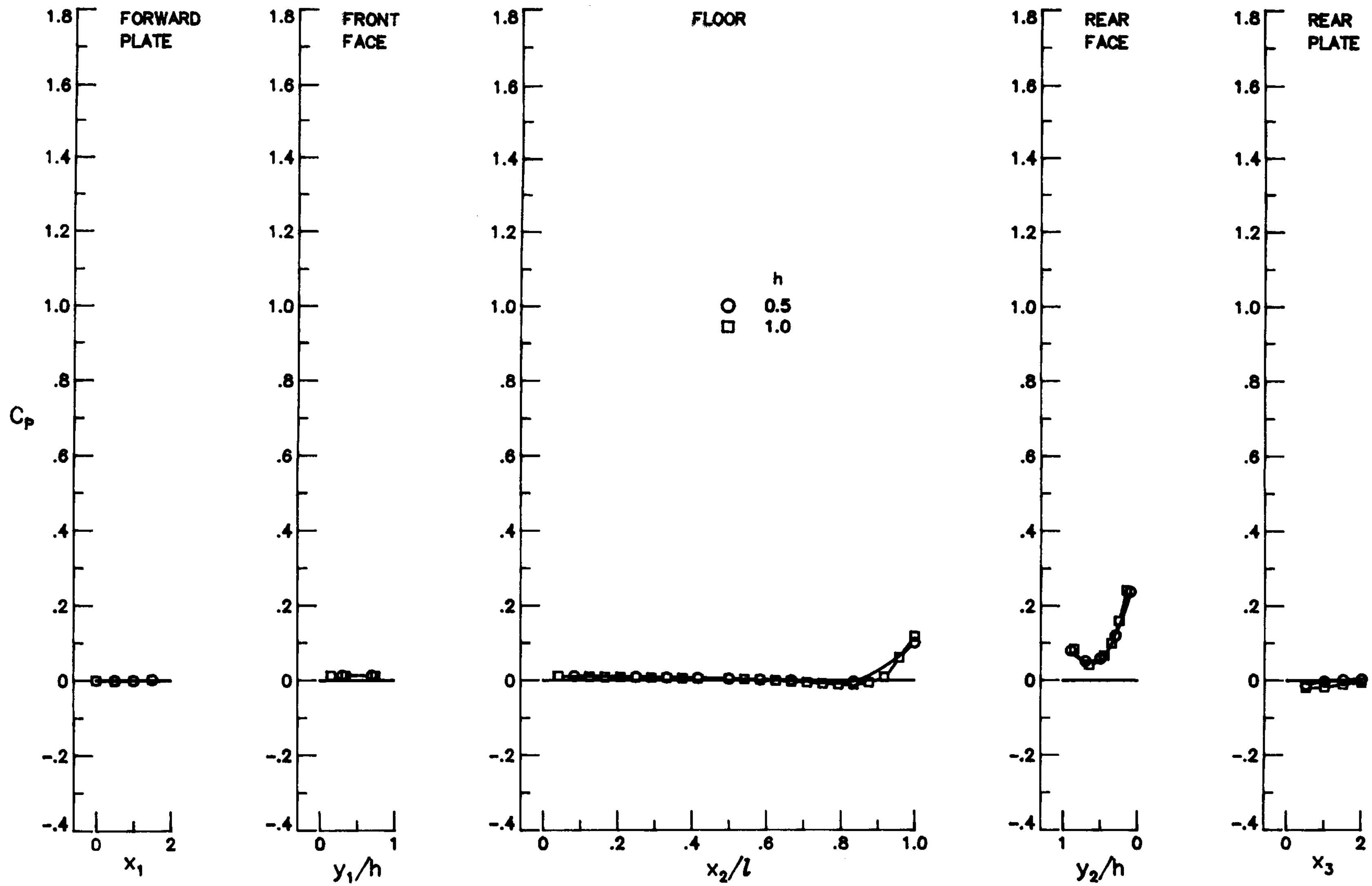

(d) $M_\infty = 2.16$; $l/h = 6$.

Figure 10. Concluded.

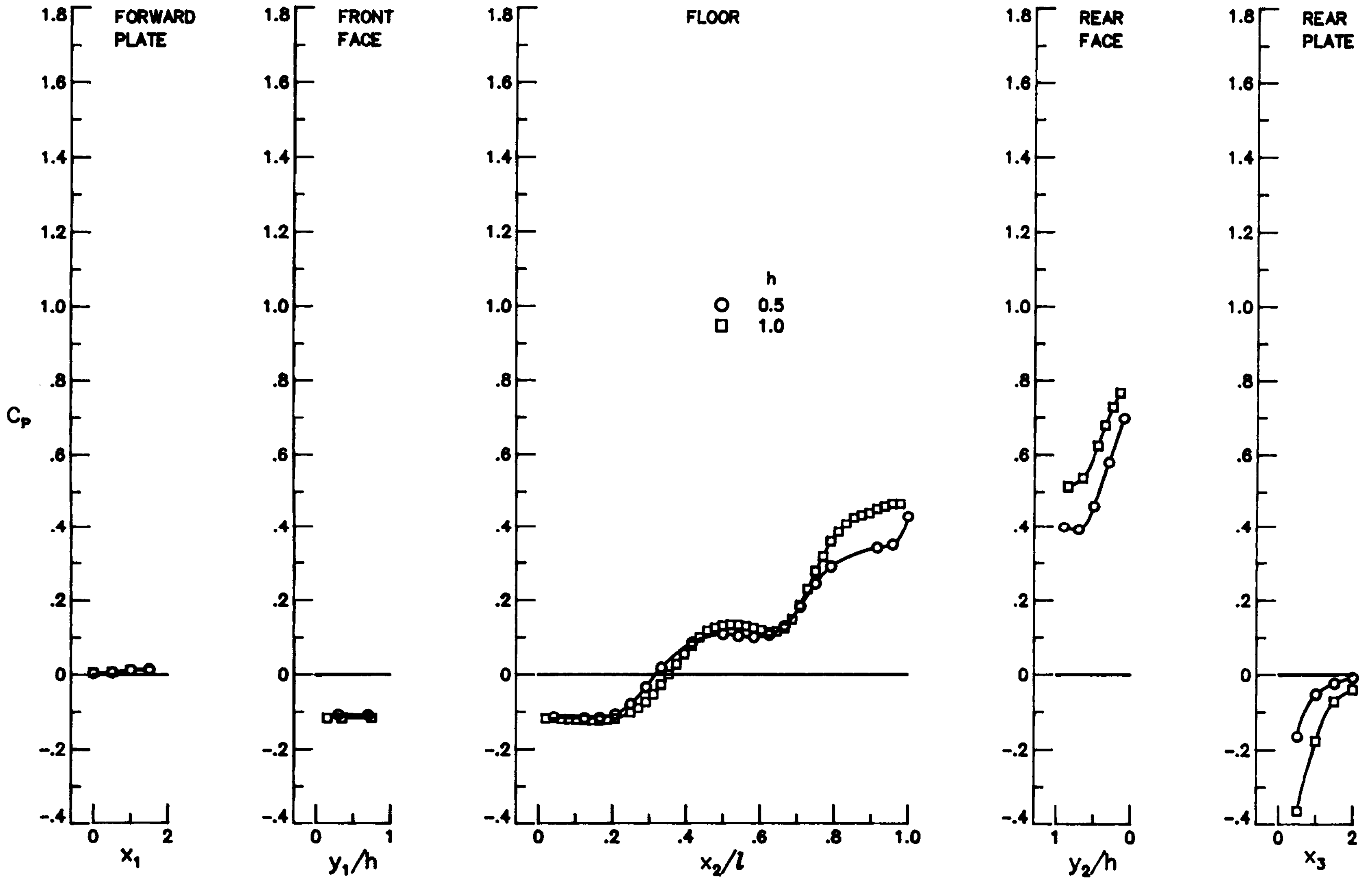

(a) $M_\infty = 1.50$; $l/h = 12$.

Figure 11. Correlation of cavity pressure distributions based on l/h and w/h. $w/h = 1.0$.

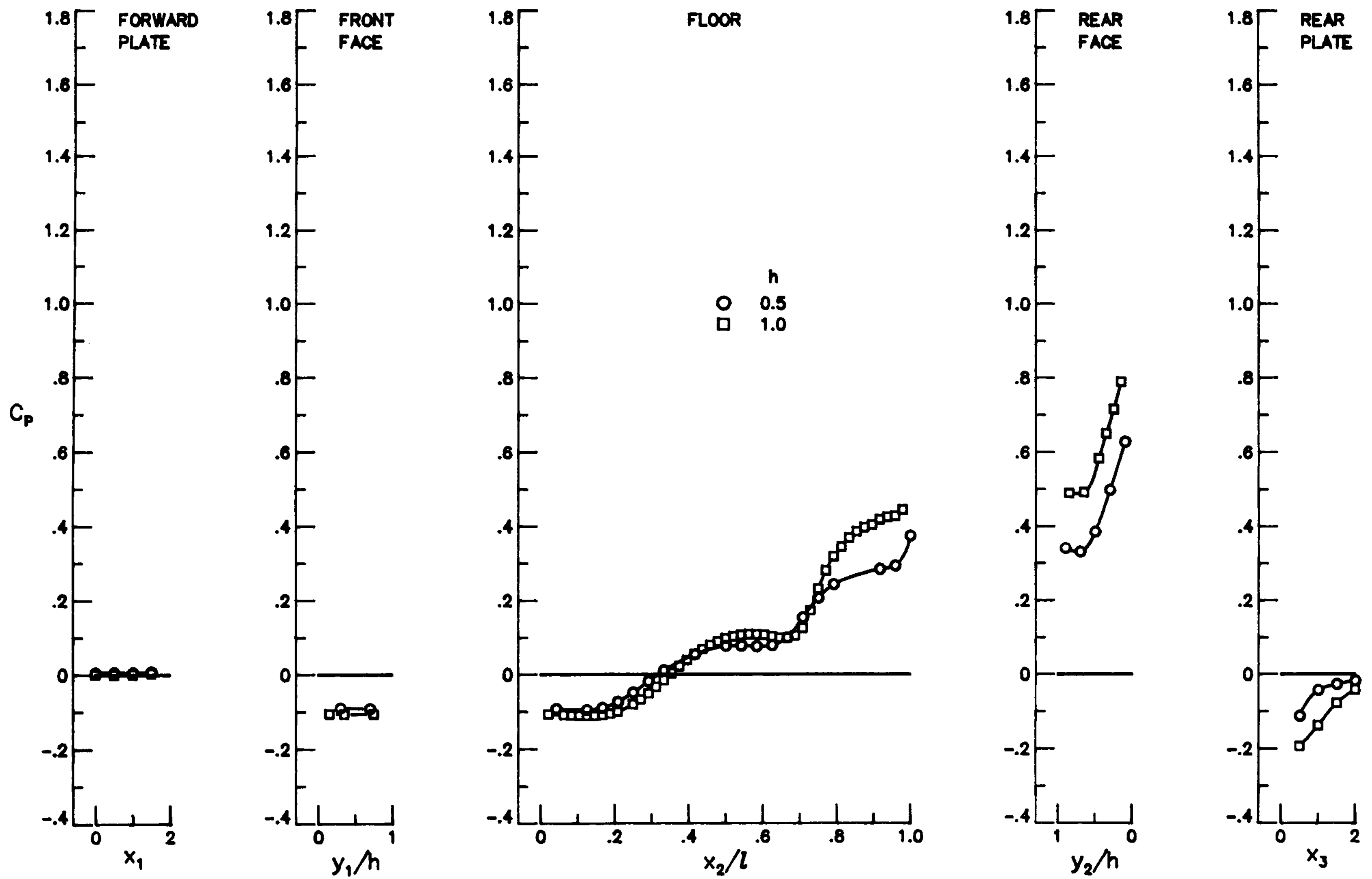

(b) $M_\infty = 2.16$; $l/h = 12$.

Figure 11. Continued.

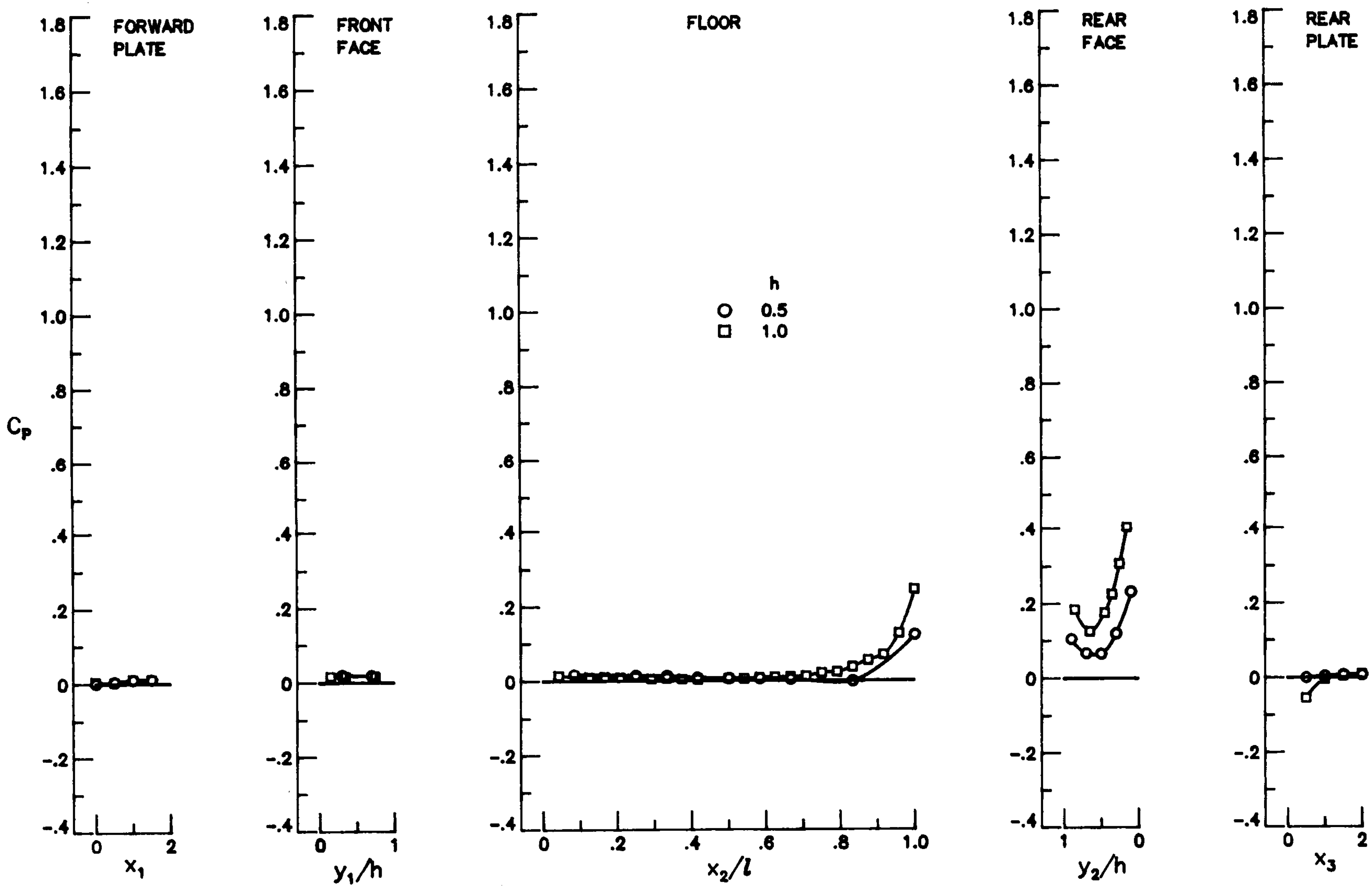

(c) $M_\infty = 1.50$; $l/h = 6$.

Figure 11. Continued.

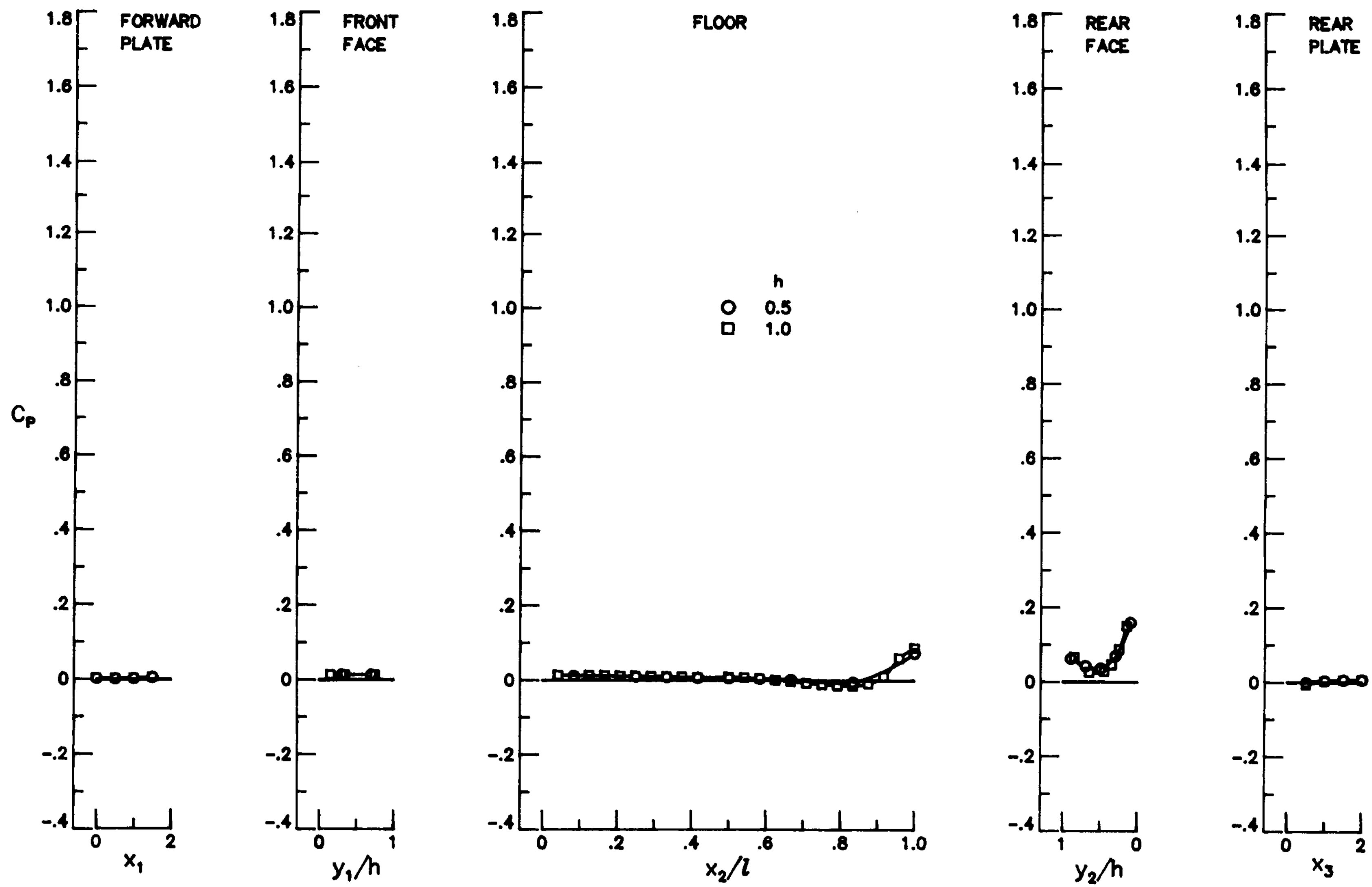

(d) $M_\infty = 2.16$; $l/h = 6$.

Figure 11. Concluded.

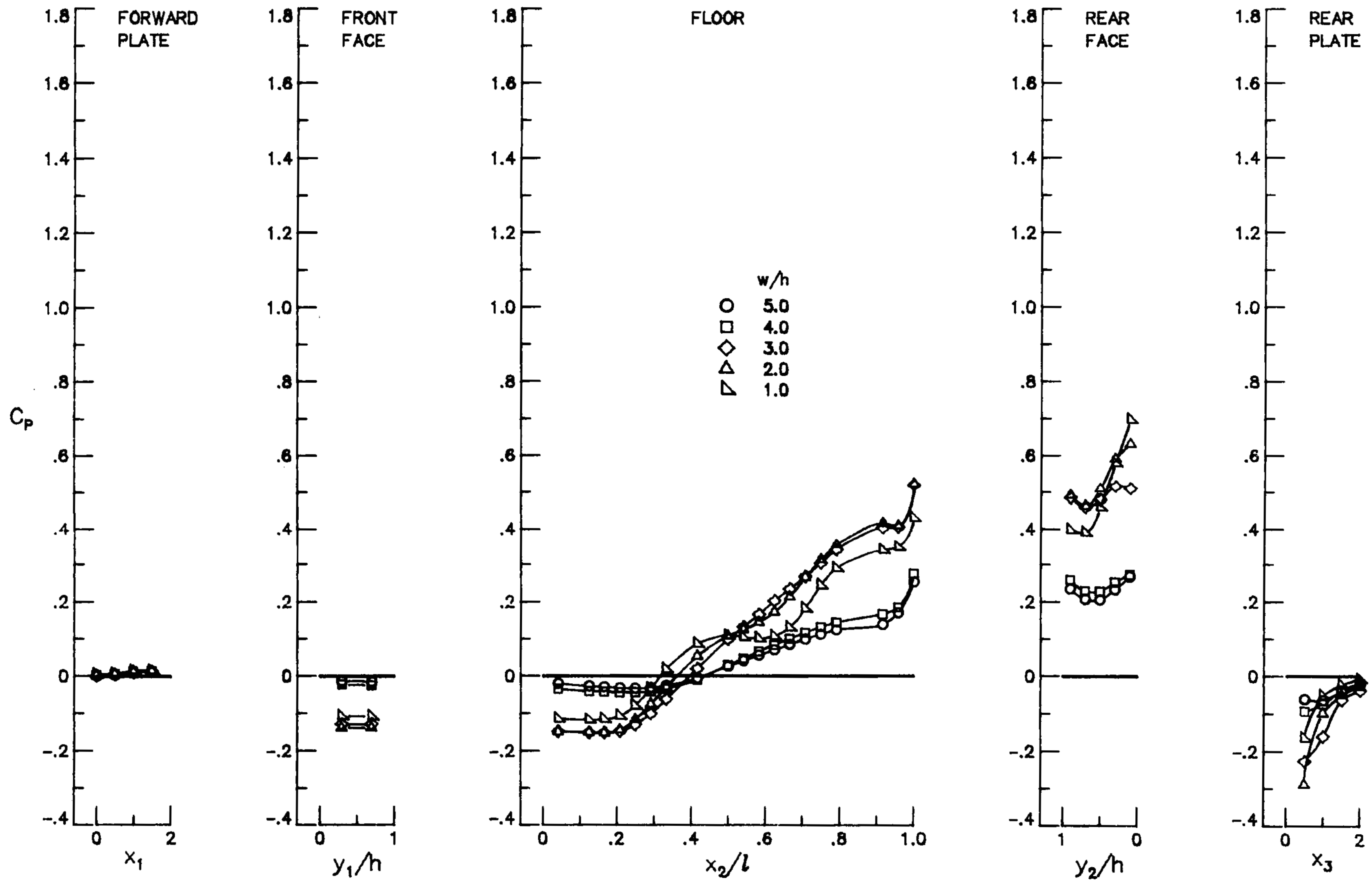

(a) $M_\infty = 1.50$; $l/h = 12$.

Figure 12. Effect of cavity width on cavity pressure distributions. $h = 0.5$ in.

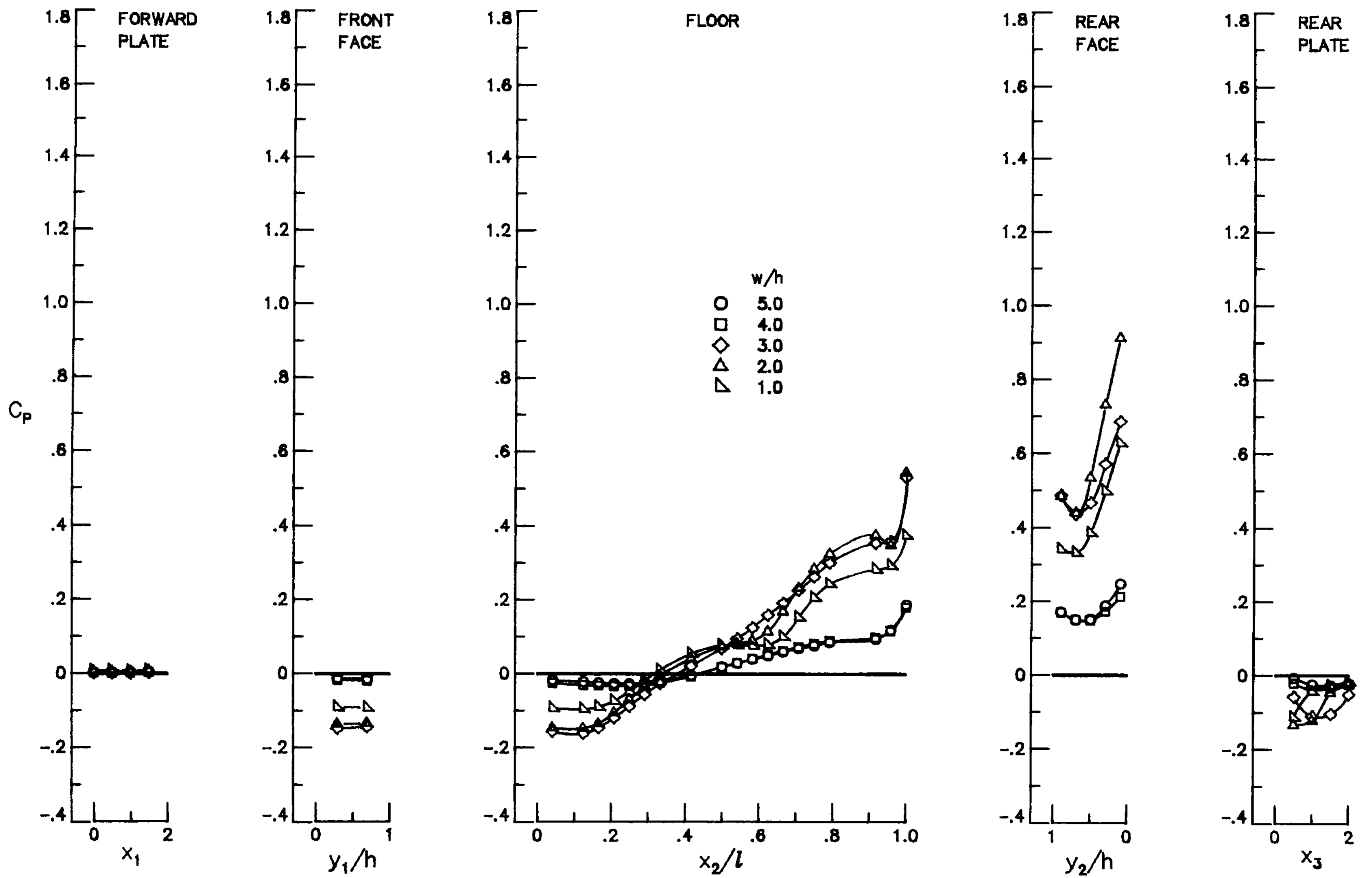

(b) $M_\infty = 2.16$; $l/h = 12$.

Figure 12. Continued.

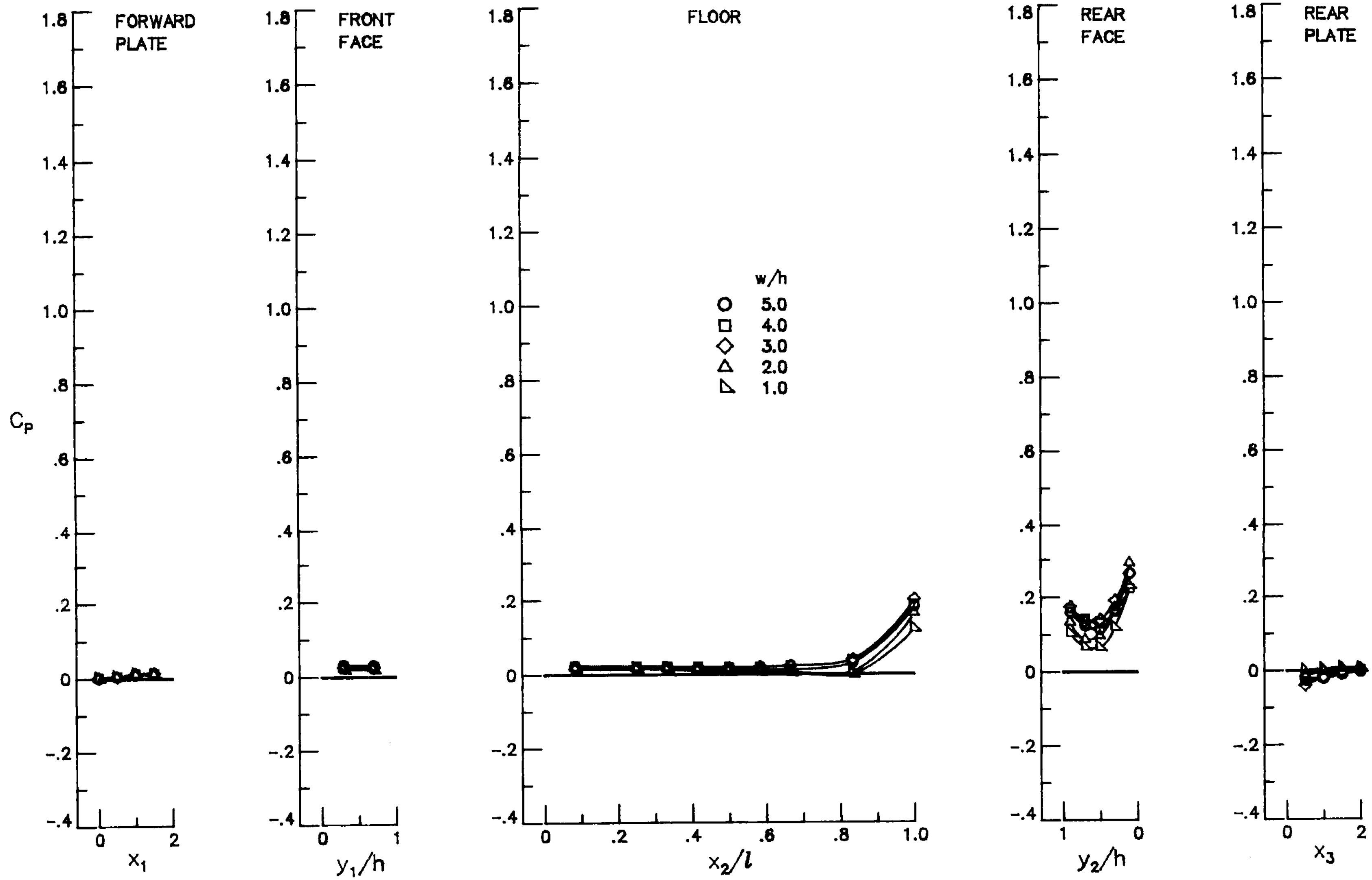

(c) $M_\infty = 1.50$; $l/h = 6$.

Figure 12. Continued.

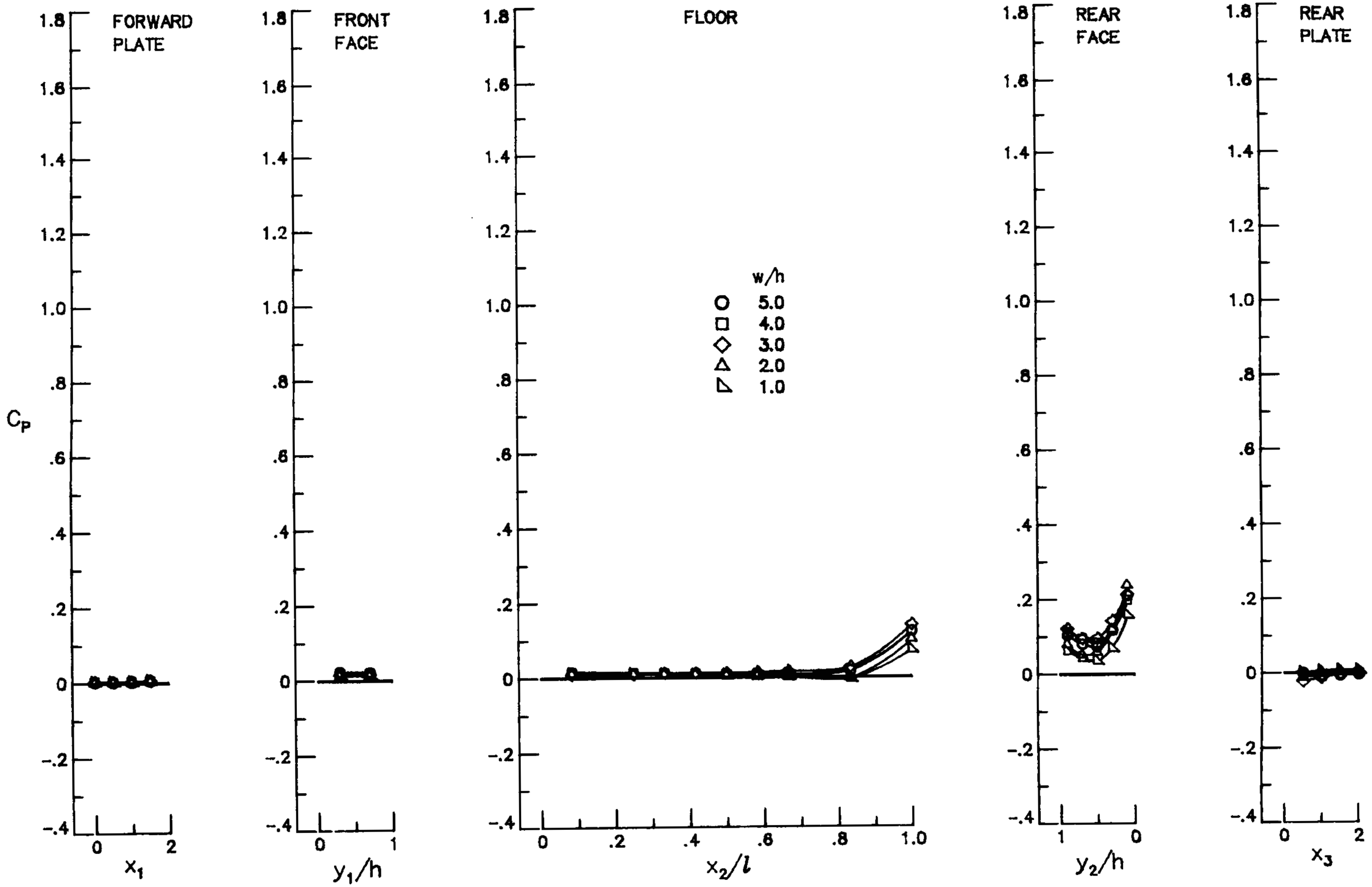

(d) $M_\infty = 2.16$; $l/h = 6$.

Figure 12. Concluded.

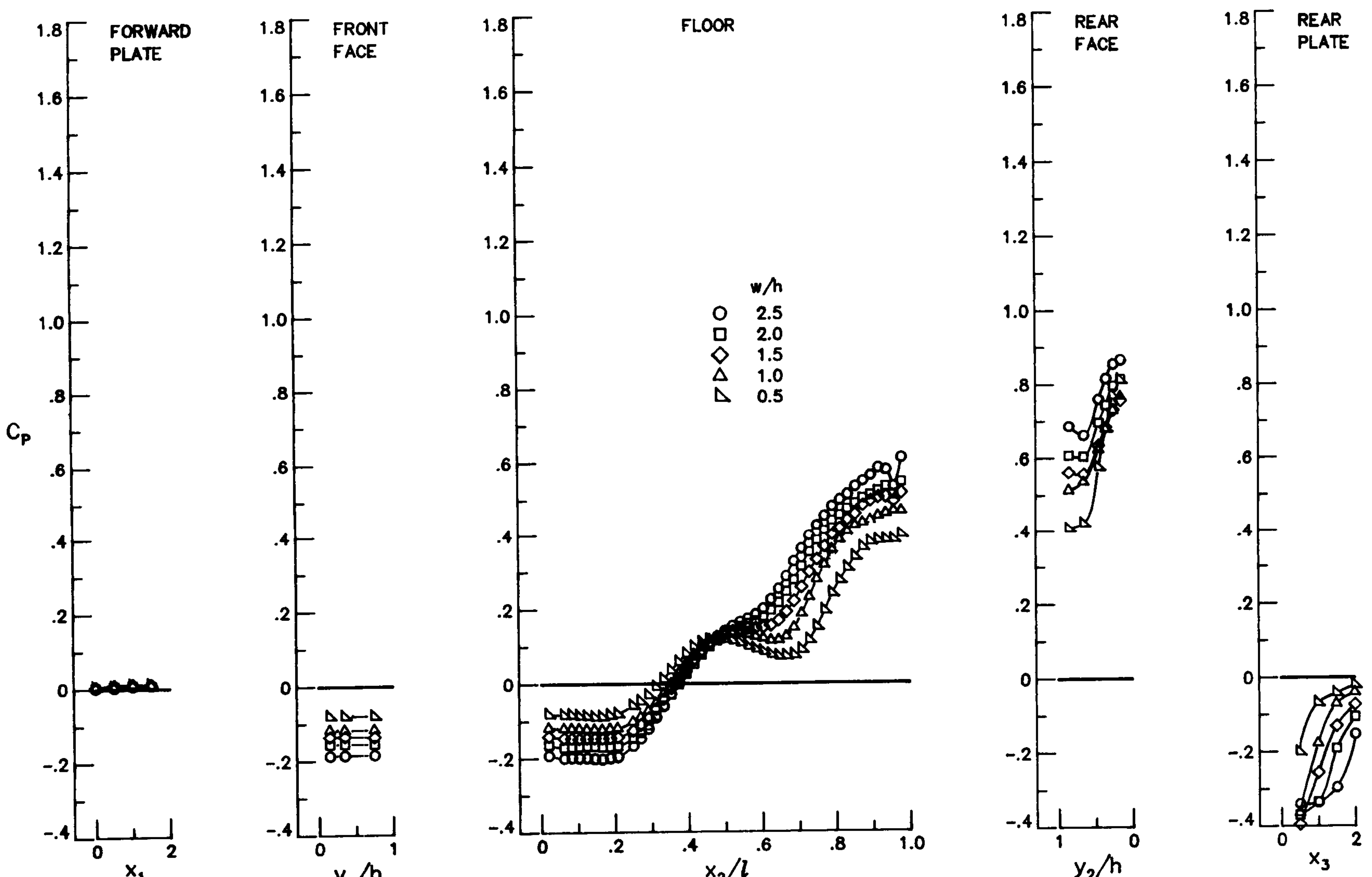

(a) $M_\infty = 1.50$; $l/h = 12$.

Figure 13. Effect of cavity width on cavity pressure distributions. $h = 1.0$ in.

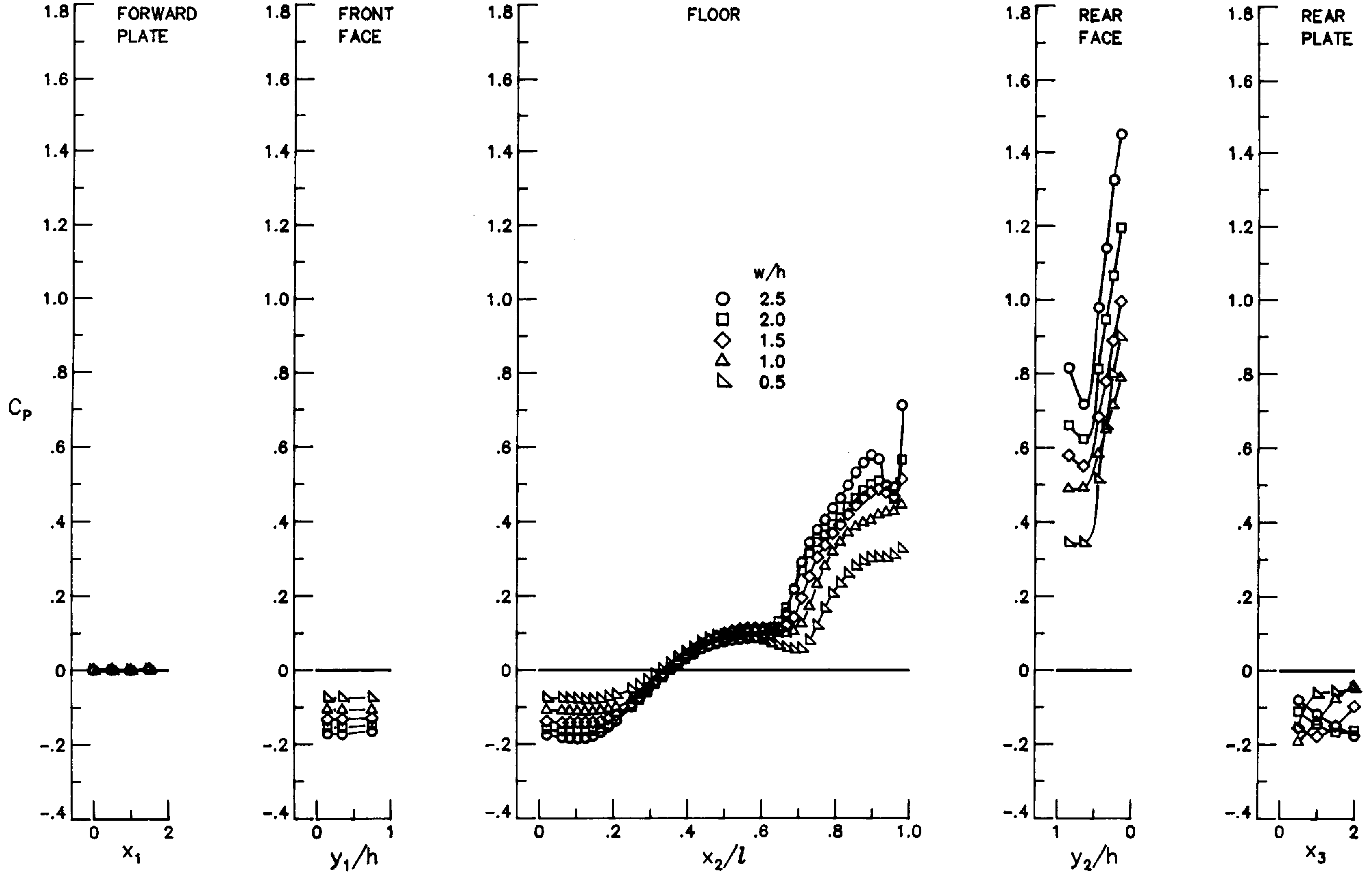

(b) $M_\infty = 2.16$; $l/h = 12$.

Figure 13. Continued.

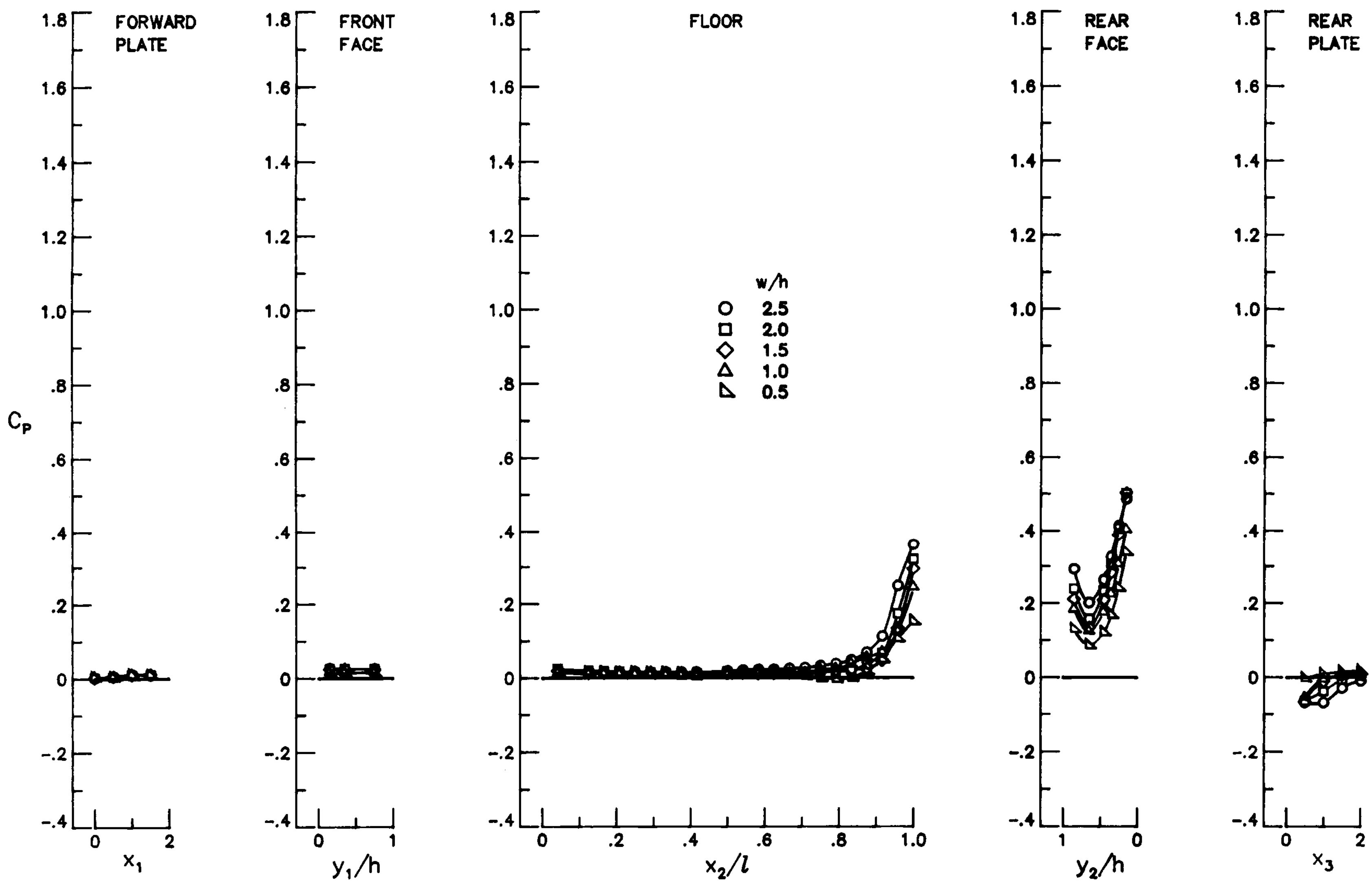

(c) $M_\infty = 1.50$; $l/h = 6$.

Figure 13. Continued.

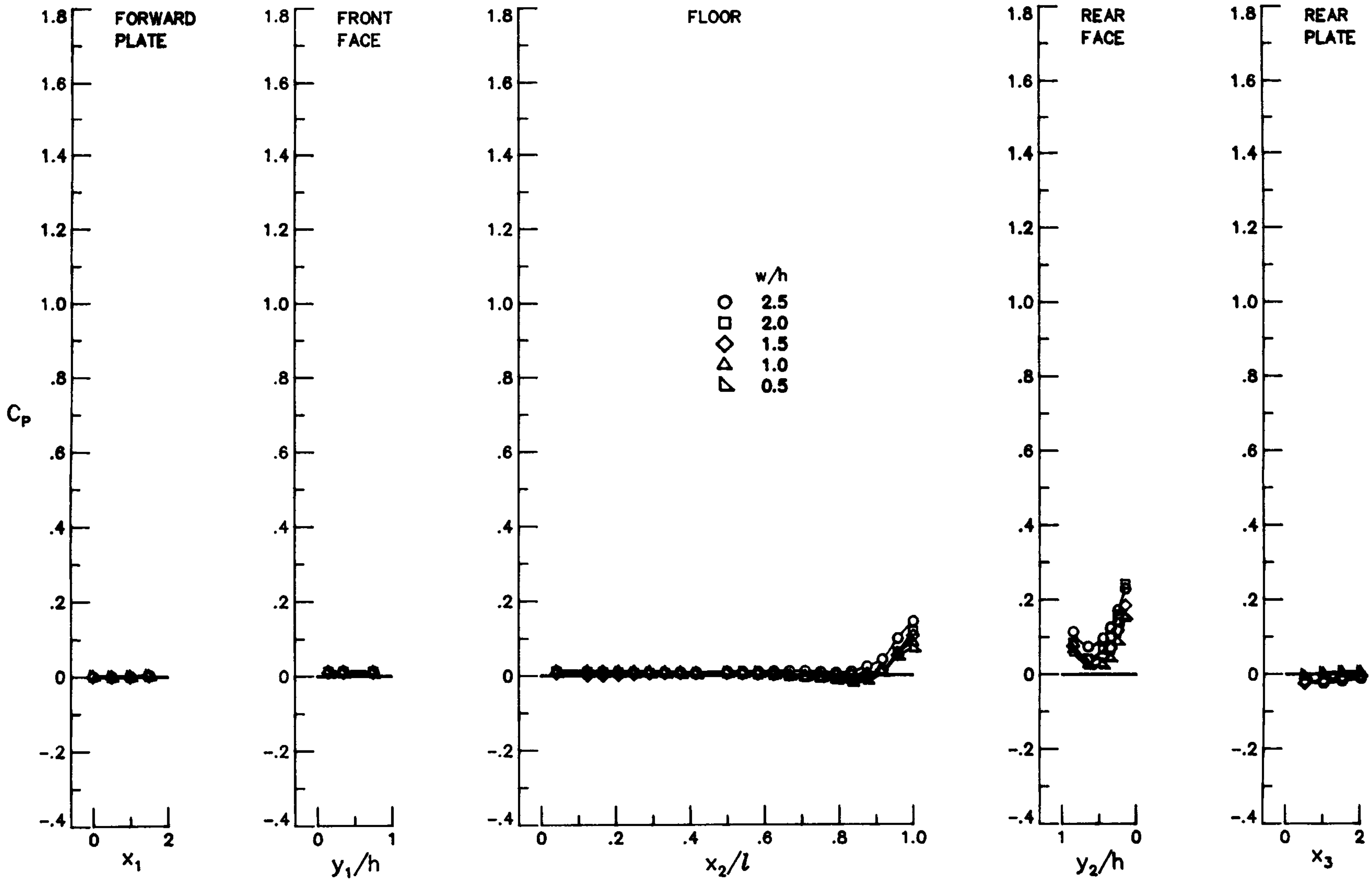

(d) $M_\infty = 2.16$; $l/h = 6$.

Figure 13. Concluded.

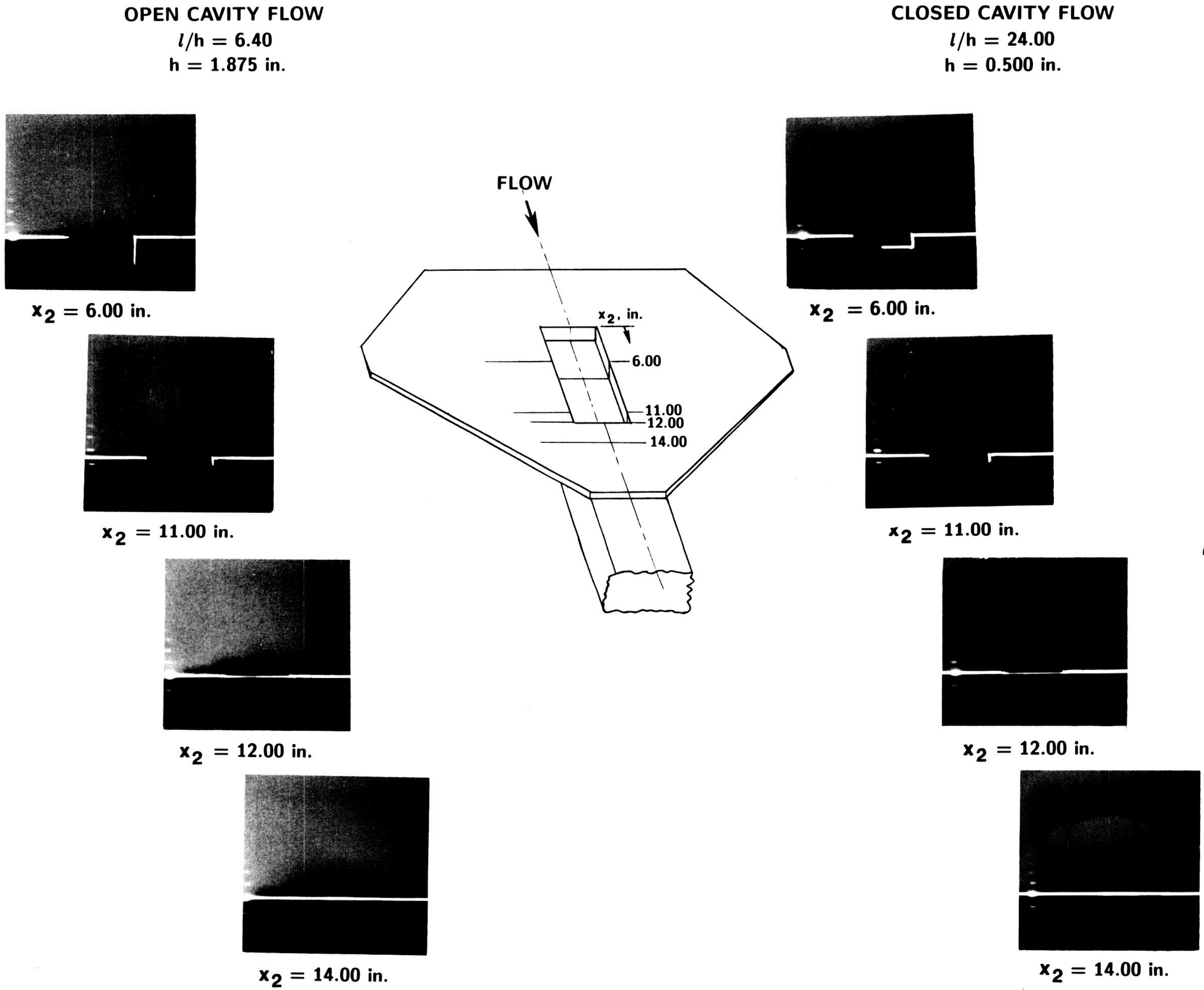

L-85-305

Figure 14. Cavity vapor screen photographs from reference 8. $M_\infty = 2.16$.

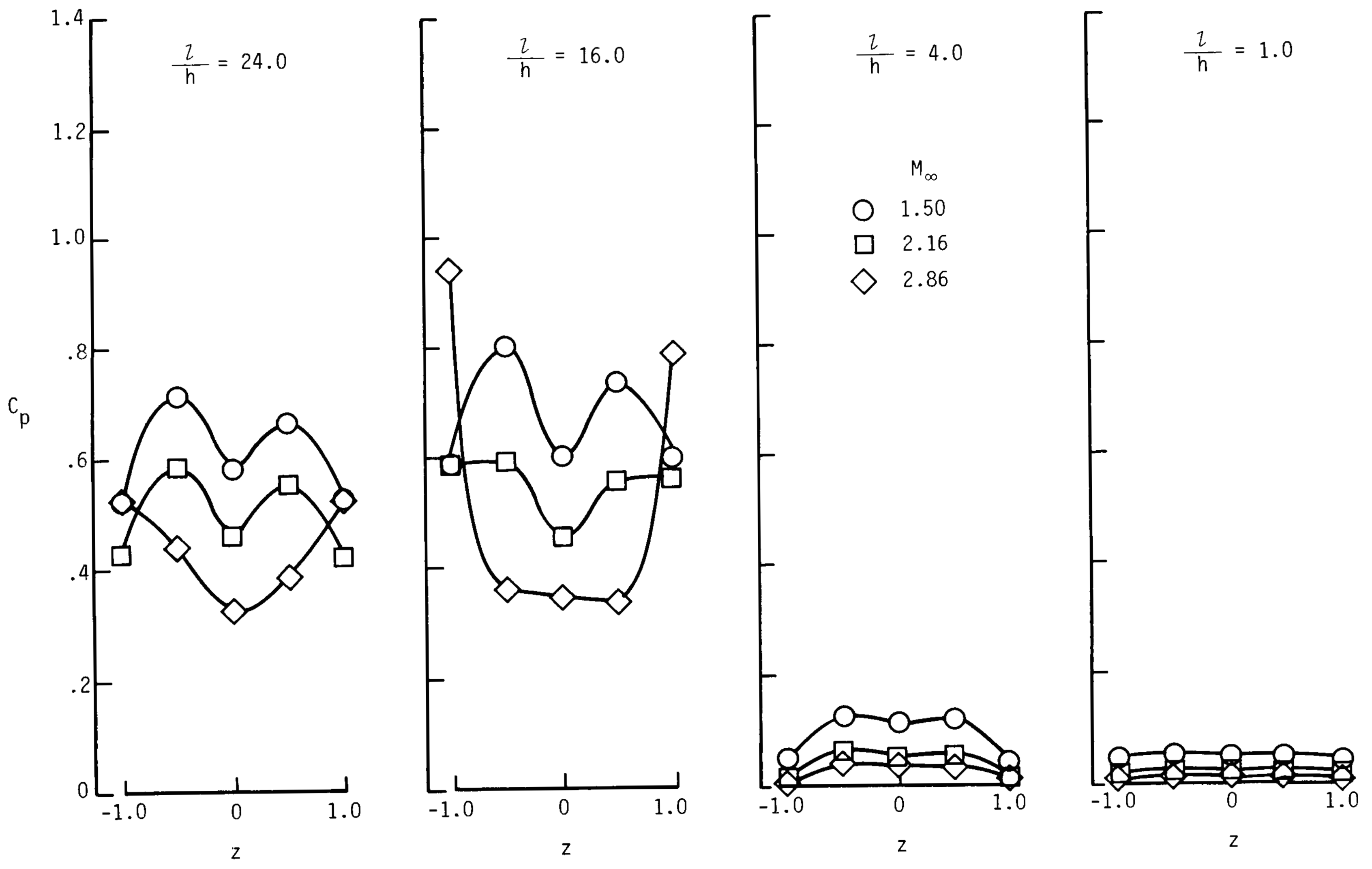

(a) $h = 0.5$ in.; $y_2/h = 0.5$.

Figure 15. Lateral pressure distributions measured on cavity rear face. $w = 2.5$ in.

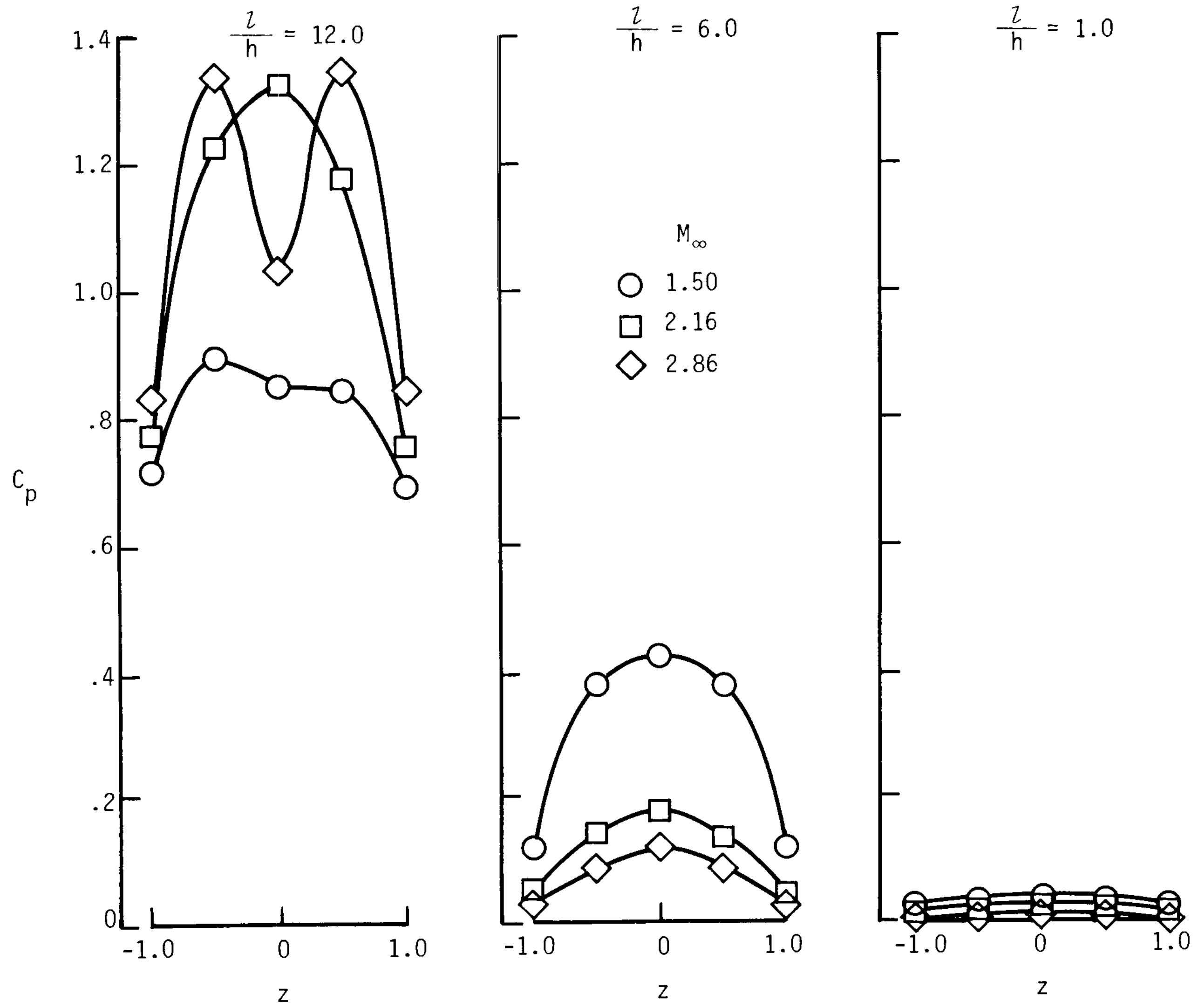

(b) $h = 1.0$ in.; $y_2/h = 0.25$.

Figure 15. Continued.

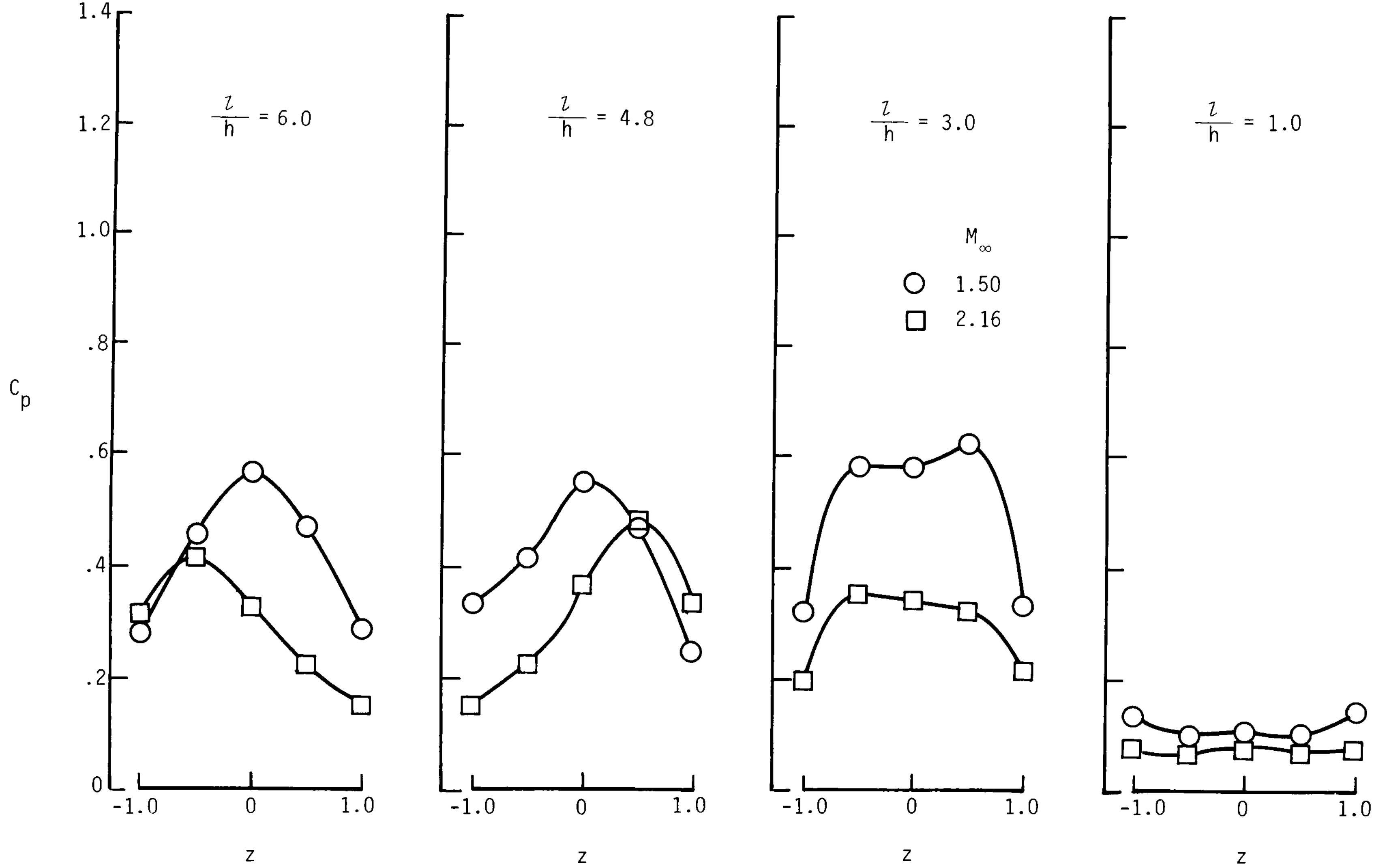

(c) $h = 2.0$ in.; $y_2/h = 0.125$.

Figure 15. Continued.

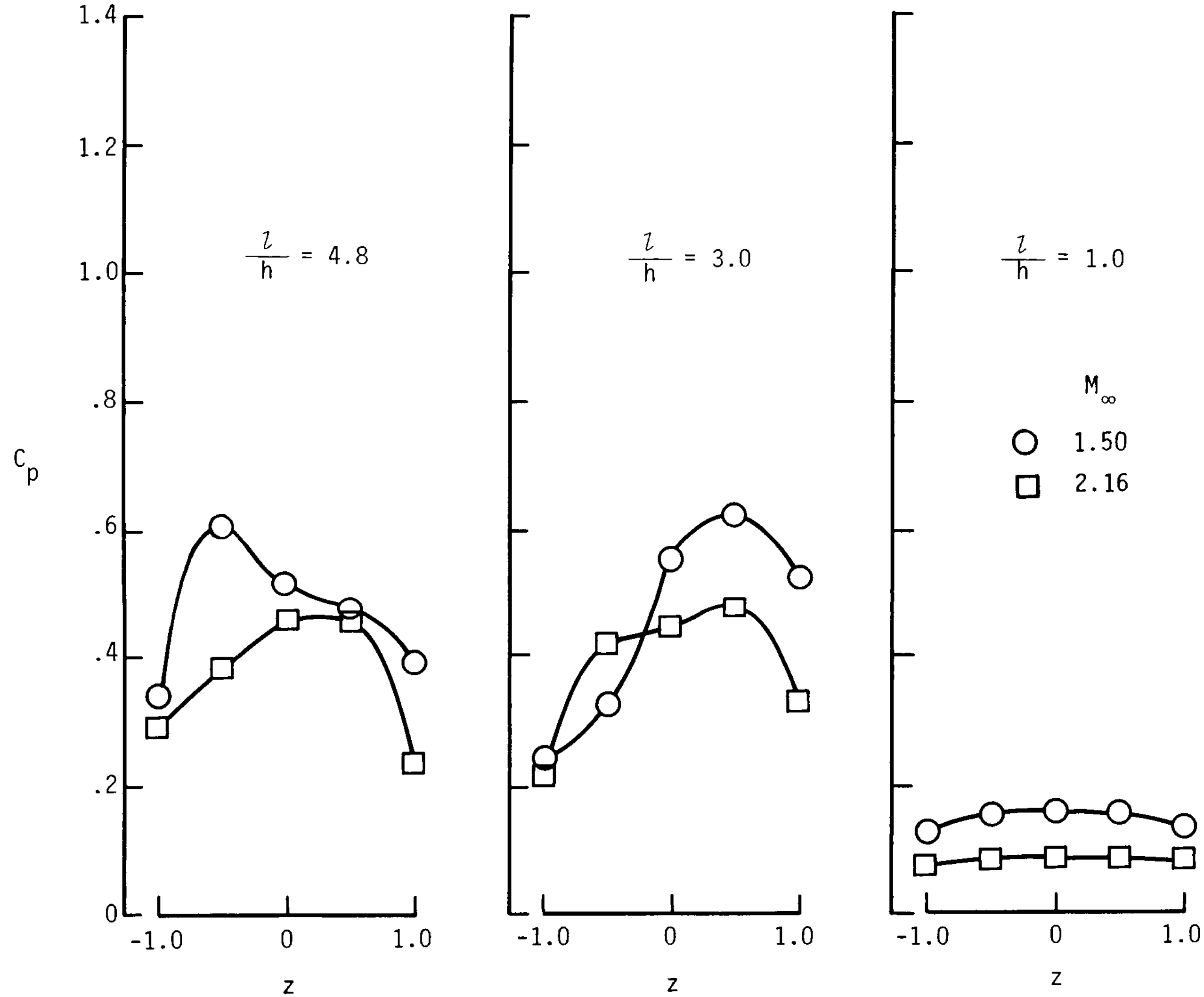

(d) $h = 2.5$ in.; $y_2/h = 0.1$.

Figure 15. Concluded.

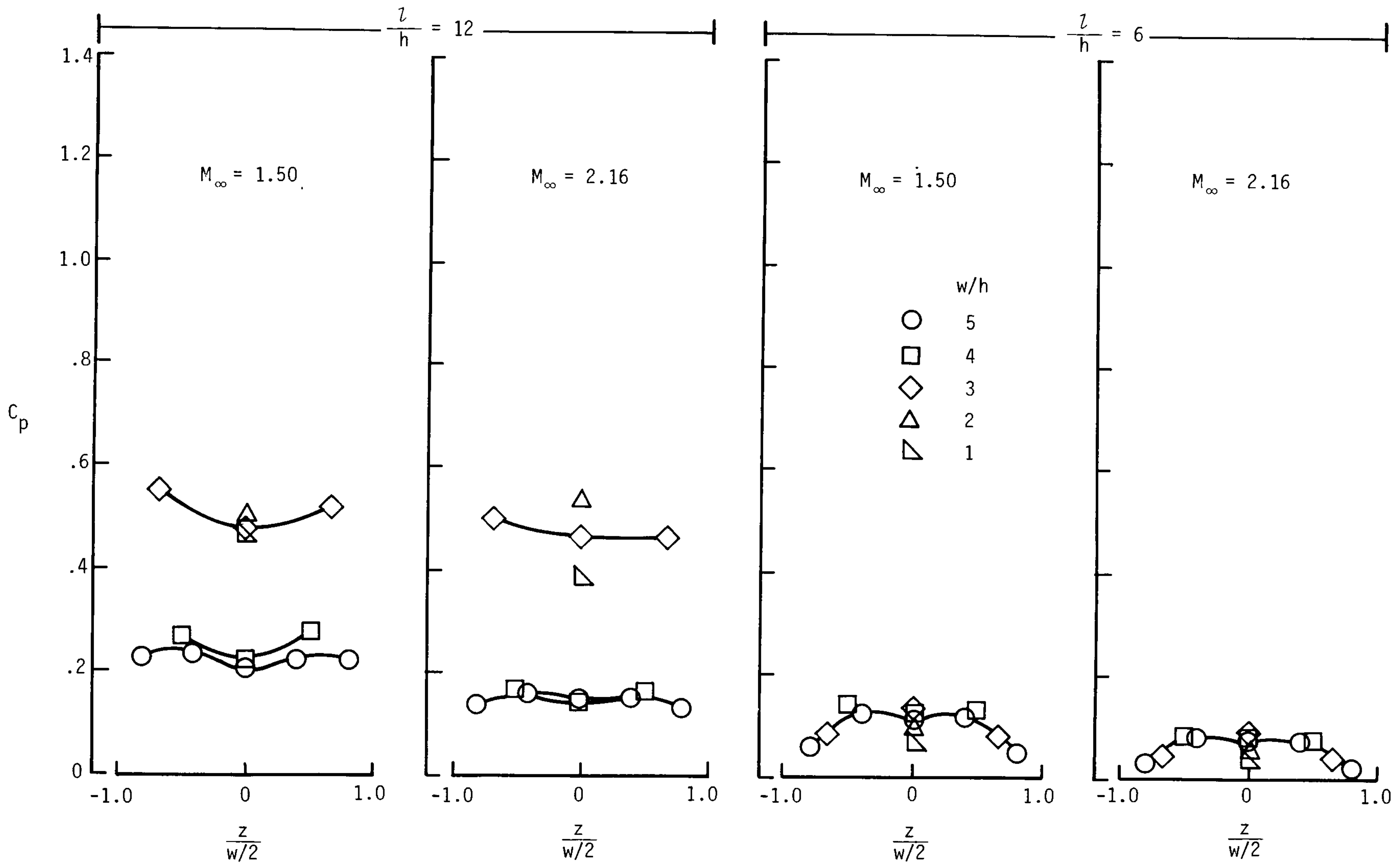

(a) $h = 0.5$ in.; $y_2/h = 0.5$.

Figure 16. Effect of cavity width on cavity rear face pressure distributions.

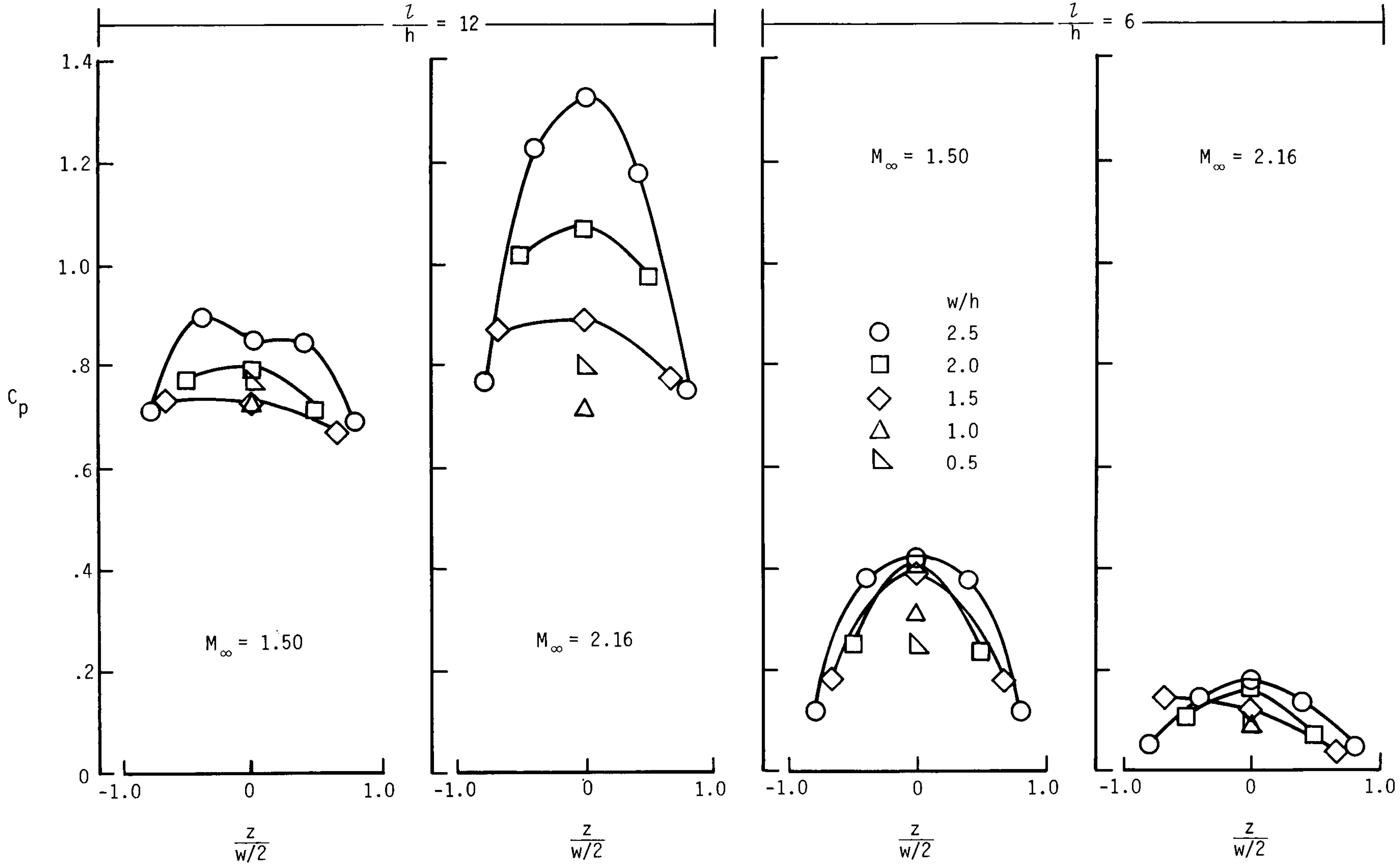

(b) $h = 1.0$ in.; $y_2/h = 0.25$.

Figure 16. Concluded.